DEVELOPMENT AND ANALYSIS OF BIOLOGICALLY INSPIRED COMMUNICATION ALGORITHMS FOR ARTIFICIAL AGENTS

By

Douglas Kirkpatrick

Thesis

Submitted to the Faculty of the

Graduate School of Vanderbilt University

in partial fulfillment of the requirements

for the degree of

MASTER OF SCIENCE

in

COMPUTER SCIENCE

May, 2015

Nashville, Tennessee

Approved:

Julie A. Adams, Ph.D.

Douglas H. Fisher, Ph.D.

ACKNOWLEDGMENTS

This work would not be possible without the support and guidance of those around me. My research advisor, Dr. Julie A. Adams, has given me invaluable assistance and direction through the difficult process of writing this Thesis. I am also grateful for the support of Dr. Douglas H. Fisher, who has been an inspiration to me.

A number of graduate students have provided assistance and guidance as I've worked through the research process and learned the ins and outs of graduate student life. In particular, I'd like to thank Sean Hayes, Electa Baker, Sayan Sen, Caroline Harriott, and Andrew Plassard for the corrections, code, and statistics that they have helped me through over the past two years.

I am indebted to the care and support that my friends and family have provided. My parents, Jackie and Brian Kirkpatrick, have been a calming influence for me, talking me through my moments of personal crisis and providing editorial feedback on this Thesis. The encouragement of my friends Zak K., Tyler G., Amber B., Amber G, and Emma C. has also helped me through long nights and busy days of the past two years. The backing and assistance that everyone has given me has been crucial to the success I have achieved here at Vanderbilt University.

This Thesis was partially supported under ONR Award N000141210987.

TABLE OF CONTENTS

Page

ACKNOWLEDGMENTS . . . . . **ii**

LIST OF TABLES . . . . . **v**

LIST OF FIGURES . . . . . **x**

I Introduction **1**

II Literature Review **4**

II.1 Biological Models 4
II.2 Motivation for Application of Biological Models 5
II.3 Artifical Swarms 5
II.4 Choice of Models 6
II.5 Alternate Models 7
II.6 Primary Models 8

III Algorithms **10**

III.1 Definitions 10
III.2 Metric Model 12
III.3 Topological Model 13
III.4 Visual Model 14
III.5 Simulator Design 17

IV Experiment **19**

IV.1 Experimental Design 19
IV.1.1 Variables 19
IV.1.2 Parameters 19
IV.1.2.1 Agent Parameters 19
IV.1.2.2 Environment Parameters 20
IV.1.2.3 Task Parameters 21
IV.1.3 Tasks 22
IV.1.3.1 Go to Location 22
IV.1.3.2 Search / Monitor 23
IV.1.3.3 Avoid Object 24
IV.1.3.4 Follow Object 26
IV.1.3.5 Disperse / Rally 26
IV.1.3.6 Maintain Group / Flocking 27
IV.1.4 Metrics 29
IV.1.4.1 Go to Location 29
IV.1.4.2 Search / Monitor 29
IV.1.4.3 Avoid Object 31
IV.1.4.4 Follow Object 32
IV.1.4.5 Disperse / Rally 33
IV.1.4.6 Maintain Group / Flocking 34

IV.1.5 Hypotheses . . . 35
IV.1.5.1 Go to Location . . . 35
IV.1.5.2 Search / Monitor . . . 36
IV.1.5.3 Avoid Object . . . 36
IV.1.5.4 Follow Object . . . 37
IV.1.5.5 Disperse / Rally . . . 37
IV.1.5.6 Maintain Group / Flocking . . . 37
IV.2 Results . . . 38
IV.2.1 Go to Location . . . 38
IV.2.2 Search / Monitor . . . 45
IV.2.3 Avoid Object . . . 61
IV.2.4 Follow Object . . . 68
IV.2.5 Disperse / Rally . . . 86
IV.2.6 Maintain Group / Flocking . . . 104
IV.3 Discussion . . . 120

V Contributions, Conclusions, and Future Work . . . 126

V.1 Conclusions . . . 126
V.2 Contributions . . . 126
V.3 Future Work . . . 127

BIBLIOGRAPHY . . . 128

LIST OF TABLES

Table		Page
II.1	Summary of alternate models and why they were eliminated.	8
IV.1	The summary of the parameters for each task, Part 1.	21
IV.2	Continued, the summary of the parameters for each task, Part 2.	22
IV.3	Summary of hypotheses by task.	35
IV.4	Summary of the results of the analyses conducted.	39
IV.5	The means and standard deviations of the Go To Location task by number of agents.	41
IV.6	The means and standard deviations of the Go To Location task by number of obstacles.	41
IV.7	The means and standard deviations of the Go To Location task by radius of repulsion.	41
IV.8	The means and standard deviations of the Go To Location task by radius of orientation.	43
IV.9	The means and standard deviations of the Go To Location task by radius of attraction.	45
IV.10	The means and standard deviations of the Search task by number of agents.	47
IV.11	The means and standard deviations of the Search task by number of obstacles.	47
IV.12	The means and standard deviations of the Search task by number of goals.	49
IV.13	The means and standard deviations of the Search task by radius of repulsion.	49
IV.14	The means and standard deviations of the Search task by radius of orientation.	50
IV.15	The means and standard deviations of the Search task by radius of attraction.	52
IV.16	The significance results from the Wilcoxon Rank-Sum Test for the Search task when the radius of attraction equals 25.	52
IV.17	The significance results from the Wilcoxon Rank-Sum Test for the Monitor task.	54
IV.18	The means and standard deviations of the Monitor task by number of agents.	54
IV.19	The significance results from the Kruskal-Wallis Test for the Monitor task by number of agents.	55
IV.20	The means and standard deviations of the Monitor task by number of obstacles.	56
IV.21	The significance results from the Kruskal-Wallis Test for the Monitor task by number of obstacles.	56

IV.22 The means and standard deviations of the Monitor task by radius of repulsion. 57

IV.23 The significance results from the Kruskal-Wallis Test for the Monitor task by radius of repulsion. 58

IV.24 The means and standard deviations of the Monitor task by radius of orientation. 59

IV.25 The significance results from the Kruskal-Wallis Test for the Monitor task by radius of orientation. 59

IV.26 The means and standard deviations of the Monitor task by radius of attraction. 61

IV.27 The significance results from the Kruskal-Wallis Test for the Monitor task by radius of attraction. 61

IV.28 The means and standard deviations of the Avoid task by number of agents. 63

IV.29 The significance results from the Kruskal-Wallis Test for the Avoid task by number of agents. 64

IV.30 The means and standard deviations of the Avoid task by radius of repulsion. 65

IV.31 The significance results from the Kruskal-Wallis Test for the Avoid task by radius of repulsion. 65

IV.32 The means and standard deviations of the Avoid task by radius of orientation. 67

IV.33 The means and standard deviations of the Avoid task by radius of attraction. 67

IV.34 The significance results from the Wilcoxon Rank-Sum Test for the Follow task using the network efficiency metric. 69

IV.35 The means and standard deviations of the Follow task by number of agents for Network Efficiency. 70

IV.36 The significance results from the Kruskal-Wallis Test for the Follow task by number of agents for Network Efficiency. 70

IV.37 The means and standard deviations of the Follow task by number of obstacles for Network Efficiency. 72

IV.38 The significance results from the Kruskal-Wallis Test for the Follow task by number of obstacles for Network Efficiency. 72

IV.39 The means and standard deviations of the Follow task by radius of repulsion for Network Efficiency. 73

IV.40 The significance results from the Kruskal-Wallis Test for the Follow task by radius of repulsion for Network Efficiency. 74

IV.41 The means and standard deviations of the Follow task by radius of orientation for Network Efficiency. 75

IV.42 The significance results from the Kruskal-Wallis Test for the Follow Task task by radius of orientation for Network Efficiency. 75

IV.43 The means and standard deviations of the Follow task by radius of attraction for Network Efficiency. . . . 77

IV.44 The significance results from the Kruskal-Wallis Test for the Follow Task task by radius of orientation for Network Efficiency. . . . 77

IV.45 The significance results from the Wilcoxon Rank-Sum Test for the Follow task using the percentage of agents within 30 degrees metric. . . . 78

IV.46 The means and standard deviations of the Follow task by number of agents for percentage of agents within 30 degrees. . . . 80

IV.47 The significance results from the Kruskal-Wallis Test for the Follow task by number of agents for percentage of agents within 30 degrees. . . . 80

IV.48 The means and standard deviations of the Follow task by number of obstacles for percentage of agents within 30 degrees. . . . 81

IV.49 The significance results from the Kruskal-Wallis Test for the Follow task by number of obstacles for percentage of agents within 30 degrees. . . . 82

IV.50 The means and standard deviations of the Follow task by radius of repulsion for percentage of agents within 30 degrees. . . . 83

IV.51 The significance results from the Kruskal-Wallis Test for the Follow task by radius of repulsion for percentage of agents within 30 degrees. . . . 83

IV.52 The means and standard deviations of the Follow task by radius of orientation for percentage of agents within 30 degrees. . . . 85

IV.53 The significance results from the Kruskal-Wallis Test for the Follow Task task by radius of orientation for percentage of agents within 30 degrees. . . . 85

IV.54 The means and standard deviations of the Follow task by radius of attraction for percentage of agents within 30 degrees. . . . 86

IV.55 The significance results from the Kruskal-Wallis Test for the Follow Task task by radius of orientation for percentage of agents within 30 degrees. . . . 87

IV.56 The means and standard deviations of the Disperse task by number of agents. . . . 89

IV.57 The significance results from the Kruskal-Wallis Test for the Disperse task by number of agents. . . . 89

IV.58 The means and standard deviations of the Disperse task by number of obstacles. . . . 90

IV.59 The significance results from the Kruskal-Wallis Test for the Disperse task by number of obstacles. . . . 91

IV.60 The means and standard deviations of the Disperse task by radius of repulsion. . . . 92

IV.61 The significance results from the Kruskal-Wallis Test for the Disperse task by radius of repulsion. . . . 92

IV.62 The means and standard deviations of the Disperse task by radius of orientation. 94

IV.63 The significance results from the Kruskal-Wallis Test for the Disperse task by radius of orientation. 94

IV.64 The means and standard deviations of the Disperse task by radius of attraction. 95

IV.65 The significance results from the Kruskal-Wallis Test for the Disperse task by radius of attraction. 96

IV.66 The significance results from the Wilcoxon Rank-Sum Test for the Rally task. 96

IV.67 The means and standard deviations of the Rally task by number of agents. 98

IV.68 The significance results from the Kruskal-Wallis Test for the Rally task by number of agents. 98

IV.69 The means and standard deviations of the Rally task by number of obstacles. 99

IV.70 The significance results from the Kruskal-Wallis Test for the Rally task by number of obstacles. 100

IV.71 The means and standard deviations of the Rally task by radius of repulsion. 101

IV.72 The significance results from the Kruskal-Wallis Test for the Rally task by radius of repulsion. 101

IV.73 The means and standard deviations of the Rally task by radius of orientation. 102

IV.74 The significance results from the Kruskal-Wallis Test for the Rally task by radius of orientation. 103

IV.75 The means and standard deviations of the Rally task by radius of attraction. 104

IV.76 The significance results from the Kruskal-Wallis Test for the Rally task by radius of attraction. 104

IV.77 The significance results from the Wilcoxon Rank-Sum Test for the Flocking task using the change in dispersion metric. 105

IV.78 The means and standard deviations of the Flocking task by number of agents for change in dispersion. 106

IV.79 The significance results from the Kruskal-Wallis Test for the Flocking task by number of agents for change in dispersion. 106

IV.80 The means and standard deviations of the Flocking task by number of obstacles for change in dispersion. 107

IV.81 The significance results from the Kruskal-Wallis Test for the Flocking task by number of obstacles for change in dispersion. 107

IV.82 The means and standard deviations of the Flocking task by radius of repulsion for change in dispersion. 108

IV.83 The means and standard deviations of the Flocking task by radius of orientation for change in dispersion. . . . 109

IV.84 The significance results from the Kruskal-Wallis Test for the Flocking Task task by radius of orientation for change in dispersion. . . . 109

IV.85 The means and standard deviations of the Flocking task by radius of attraction for change in dispersion. . . . 110

IV.86 The significance results from the Kruskal-Wallis Test for the Flocking Task task by radius of orientation for the change in dispersion. . . . 111

IV.87 The means and standard deviations of the Flocking task by number of agents for the change in center of gravity. . . . 112

IV.88 The significance results from the Kruskal-Wallis Test for the Flocking task by number of agents for the change in center of gravity. . . . 113

IV.89 The means and standard deviations of the Flocking task by number of obstacles for change in center of gravity. . . . 114

IV.90 The significance results from the Kruskal-Wallis Test for the Flocking task by number of obstacles for change in center of gravity. . . . 114

IV.91 The means and standard deviations of the Flocking task by radius of repulsion for the change in center of gravity. . . . 115

IV.92 The significance results from the Kruskal-Wallis Test for the Flocking task by radius of repulsion for the change in center of gravity. . . . 116

IV.93 The means and standard deviations of the Flocking task by radius of orientation for the change in center of gravity. . . . 117

IV.94 The significance results from the Kruskal-Wallis Test for the Flocking Task task by radius of orientation for the change in center of gravity. . . . 117

IV.95 The means and standard deviations of the Flocking task by radius of attraction for the change in center of gravity. . . . 119

IV.96 The significance results from the Kruskal-Wallis Test for the Flocking Task task by radius of orientation for the change in center of gravity. . . . 120

IV.97 A summary of the hypotheses and if they were supported, either fully, partially, or not at all. 120

IV.98 Summary of recommended models for tasks. . . . 125

LIST OF FIGURES

Figure		Page
III.1	A visualization of the sensing abilities of the metric model agent.	13
III.2	A visualization of the sensing abilities of the topological model agent.	14
III.3	A visualization of the sensing abilities of the visual model agent.	16
IV.1	Example start and end states for the Go To Location Task.	23
IV.2	Example start and end states for the Search Task.	24
IV.3	Example start and end states for the Monitor Task.	25
IV.4	Example start and end states for the Avoid Task.	25
IV.5	Example start and end states for the Follow Task.	26
IV.6	Example start and end states for the Disperse Task.	27
IV.7	Example start and end states for the Rally Task.	28
IV.8	Example start and end states for the Maintain Group / Flocking Task.	28
IV.9	The distributions for each model in the Go To Location task.	40
IV.10	The distributions of PercentReached by number of agents and model.	40
IV.11	The distributions of PercentReached by number of obstacles and model.	42
IV.12	The distributions of PercentReached by radius of repulsion and model.	42
IV.13	The distributions of PercentReached by radius of orientation and model.	43
IV.14	The distributions of PercentReached by radius of attraction and model.	44
IV.15	The distributions for each model in the Search task.	46
IV.16	The distributions of PercentFound by number of agents and model.	46
IV.17	The distributions of PercentFound by number of obstacles and model.	48
IV.18	The distributions of PercentFound by number of goals and model.	48
IV.19	The distributions of PercentFound by radius of repulsion and model.	50
IV.20	The distributions of PercentFound by radius of orientation and model.	51
IV.21	The distributions of PercentFound by radius of attraction and model.	53

IV.22 The distributions for each model in the Monitor task 53
IV.23 The distributions of PercentCoverage by number of agents and model. 55
IV.24 The distributions of PercentCoverage by number of obstacles and model. 57
IV.25 The distributions of PercentCoverage by radius of repulsion and model. 58
IV.26 The distributions of PercentCoverage by radius of orientation and model. 60
IV.27 The distributions of PercentCoverage by radius of attraction and model. 62
IV.28 The distributions for each model in the Avoid task. 62
IV.29 The distributions for each model in the Avoid task by number of agents. 64
IV.30 The distributions for each model in the Avoid task by radius of repulsion. 66
IV.31 The distributions of expanse by radius of orientation and model. 66
IV.32 The distributions of expanse by radius of attraction and model. 68
IV.33 The distributions of network efficiency for each model in the Follow task. 69
IV.34 The distributions of Network Efficiency by number of agents and model. 71
IV.35 The distributions of Network Efficiency by number of obstacles and model. 73
IV.36 The distributions of Network Efficiency by radius of repulsion and model. 74
IV.37 The distributions of Network Efficiency by radius of orientation and model. 76
IV.38 The distributions of Network Efficiency by radius of attraction and model. 78
IV.39 The distributions of percentage of agents within 30 degrees for each model in the Follow task. 79
IV.40 The distributions of percentage of agents within 30 degrees by number of agents and model. 81
IV.41 The distributions of percentage of agents within 30 degrees by number of obstacles and model. 82
IV.42 The distributions of percentage of agents within 30 degrees by radius of repulsion and model. 84
IV.43 The distributions of percentage of agents within 30 degrees by radius of orientation and model. 86
IV.44 The distributions of percentage of agents within 30 degrees by radius of attraction and model. 88
IV.45 The distributions for each model in the Disperse task. 88
IV.46 The distributions for each model in the Disperse task by number of agents. 90

IV.47 The distributions for each model in the Disperse task by number of obstacles. 91
IV.48 The distributions for each model in the Disperse task by radius of repulsion. 93
IV.49 The distributions for each model in the Disperse task by radius of orientation. 95
IV.50 The distributions for each model in the Disperse task by radius of attraction. 97
IV.51 The distributions for each model in the Rally task. 97
IV.52 The distributions for each model in the Rally task by number of agents. 99
IV.53 The distributions for each model in the Rally task by number of obstacles. 100
IV.54 The distributions for each model in the Rally task by radius of repulsion. 102
IV.55 The distributions for each model in the Rally task by radius of orientation. 103
IV.56 The distributions for each model in the Rally task by radius of attraction. 105
IV.57 The distributions of change in center of gravity for each model in the Flocking task. . . . 112
IV.58 The distributions of the change in center of gravity by number of agents and model. . . . 113
IV.59 The distributions of change in center of gravity by number of obstacles and model. 115
IV.60 The distributions of the change in center of gravity by radius of repulsion and model. . . . 116
IV.61 The distributions of the change in center of gravity by radius of orientation and model. . . 118
IV.62 The distributions of the change in center of gravity by radius of attraction and model. . . 119

CHAPTER I

Introduction

The natural emergence of swarm behaviors has long been one of the marvels of the natural world (Wilson, 1962; Aoki, 1982). Complex patterns that arise in biological swarms serve many purposes and allow the group to function more effectively as a whole. Many species have developed some form of swarm interaction, from flocks of birds (Ballerini et al., 2008) to schools of fish (Aoki, 1982; Huth and Wissel, 1992) or colonies of insects (Wilson, 1962; Hecker and Moses, 2015; Karaboga and Akay, 2009; Brito et al., 2012). Biological swarming tasks can consist of gathering food (Wilson, 1962; Hecker and Moses, 2015), constructing shelter (Brito et al., 2012), avoiding predators (Krause and Ruxton, 2002), and traveling long distances (Couzin, 2009). The astounding fact about the described swarms is that their capabilities do not require centralized control for the swarm, but result from the interactions of individual agents (Aoki, 1982; Reynolds, 1987; Couzin et al., 2002; Huth and Wissel, 1992). The capabilities of swarms have long been considered for use in artifical settings (Reynolds, 1987), but more recent results in swarm robotics are more practical and relevant (Dorigo et al., 2004; Beni, 2005; Murray et al., 2013; Hecker and Moses, 2015). Robots' increased capabilities and features, coupled with decreasing costs permits the use of many smaller, less intelligent robots, rather than relying on one robot with extensive capabilities (Seyfried et al., 2005; Cianci et al., 2007). Swarm robotics requires comprehensive algorithms capable of completing complex tasks using large numbers of robots. These requirements for a controller algorithm in swarm robotics can be solved by using biological models from the natural world. The research objective of this Thesis is to assess the performance of biologically inspired swarm communication models for use in swarm robotics tasks. Communication in this Thesis refers to a swarm member reacting to the presence of another member or environmental object in a well defined manner. This Thesis provides an analysis of several different biological swarm communications models to assess their ability to complete swarm robotics tasks and demonstrate that different models are significantly better at completing specific tasks.

There are many potential behavior models outlined in the swarms literature (Kolpas et al., 2013; Strandburg-Peshkin et al., 2013; Ballerini et al., 2008; Huth and Wissel, 1992; Hecker and Moses, 2015). However, this Thesis does not consider every model. While fluid dynamics or Voronoi graphs may be apt descriptors of the collective swarm's motions (Kolpas et al., 2013; Attanasi et al., 2013), these models do not sufficiently describe the actions taken by individual swarm members. Voronoi and fluid dynamics models address the swarm as a single entity, rather than as individual entities. Artificial implementations of a biological model, like the Boids model, can be too simplistic and do not consistently produce prototypical swarm behavior

(Reynolds, 1987). Other models require interaction with the environment or are focused on a specific tasks, as in the ant pheromone models used to gather food (Wilson, 1962).

The chosen communication models for this Thesis share a background in the biological world, and describe how agents move and react to the immediate environment. Each model sufficiently describes biological phenomena (Aoki, 1982; Ballerini et al., 2008; Strandburg-Peshkin et al., 2013) and can be extended to complete the robotics tasks studied in this Thesis. A consistent nomenclature must be established to define the communication models and the studied tasks. An object, for the purposes of this Thesis, is any concrete item or actor in the environment, while an agent reacts to objects in the environment. The foundational swarm communication model is the metric model (Aoki, 1982; Couzin et al., 2002), which operates under the assumption that an agent reacts to all objects within a given radius, with varying reactions depending on how far away a given object is located relative to the agent. The biological analysis of swarms demonstrated that the metric model is not always a highly accurate representation of starling swarm patterns (Ballerini et al., 2008). Based on the starling results, the topological model was proposed. The topological model is developed using the metric model rules, but posits that an agent only reacts to the closest n objects in the environment. This model's underlying assumption is that, in dense swarms, the agents are unable to track and respond to every other bird in the flock; thus, a constraint on the number of objects considered was added (Ballerini et al., 2008). The topological model ignores that the closest agents in a swarming environment may be occuluded, or not visible to the agent, which led to a model focused on the realities of biological visual systems (Strandburg-Peshkin et al., 2013). The visual communication model is also based on the metric model's interaction rules, but assumes that the agent interacts with the objects that are visible to the agent. An object is visible to an agent when a minimal portion of that object is within the agent's field of view.

The prior swarm robotics research has focused primarily on the application of ant-based models (Dorigo et al., 2004; Hecker and Moses, 2015) or specific models developed for unique properties of the robots (Murray et al., 2013). Some work has been done to simulate the topological model and associate the results with biological systems (Bode et al., 2011; Abaid and Porfiri, 2010), but only on a limited basis. Abaid's modeling was restricted to a one-dimensional ring around which the agents operated. Each of the three communication models considered in this Thesis have been shown to be plausible explanations for collective biological swarm behavior (Couzin et al., 2002; Ballerini et al., 2008; Strandburg-Peshkin et al., 2013).

The most common swarm activities can be reduced to combinations of several independent, simplistic, and in some cases, atomic tasks, which have been mapped to common robotic swarm tasks (Hayes, 2014). An analysis of these communication models for different robotic swarm tasks is required in order to understand under which circumstances particular communication models provide the most impact on the swarm's ability to complete particular tasks. The overall hypothesis for this Thesis is that different tasks require unique

swarm communication models for optimal completion of each task. Therefore, a simulation-based evaluation incorporating the three communication models assessed the models' relative performance on swarm robotics based tasks such as searching for goals, avoiding adversaries, flocking, and moving to a specified area.

Chapter 2 provides a review of the pertinent literature, and further explores the motivation for the considered communication models. Chapter 3 defines the various communication models examined in the experiments, along with the developed, implemented, and evaluated algorithms. Further, Chapter 3 describes the simulator developed as the experimental platform. Chapter 4 presents the experimental design, experimental results, and a discussion of the resulting implications. Chapter 5 presents the conclusions, contributions to the field, and future work.

CHAPTER II

Literature Review

Biological swarms present many promising concepts that can be applied to robotics, and serve as a motivation for this Thesis. A review of the relevant biological swarm models was completed and narrowed to three primary models. A general outline of the considered models is provided, along with the relevance of the chosen models.

II.1 Biological Models

Biological swarms have repeatedly been shown to be the result of simple interactions between swarm members (Aoki, 1982; Reynolds, 1987; Huth and Wissel, 1992). The simple interactions that define the biological world lead to layers of complexity and completion of tasks that no single individual is able to handle. The swarming patterns of bees allow for the construction of complex hives (Brito et al., 2012). Fish use swarm behaviors to avoid predators and travel vast distances under the sea (Huth and Wissel, 1992; Makris et al., 2009). Foraging for food drives the use of swarming behavior in ants (Wilson, 1962; Hecker and Moses, 2015). Birds demonstrate flocking patterns for a variety of tasks, from migration to foraging for food (Ballerini et al., 2008). One point remains consistent across these biological examples; swarming behavior allows for the execution of more complex actions than is otherwise possible with an individual entity.

Observations and simulations over the years have allowed for the development and refinement of biological models. The vast majority of the research has focused on fish (Aoki, 1982; Huth and Wissel, 1992). Information from the oceans, lakes, and rivers (Huth and Wissel, 1992; Makris et al., 2009) in conjunction with simulation of proposed swarming models (Aoki, 1982) has demonstrated that simple interaction models can accurately describe biological swarming actions. Insects - in particular ants and bees - represent another common class of biological swarm literature (Karaboga and Akay, 2009; Wilson, 1962). The ant's foraging abilities has been of particular interest (Wilson, 1962), specifically their use of pheromones. Modeling of the interactions of ants in the presence of pheromones has proven particularly fruitful in understanding the patterns of movement in ants. The more recent research has also focused on birds, more specifically starlings. High resolution stereophotography allows for reconstruction of the three-dimensional swarming patterns (Ballerini et al., 2008), which has motivated the further analysis of the specific patterns involved with swarming behavior (Attanasi et al., 2013).

II.2 Motivation for Application of Biological Models

Biological swarms demonstrate a cohesiveness and unity, even when faced with threats and obstacles, which makes the swarm robust to the loss of swarm entities without negatively impacting the overall task performance (Ballerini et al., 2008). It has been found that hungrier swarm members form an ad-hoc leadership sub-group that better guides the swarm towards a food source, when those entities have knowledge of the food source (Krause et al., 2000). This emergent leadership allows the swarm to perform efficient decision-making (Couzin et al., 2005) and act with more coordination. Thus, these biologically inspired models have been shown to perform a required search behavior, with high efficacy. Biological swarm behavior is also well suited to handle for predator/prey situations. Work by Olson, Knoester, and Adami (2013) shows that swarming behavior likely arose in the biological world as a result of interactions with predators. As a result of evolution, the swarming behavior will be highly effective in avoiding obstacles or predators (Olson et al., 2013). The biological predator and obstacle avoidance behaviors are key to several of the robotic swarm tasks.

Another primary advantage of biological swarms is their ability to transfer information quickly across the swarm. Handegard, Boswell, Iannou, Leblanc, Tjøstheim, and Couzin (2012) showed that information about predators quickly travels through the swarm of biological prey. This information transfer property can allow swarm members to react to potential threats before the predators come into the individual swarm member's sensory range (Handegard et al., 2012). This information transfer has been shown to be effective, regardless of the scale of the group (Cavagna et al., 2010). Additionally, the information spread correlates linearly with the swarm's size (Cavagna et al., 2010), and can even bypass parts of the swarm to inform the whole group (Cavagna et al., 2013). The scalability and effectiveness of information transfer is promising, because as swarm robots become a reality, the communication between swarm members must increase with the group size (Seyfried et al., 2005; Cianci et al., 2007). Quick information transfer allows for increased decision-making capabilities at a low cost in starling flocks (Young et al., 2013), which are the basis for the topological communication model (Ballerini et al., 2008). Biological swarms allow for the emergence of leadership, efficient communication, avoidance of obstacles or predators, and concise decision making, which are ideal properties for robotic swarm intelligence.

II.3 Artifical Swarms

Prior work in artificial swarm intelligence confirms the efficacy of biological models. Reynolds was one of the first to verify that the simple artifical models were able to lead to emergent swarming behaviors (Reynolds, 1987). A significant amount of the research thus far has been simulation based (Couzin et al., 2002; Aoki, 1982; Huth and Wissel, 1992), as the capabilities of the existing swarm robots have been mostly limited

to only basic functionalities (Dorigo et al., 2004). The models for artificial swarms fall into two primary categories, biologically inspired or artificially generated. The most prominent biologically inspired artificial swarms are based on insectiod movement patterns and capabilities. Ants and their pheromone trails have been simulated both for use in robotics (Fujisawa et al., 2014; Hecker and Moses, 2015), and also in the pursuit of pathfinding or clustering algorithms (Shen and Jaikaeo, 2005; Handl and Meyer, 2007). Hecker and Moses (2015) have created actual robotic swarms using ants as inspiration. The pheromones associated with the ant models have been both virtually (Handl and Meyer, 2007; Hecker and Moses, 2015) and chemically (Fujisawa et al., 2014) generated for different purposes. For example, a routing algorithm was implemented that leaves a virtual breadcrumb trail of pheromones, using the ants' foraging algorithm to find the best path (Hecker and Moses, 2015). These biologically inspired algorithms establish the efficacy of using biological models to complete robotics tasks.

The artifically generated models focus on the robotic capabilities in the swarm. The e-puck robots have specific capabilities (e.g., sensors and actuators) that allow them to self-assemble and configure into different shapes (Murray et al., 2013). A second model, incorporating the boids model, has been used to stabilize unmanned aerial vehicles (Saska et al., 2014) without additional equipment. Swarm models, however, do not need to be specifically developed for a particular platform. Brutschy et. al. developed a method to integrate general swarm models into artifical swarm agents. The system requires an abstraction layer that provides the model with relevant input (Brutschy et al., 2015). The implication is that the models and algorithms based on biological swarms can be useful for developing robotic swarms for use in a variety of tasks.

II.4 Choice of Models

The chosen biological models were selected to facilitate illustration of how small differences between similar models can lead to varied outcomes. Each model demonstrates a biologically verified model for swarm behavior (Couzin et al., 2002; Ballerini et al., 2008; Strandburg-Peshkin et al., 2013). The models define the communications between individual swarm members, but do not require excessive computation or hardware requirements to the swarm robots or an associated simulator. The numerous models not selected for this Thesis failed to fufill these requirements for the models: the model consistently demonstrates swarming patterns and behaviors, provides a specific controller for individual agents, implements a biologically inspired swarm communications model, uses only position and heading information from neighboring agents, and does not require excessive or unusual computational or hardware capabilities.

II.5 Alternate Models

A number of models exist that are not considered for this Thesis. Some models focused on the group properties and were not specific with regards to individual agents, modelling interactions that are not realistic in robotic applications because they do not provide a clear controller for individual swarm members (Kolpas et al., 2013; Nunnally et al., 2012). An interesting model of starling flocks relies on theories related to super fluids, normal liquids transformed under extreme pressure or temperature changes, was shown to explain the rapid information transfer across the swarm (Attanasi et al., 2013). However, this model focuses on the propagation of information across the swarm without regard for the movement of individual swarm members. The fluid dynamics model is unsuitable for this Thesis because it does not provide an algorithm to determine individual behavior.

Voronoi diagrams, as generated from a Delaunay triangulation process, represent another alternative model of swarm dynamics (Du et al., 1999). This model has a comparable descriptive ability to the topological model (Kolpas et al., 2013), but is not entirely feasible with swarms of robots due to its reliance on the relative positioning of individuals. The relative positions of the swarm members may not be known by an individual agent, due to environmental or sensor inaccuracies (Nunnally et al., 2012). The Voronoi model requires relative positions to compute the Delaunay triangulation, and does not always have the information required to do so in robotic swarms. Koilpas et. al. (2013) compared the capabilities of the Voronoi model and the topological model in simulating a swarm and found both models to have comparative descriptive abilities. Thus, the Voronoi model is less realistic and extraneous, and was not considered for the purpose of this Thesis. Additional results by Cavagna et al. (2013) and Bialek et al. (2012) provide the statistical probabilities of where birds will be positioned in a flock, whether the bird will lead the flock or follow along the back edge; and which other individuals will be their neighbors. Both an analysis of change in neighbors over time (Cavagna et al., 2013) and an entropic model of the entire flock (Bialek et al., 2012) do not address the movements of the specific swarm members, but rather properties of the entire swarm. Although the entropic model of the entire swarm is an interesting concept, this theory does not describe the swarm member's specific actions or reactions, and is thus unsuitable for the research focus of this Thesis.

Ant models focus on using pheromones, either as virtual tokens (Hecker and Moses, 2015) or as actual chemical scents (Fujisawa et al., 2014), to set markers within the environment. Actual scents may not be effectively monitored by robots in outdoor environments, and the swarm may not have consistent communication necessary to use artificial pheromones (Nunnally et al., 2012). Bees use dancing and other movements as a form of communication to pass along information to the swarm (Dornhaus and Chittka, 1999; Karaboga and Akay, 2009). The models of bees and ants require the use of communication techniques or capabilities

that may not be readily available for artificial agents and are thus unsuitable for this Thesis. On the other hand, the Boid model operates at too simple a level, using the rules of repulsion, orientation, and attraction on all objects neighboring the agent (Reynolds, 1987). Flocking under this model can become confused with a disturbance to the environment or environmental properties. The algorithm, which can be quite effective in demonstrating some swarm capabilities, does not fit the criteria defined for the chosen models. The full list of alternate models and the reasons the models were disqualified is contained in Table II.1.

Model	**Source**	**Reason Eliminated**
Voronoi	Du et al., 1999	Inaccuracy Concerns
Entropic Model	Bialek et al., 2012	Does not predict individual behavior
Neighbor Analysis	Cavagna et al., 2013	Does not predict individual behavior
Fluid Dynamics	Attanasi et al., 2013	Does not predict individual behavior
Boids	Reynolds, 1987	Too Simple
Ants	Fujisawa et al., 2014; Hecker and Moses, 2015	Pheremones
Bees	Karaboga and Akay, 2009	Complex Communicaitons

Table II.1: Summary of alternate models and why they were eliminated.

II.6 Primary Models

Historically, the most prominent biological swarm communication model is the metric model. The metric model, originally discovered in fish (Aoki, 1982), incorporates several different zones, defined by relative radii, where an agent reacts differently to other objects in different zones. The three zones include a zone of repulsion, where the agent moves away from the objects within, a zone of orientation, where the agent orients its heading to the objects within the zone, and a zone of attraction, where the agent moves towards the objects within the zone. This model is simplistic and effective in describing different swarm behavior states and the associated transitions between these states (Couzin et al., 2002). This model serves as the foundation for two biologically-based communication models that have been shown to better represent biological swarm communications (Ballerini et al., 2008; Strandburg-Peshkin et al., 2013) and are considered in this Thesis, the topological and visual models.

The topological model incorporates principles similar to the metric models, with one decisive difference. The primary feature of the topological model is that the agent interacts with a fixed number of nearest neighbors, instead of all those within a radius, as the metric model does. The topological model was originally verified by analyzing migrating flocks of birds, comparing the actual bird's movements to those predicted by the model (Ballerini et al., 2008). Further work has modeled the swarms and compared the results to data from the biological bird flocks to verify the model's accuracy (Bode et al., 2011). A simplistic, one-dimensional topological model verified that the model accurately describes schools of fish (Abaid and Porfiri, 2010).

The most intuitive and biologically compelling communication model is the visual communication model (Strandburg-Peshkin et al., 2013), in which the agent only communicates with the adjacent swarm members that are visible (e.g., within the field of view) to the current agent. This model requires ranges of repulsion, attraction, and orientation, but a different group of agents is visible to the agent compared to those that are within the metric model's radius. The ability of the agents to see an object is generally thought to have an upper limit, denoted as the visual range in this Thesis. The model was originally compared both to the performance of other models and that of fish schools to verify its predictive abilities (Strandburg-Peshkin et al., 2013).

While having different properties, some similarities exist in how the agents interact in the swarm, given that all three follow the metric model's concepts of repulsion, orientation, and attraction. The visual model performs closely to the metric model when the visual range is equal to or not much larger than the metric model and when not many objects are occluded in the visual field (e.g., in a sparse or lowly populated environment), as the objects that both models interact with are similar. The topological model performs like the metric model when the topological number is high and the metric model has a small outer radius, because the groups of agents that the models interact with are similar. Chapter III formally defines algorithms for the three models.

CHAPTER III

Algorithms

Three robotic swarm communication algorithms have been derived based on the biological literature. The metric, topological, and visual algorithms have been designed to follow the biological definitions as closely as possible.

III.1 Definitions

An object in the context of this Thesis is defined as any concrete item in the environment. An object can represent an agent, an obstacle, an objective, a target, or an adversary. An agent (i.e., an individual) is a swarm member that reacts and responds to other objects in the environment. An obstacle exists in the environment and is to be avoided; an analogue in the real world is a rock or a wall that the agent must avoid. An objective is an object or area that the agents must find in the environment and approach or access directly, like a victim in a search and rescue scenario, or a rendezvous point. A target is something (e.g. a person, a vehicle) that must be pursued, but not necessarily reached, with the implication that the target may move on its own. An adversary is something that can harm the swarm, a predator in the natural world, that the agents must avoid.

There are three central swarm communication models used in the context of this Thesis. The metric model defines that each agent reacts to other agents depending on whether or not they are in one of several different zones. The three zones are the zone of repulsion, wherein an agent reacts by moving in the opposite direction of the agent in that zone; the zone of orientation, wherein the agent attempts to orient with the agents in that zone; and the zone of attraction, where agents move towards the other agents in that region. The three zones are generally concentric circles, designated by their radii, with repulsion being the interior zone, orientation the middle zone, and attraction the exterior zone. Repulsion takes precedence over the other two zones in order to prevent collisions. All agents within any of the three zones are considered for interaction with the agent being modeled (Couzin et al., 2002). The topological model uses the same zones and preferences as the metric model, but only considers the closest n agents, where n usually takes a value of 6 or 7 (Ballerini et al., 2008). The visual model uses the same zones, but considers only those agents that are visible to the original agent, or within the agent's field of view (Strandburg-Peshkin et al., 2013). The three zones are denoted in the algorithms by the radii that define them, namely the radius of repulsion (denoted *RadRepulsion*) for the zone of repulsion, the radius of orientation (denoted *RadOrientation*) for the zone of orientation, and the radius of attraction (denoted *RadAttraction*) for the zone of attraction.

Algorithm 1 The GetNewDirection algorithm, which determines how agents respond to other objects.

GetNewDirection[Agent a, Objects o_i]

```
1: Create vectors newDir, PositionComponent, DirectionComponent
2: for all o_i do
3:    if o_i is an Objective AND distance(a, o_i) <Rad Orientation  then
4:       mark o_i as found
5:    end if
6: end for
7: if distance(a, o_1) <Rad Repulsion then
8:    while distance(a, o_1) <Rad Repulsion do
9:       if o_1 is an Obstacle or an Adversary then
10:         PositionComponent = PositionComponent - (o_1.position - a.position).normalize * 30 / distance(a,
            o_1)
11:      else if o_1 is an Objective then
12:         Do Nothing
13:      else
14:         PositionComponent = PositionComponent - (o_1.position - a.position).normalize
15:      end if
16:      Remove o_1 from front of Objects
17:   end while
18:   newDir = temp1
19: else
20:   for all o_i do
21:      if o_i is an Obstacle or an Adversary then
22:         vector PositonDiff = o_1.position - a.position
23:         PositionComponent = PositionComponent - PositonDiff.normalize * 30 / distance ( a, o_i )
24:      else if o_i is an Objective then
25:         if o_i has not been found then
26:            PositionComponent = PositionComponent + (o_i.position - a.position).normalize * 20 / sqrt (
               distance ( a, o_i ) )
27:         end if
28:      else if o_i is an Agent or a Target then
29:         if distance(a, o_i) <Rad Orientation then
30:            PositionComponent = PositionComponent + o_i.direction
31:         else
32:            DirectionComponent = DirectionComponent + (o_i.position - a.position).normalize
33:         end if
34:      end if
35:   end for
36:   if PositionComponent exists and DirectionComponent exists then
37:      newDir = (PositionComponent + DirectionComponent)/2
38:   else if PositionComponent.exists then
39:      newDir = PositionComponent
40:   else if DirectionComponent.exists then
41:      newDir = DirectionComponent
42:   end if
43: end if
44: return newDir
```

These definitions only apply to the agent-to-agent communications, while the interactions between agents and the other objects in the environment must also be defined. Obstacles and adversaries always have a repulsive effect, with the repulsive force based on an inverse power law with regard to distance from the object. An objective follows the same inverse power law as an obstacle, but with an attractive force, rather than a repulsive force. A target is treated in the same manner as another agent, as it must be tracked, but not necessarily approached. The agent's reactions to objects in the environment and the resulting effect on the agent's new direction are outlined in Algorithm 1. Lines 9, 10, 22, and 23 describe the repulsive force of adversaries, as a vector directing the agent away from the repulsive objects is added to the new direction. Lines 14, 30, and 32, respectively describe the repulsive, orientative, and attractive forces caused by other agents. These repulsive, orientative, and attractive forces are effected by adding vectors corresponding to a direction away from the agent in the repulsive zone, the heading of the agent in the orientative zone, and the direction towards the agents in the attractive zone, respectively, to the new direction object. Line 26 describes the attractive force of goals while line 4 describes the discovery of goals. When a goal is considered discovered, it is marked as found by the algorithm. The attractive force is effected by adding a vector in the direction from the agent to the goal to the agent's new direction. This algorithm requires a list of relevant objects and determines a new heading for the agent based on the defined rules. All objects have a position, which describes their position (x_p,y_p), and a direction vector (θ,r) that indicates their heading and magnitude, respectively.

III.2 Metric Model

The metric model agents respond to all objects within the radius of attraction, with the responses as defined in Algorithm 1 (Couzin et al., 2002). The metric model algorithm is provided in Algorithm 2. The agent in this algorithm observes the positions and directions of other objects within the agent's radius of orientation. The radius of attraction is the maximum distance that an object can be from the agent and still interact with the agent. When all objects within the radius of attraction are determined, lines 3 through 5 in Algorithm 2, the metric model algorithm executes Algorithm 1's interaction rules with the current agent and the associated agents within the radius of attraction, and sets the resulting direction as the new direction for the agent, line 7 of Algorithm 2. An example of the range of sensing for an agent using the metric model is depicted in Figure III.1. The shaded area emitting from the agent represents the agent's blind spot, the center solid circle represents the metric model agent, the squares represent objects within the agent's communication range, and the triangles represent objects outside of the agent's radius of repulsion with which the agent is unable to communicate. The dotted circle represents the radius of repulsion, the dashed circle represents the radius of orientation, and the solid circle represents the radius of attraction.

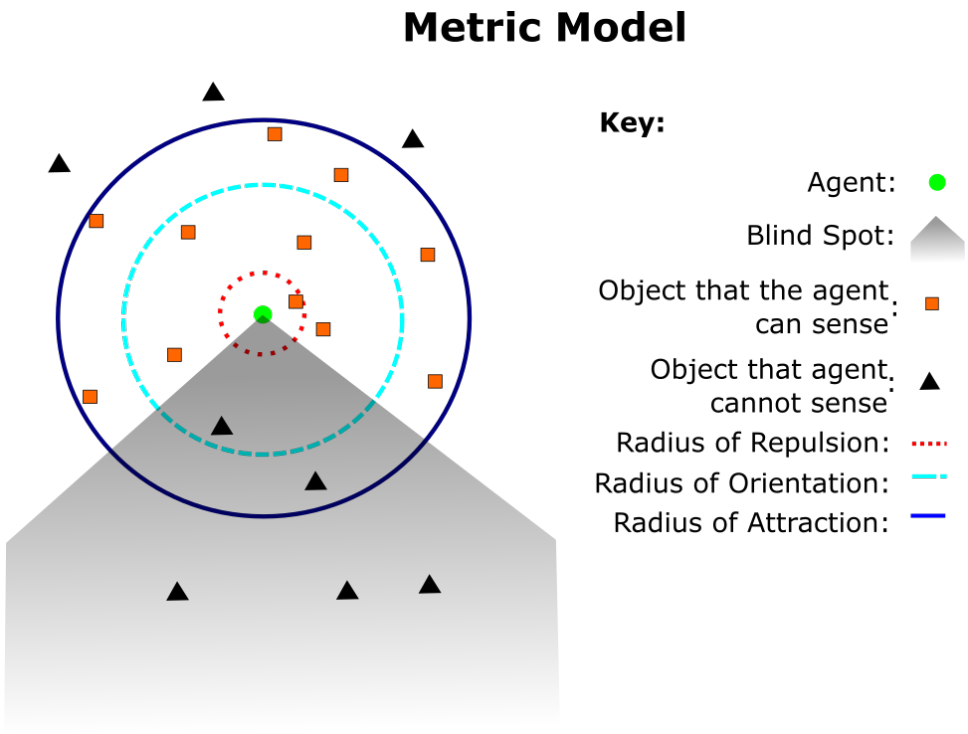

Figure III.1: A visualization of the sensing abilities of the metric model agent.

Algorithm 2 The Metric Model algorithm.

MetricModel[Agent a, Objects o_i]

1: Create a priority queue *withinRange* of objects ordered by distance
2: **for** all o_i **do**
3: **if** distance(a, o_i) <RadAttraction **then**
4: add o_i to *withinRange* with associated distance
5: **end if**
6: **end for**
7: a.direction = **GetNewDirection**[a, *withinRange*]

III.3 Topological Model

The topological model considers the closest c objects, independent of if they are goals, agents, or obstacles. An agent's response to each type of object is the same as the metric model (Ballerini et al., 2008). The topological model is defined in Algorithm 3. The agent finds the closest c objects, lines 1 through 5, by adding objects and their distances to a priority queue sorted by lowest distance to the current agent. The closest c objects are identified from this ordering, lines 7 and 8, so that the agent can interact with the objects. The agent then applies the interaction rules, as defined in Algorithm 1, and sets the resulting direction as the

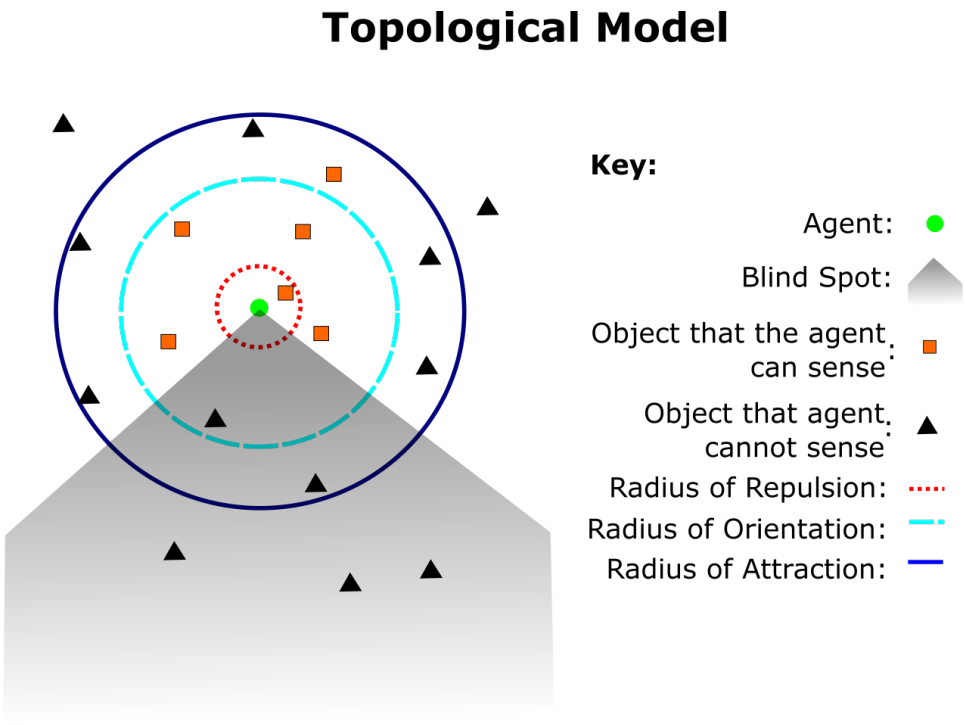

Figure III.2: A visualization of the sensing abilities of the topological model agent.

new direction for the agent in line 9. An example of the range of sensing for an agent using the topological model (with $c = 6$) is provided in Figure III.2. The squares represent the six closest objects closest to the agent. Note the difference from the metric model, which senses all objects within the radius of attraction.

Algorithm 3 The Topological Model algorithm.

TopologicalModel[Agent a, Objects o_i]

1: Create a priority queue $allObjects$ of objects ordered by distance
2: **for** all o_i **do**
3: add o_i to $allObjects$ with associated distance
4: **end for**
5: Create a list of objects of size n named $closestObjects$
6: Add the first c objects from $allObjects$ to $closestObjects$
7: a.direction = **GetNewDirection**[a, $closestObjects$]

III.4 Visual Model

The visual model is also a similar modification of the metric model, as all objects that are visible to the agent generate a response from the agent. An object is visible to an agent if the object occupies at least a minimum portion of the agent's field of view. Again, the responses to each object type are identical to the responses

described for the metric model (Strandburg-Peshkin et al., 2013). Algorithm 4 provides the primary visual communication model, which also requires a visibility algorithm (Algorithm 5). The portion of the visual algorithm in Algorithm 4 performs the same function as those in Algorithms 2 and 3; it observes objects in the environment, and identifies those that are visible to the agent by applying Algorithm 5 in line 12. When all visible agents are determined, the same interaction rules are applied by invoking Algorithm 1, and then a new direction is provided.

The visibility algorithm (Algorithm 5) considers an object and a list of objects closer to the agent than the object that is being considered. The algorithm then verifies if the agent can see the object by checking that the object in question is not behind any of the objects in the list of closer objects. If there is a portion of the agent's field of view, above a defined threshold, that the object occupies, then the object is considered to be within the agent's field of view, and the algorithm returns true. If there are no objects between the object being considered and the agent, then the object is clearly visible, and the algorithm returns true. The threshold of the visibility algorithm is defined as the portion of the visual field that an object occupies when it is positioned at the visual range of the agent. The visual model's behavior differs from the topological model, which considers only the closest n objects, and the metric model, which considers all agents, regardless of visibility, within a certain range. Figure III.3 illustrates the objects that a visual algorithm agent is able to sense. The squares are those objects that the circle visual agent is able to sense; while the objects within the visual model's agent's field of view fall within the outer circle. Note that even though an object is within the field of view, some objects are occluded and are not visible to the agent.

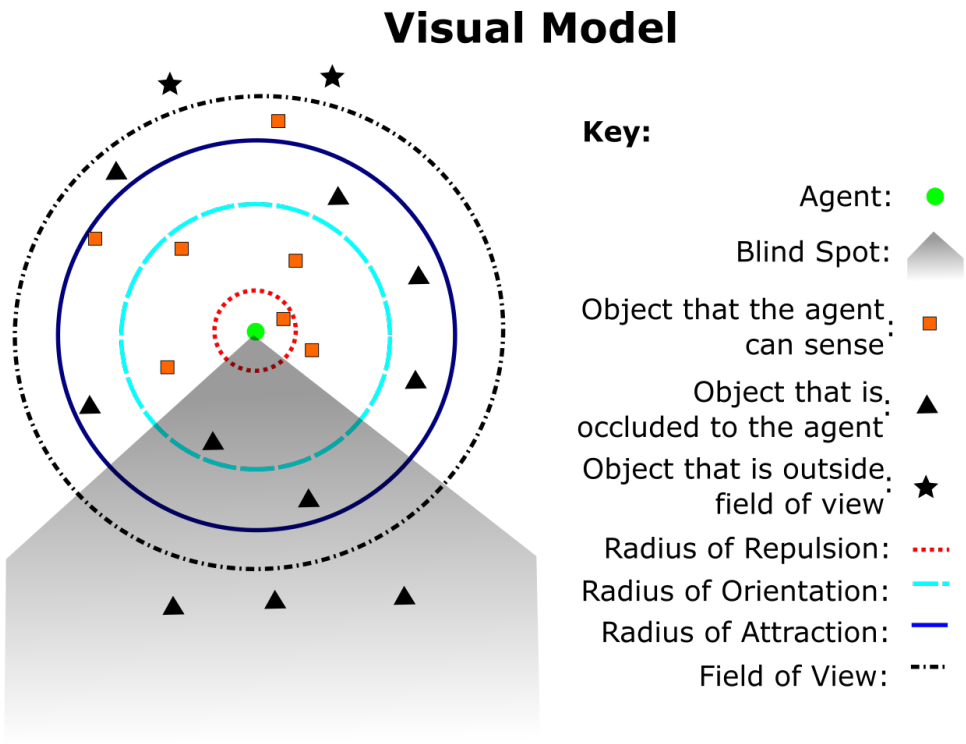

Figure III.3: A visualization of the sensing abilities of the visual model agent.

Algorithm 4 The Visual Model algorithm.

VisualModel[Agent a, Objects o_i]

Create a priority queue *withinRange* of objects ordered by distance
for all o_i **do**
  if distance(a, o_i) <VisualRange **then**
    add o_i to *withinRange* with associated distance
  end if
end for
Create a list *visibleObjects*
Add closest object from *withinRange* to *visibleObjects*
Remove closest object from *withinRange*
for all o_j in *withinRange* **do**
  if isVisible[a, o_j, *visibleObjects*] **then**
    Add o_j to *visibleObjects*
  end if
end for
a.direction = **GetNewDirection**[a, *visibleObjects*]

Algorithm 5 The visibility algorithm. Returns whether o_j is occluded by o_i from the viewpoint of a.

isVisible[Agent a, Object o_j, Objects o_i]

Calculate the arc a_j in a's visual field that o_j comprises
for All o_i **do**
    Calculate the arc a_i in a's visual field that o_i comprises
    if a_i covers some part of a_j **then**
        Remove the overlap area from a_j
    end if
end for
if the arc a_j has a value greater than the threshold **then**
    return true
else
    return false
end if

III.5 Simulator Design

The simulator consists of four main components; the application, the simulator, the objects, and the controllers. The application component handles all file input and output, and defines the necessary variables and records the results. The file input includes reading in the objects, environmental constraints, and agent parameters. There is a set of two JSON documents that define the input. The configuration file contains the information regarding the agent's communication model, specifically the model type and the different radii or other parameters. The object file contains the locations and original directions of the objects within the simulation, as well as any other environmental constraints. The file output is concerned primarily with writing the results to a specific file in Comma Separated Value (CSV) format. The objects consist of the agents, objectives, adversaries, and obstacles. Each of the objects maintains an internal state representing their position, direction, and other internal properties. The simulator manages the environment, which is the rectangular area within which the agents operate and objects are contained. The environment also contains states associated with the objects (e.g., the state of a goal is whether or not it has been discovered). The simulator calls the functions that update each of the objects over a timestep. The object's position is updated by moving the object along the given heading θ for a distance specified by the magnitude r. The final component is the controller, which is contained inside each object. The controller regulates the object's movement, providing the object's direction and magnitude value either by applying the respective communication mode algorithm for the agents or by providing a constant direction and magnitude for the other types of objects.

The simulator is written in C++ with the use of the Qt framework. The individual trials of the experiment are run from the command line. A batch file calls the program with the corresponding object and configuration files as arguments. There is an option to use a graphic user interface to view the swarm in motion if necessary.

CHAPTER IV

Experiment

The experimental design contains the definitions of the tasks, the hypotheses for each experimental task, and the metrics associated with each experimental tasks. The results, including descriptive statistics and a formal statistical analysis, are presented. The discussion frames the importance of the results.

A task is an action or series of actions that the swarm must complete. A trial is a run of a specific task with a given set of parameters and objects, while an experiment is a collection of trials over all the valid parameters designed to evaluate a specific research hypotheses.

IV.1 Experimental Design

IV.1.1 Variables

The independent variables for each trial are the task being assessed in the trial, and the communication model that the swarm uses to interact: metric, topological, or visual. The dependent variable for each trial is the metric or metrics used to evaluate the swarm's ability to complete the task.

IV.1.2 Parameters

There are four parameters common to all algorithms, while two additional parameters apply to specific algorithms. There are three parameter classifications: those that are related to agents, those that relate to the environment in which the swarm is operating, and those specific to the tasks.

IV.1.2.1 Agent Parameters

The *number of agents* in the swarm was 50, 100, 250, 500, and 1000. These values represent a broad range of swarm sizes and ensure that the models generalize to different sizes.

The *radius of repulsion*, as defined for the communication model (Chapter III), represents the area in which an agent reacts by moving in the opposite direction of an object within that radius. The radius of repulsion values were set to 5, 25, 50, and 100 units. Units are an abstract measurement defined for the simulator and are intended to be on the same scale as one-tenth of a meter. The *radius of orientation* is the radius within which the agent attempts to orient with agents in that zone. The radius of orientation values were set to 20, 40, 75, 150, 200, and 300 units. The constraint for the radius of orientation is that the value must be strictly greater than the radius of repulsion for a particular trial. The *radius of attraction* is the radius within which an agent will attempt to move toward objects in that region. The radius of attraction had the

values of 25, 35, 80, 200, 400, and 600 units. The constraint for the radius of attraction is that each value must be strictly greater than the value of the radius of orientation for a particular trial. The values for these three radii were chosen to evaluate a variety of relative distances and ratios. The combination of 5-10-15 is a smaller relative distance as compared to 100-300-600. The radii of 5-10-15 as compared to 5-10-50, is an example of different ratios among the radii, as the ratio of the radius of attraction to the radius of repulsion in the first grouping is much lower than in the second grouping. These different relative distances and ratios caused the swarm to exhibit different types of behavior (Couzin et al., 2002).

Trials involving the topological model require an additional parameter, the *number of closest agents, c*, which was set to 6, 7, 8, and 10. These values were chosen to fall around the ideal values for *c* (i.e., 6 or 7), as defined in literature (Ballerini et al., 2008), while still providing some variability.

Trials involving the visual model agents require the *maximum visual range, maxVisRange* of the agent as a parameter. The associated variable values are constrained for each trial to equal the radius of attraction, double the trial's radius of attraction, or equal the maximum diagonal length of the trial environment. These values permit demonstration of the effect that different field of view ranges have on the model. Swarms may be able to see more or less distance dependent on environmental conditions; thus, the model must compensate for the ability to sense objects at different distances if the objects are not occluded.

Each agent has a *heading* and a *position* randomly assigned within a set area, where the area is proportional to the swarm size. The heading was either completely random or constrained within a certain range around a specific heading.

IV.1.2.2 Environment Parameters

The environment was represented as a rectangle proportional to the swarm size. That is, a larger swarm size required a larger environment in which to operate. The *x*-axis was the longer of the two sides of the rectangle, and the *y*-axis the shorter. Each environment had a corner at (0, 0) and a corner at ($2d$, d) in a unit coordinate plane, with d being the length of the shorter side of the rectangle. Swarms with 50 or 100 agents operated in the smallest sized environment, with dimensions of 1000 units by 2000 units. Swarms of 250 or 500 agents operated in a middle sized environment, with dimensions of 2000 units by 4000 units. Swarms of 1000 agents operated in the largest environment,k with dimensions of 4000 units by 8000 units. The environment sizes were chosen to ensure that the available area was roughly proportional to the swarm's size. A larger swarm size (e.g., size 1000) in a small environment (e.g., 1000 units by 2000 units) will not be effective, since a large majority of agents will always have other objects within the radius of repulsion. Thus, the dominant agent behavior will be avoiding other objects. Similarly, the small swarm (50 agents) within a large environment (2000 units by 4000 units) is ineffective. The swarm will be dispersed over too large of an area; thus, the

agents will be unable to interact with one another.

Obstacles were randomly placed throughout the environment. The *number of obstacles* present was set to 0, 25, 50, 100, or 250 obstacles. The number of obstacles was constrained based on the environment size; thus, for the smallest environment, the maximum number of obstacles was 50. The maximum number of obstacles allowed for the middle sized environment was 100. These number of obstacles were chosen to ensure that the presence of obstacles does not significantly hinder the swarm's communication. It is important for swarms to operate efficiently in noisy environments (i.e., one that contains obstacles and other objects).

IV.1.2.3 Task Parameters

Eight tasks were evaluated for each algorithm. The only task requiring a specific task parameter is the Search task, which requires the *number of targets* in the environment. The number of targets was 5, 10, 25, or 50. These values were chosen to ensure that the swarms can find both smaller and larger numbers of targets. The avoid task was constrained to only have a single adversary in the environment, and thus did not require variation in the *number of obstacles* parameter. The variation in parameters, as defined in Chapter IV.1.2, for specific tasks are delineated in Tables IV.1 and IV.2. A single trial was run for each combination of the potential values for each parameter and variable for a given task.

Task	**Model**	**numAgent**	**numObst**	**numGoal**	**RadRep**
Go To Location	Metric	•	•		•
	Topological	•	•		•
	Visual	•	•		•
Search	Metric	•	•	•	•
	Topological	•	•	•	•
	Visual	•	•	•	•
Monitor	Metric	•	•		•
	Topological	•	•		•
	Visual	•	•		•
Avoid	Metric	•			•
	Topological	•			•
	Visual	•			•
Follow	Metric	•	•		•
	Topological	•	•		•
	Visual	•	•		•
Disperse	Metric	•	•		•
	Topological	•	•		•
	Visual	•	•		•
Rally	Metric	•	•		•
	Topological	•	•		•
	Visual	•	•		•
Maintain Group / Flocking	Metric	•	•		•
	Topological	•	•		•
	Visual	•	•		•

Table IV.1: The summary of the parameters for each task, Part 1.

Task	Model	RadOrient	RadAttr	topological c	Visual Range
Go To Location	Metric	•	•		
	Topological	•	•	•	
	Visual	•	•		•
Search	Metric	•	•		
	Topological	•	•	•	
	Visual	•	•		•
Monitor	Metric	•	•		
	Topologica	•	•	•	
	Visual	•	•		•
Avoid	Metric	•	•		
	Topological	•	•	•	
	Visual	•	•		
Follow	Metric	•	•		•
	Topological	•	•	•	
	Visual	•	•		
Disperse	Metric	•	•		
	Topological	•	•	•	
	Visual	•	•		•
Rally	Metric	•	•		
	Topological	•	•	•	
	Visual	•	•		•
Maintain Group / Flocking	Metric	•	•		
	Topological	•	•	•	
	Visual	•	•		•

Table IV.2: Continued, the summary of the parameters for each task, Part 2.

IV.1.3 Tasks

Eight tasks were evaluated. These tasks represent real robot swarm tasks derived from biological swarm tasks. The tasks also provide a broad representation of swarm capabilities and are comprehensive.

IV.1.3.1 Go to Location

The Go to Location task requires an area to be defined to which all agents attempt to move towards. A point was randomly generated in the environment, with the point's x location value being greater than $3d/2$. The target area was defined as the circle with radius equalling $1.25 * \sqrt{numAgents * RadRep^2}$, with the center at a randomly generated point. This radius defined an area large enough for the entire swarm to reach without overcrowding and experiencing excessive repulsion effects. The swarm's members were assigned independent start locations in which the x value for each agent was less than d. The swarm moved throughout the environment for 90 timesteps, at which point the percentage of swarm members that reached the goal area was recorded. Example Go To Location task start and end states are presented in Figure IV.1. The triangles represent obstacles randomly placed within the environment. The circles represent agents, and the dashed circle represents the area that the agents must reach. The obstacles are distributed randomly throughout the

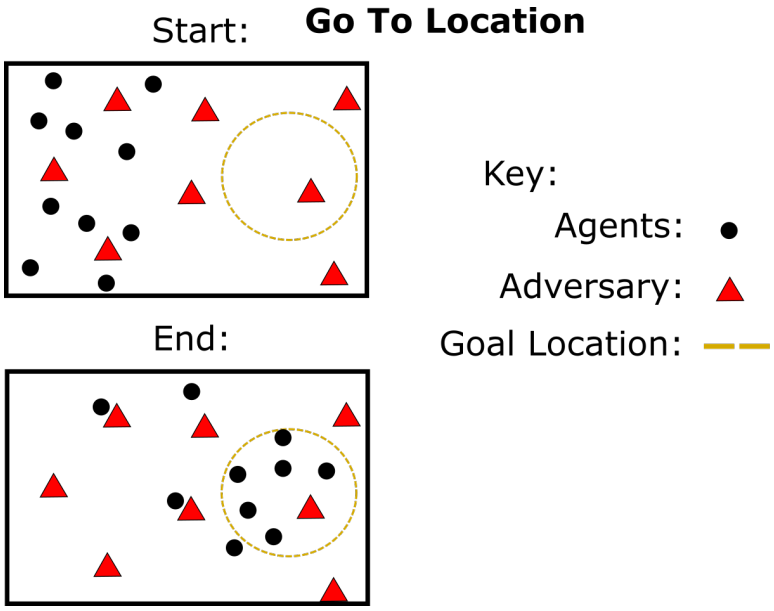

Figure IV.1: Example start and end states for the Go To Location Task.

environment at the beginning of the trial and the agents are distributed in the left half of the environment. The goal circle is designated in the right half of the environment. A number of agents have reached the goal area at the end of the trial. Some agents did not reach the goal area, either because the group was not cohesive or because an obstacle impeded movement to the goal area.

IV.1.3.2 Search / Monitor

The Search task required the agents to discover a number of goal objects distributed throughout the environment. The Search task began with target objects placed randomly throughout the environment. The swarm agents were also placed randomly in the environment, and moved throughout the environment for 90 timesteps. When each target was discovered by an agent, the target was marked as found. At the end of the trial, the number of discovered targets was recorded. A demonstration of a potential start and end states for the Search task are presented in Figure IV.2. The triangles represent obstacles within the environment, and the circles represent agents. The pentagons are goals that have not been discovered, and the stars are goals that the agents have found. The obstacles, agents, and undiscovered goals are distributed randomly throughout the environment at the beginning of the trial. Some goals, denoted as stars, were discovered by the end of the trial, while others remain undiscovered by the swarm.

The Monitor task required the agents to observe the entire environment and began with the swarm members distributed randomly across the environment. The environment had no or several obstacles positioned randomly, as described in Chapter IV.1.2. The agents moved and interacted under the direction of the commu-

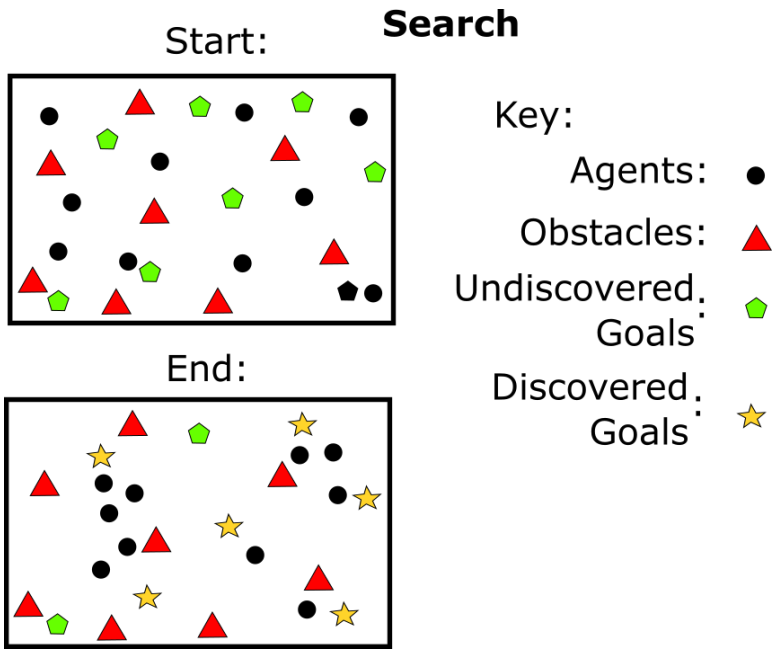

Figure IV.2: Example start and end states for the Search Task.

nication models for 90 timesteps, after which the total coverage of the swarm was calculated. A Monitor task example start and end states are presented in Figure IV.3. The triangles represent obstacles within the environment, and the circles represent agents. The start state has the circle agents and triangle obstacles randomly placed throughout the environment, while the end state has the agents relocated by swarming behaviors.

IV.1.3.3 Avoid Object

The Avoid Object task required the swarm agents to avoid a certain object. An object was placed at the midpoint of the environment, point (d, d/2), and was designated as an adversary, with a heading of 180 degrees and a magnitude of 10, directed towards the swarm. The swarm was generated randomly with x position values less than that of the adversary. The direction vectors of the individual swarm agents were required to be within thirty degrees of the vector from the agent to the adversary object. The swarm moved throughout the environment until 90 percent of the swarm had an x position value greater than that of the adversary, at which point the simulation was stopped, and the dispersion was recorded. The adversary was the only obstacle in the environment, as shown in Figure IV.4, in order to measure the specific effect of the adversary without confounding the results by the impact of other types of obstacles. The start state has the triangle adversary at the midpoint of the environment, and the circle agents randomly distributed to the left of the adversary. The end state occurs when the agents have passed the adversary, while maintaining a semblance of a swarm.

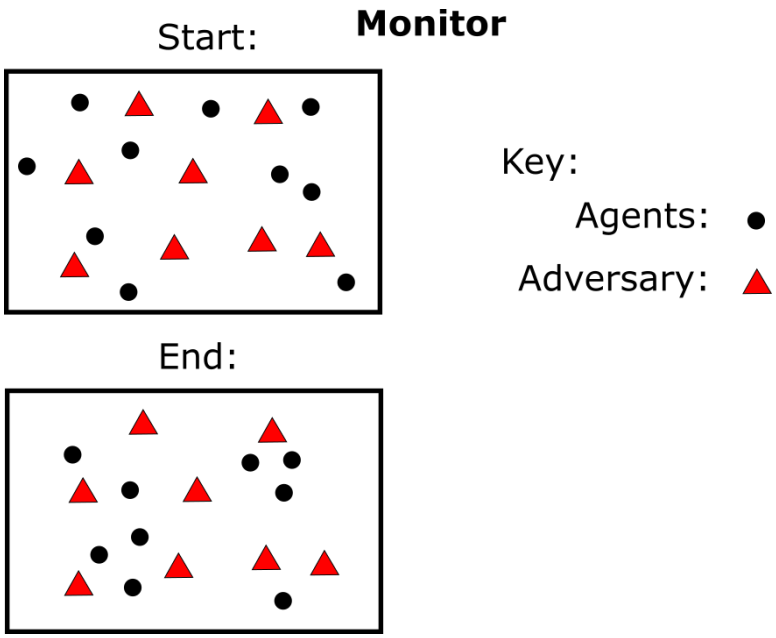

Figure IV.3: Example start and end states for the Monitor Task.

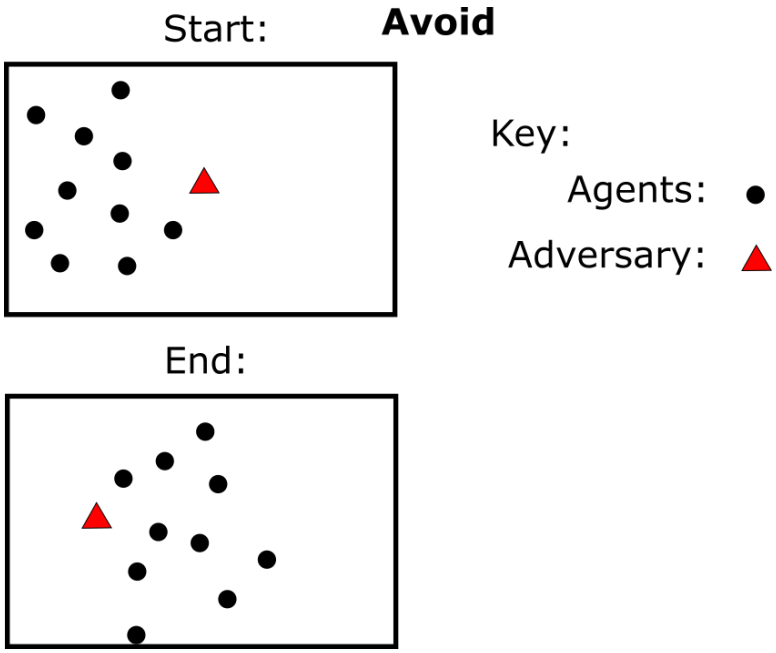

Figure IV.4: Example start and end states for the Avoid Task.

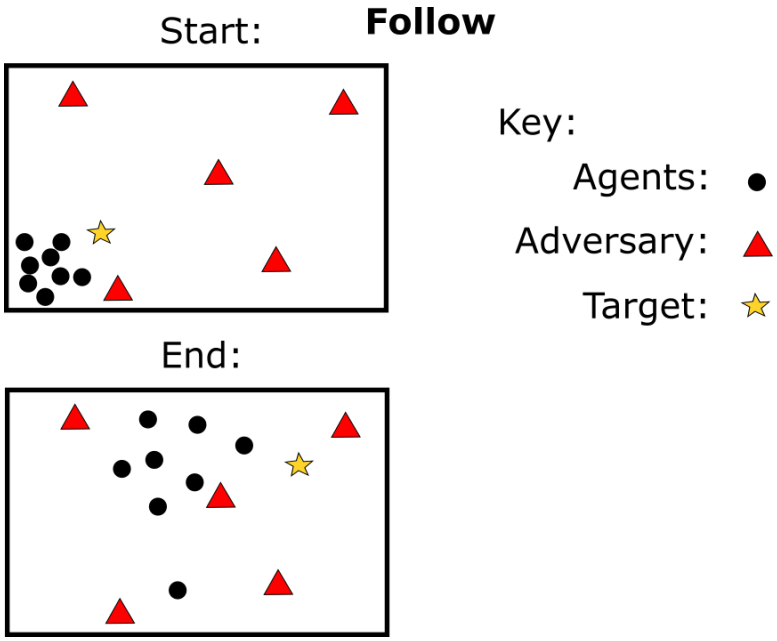

Figure IV.5: Example start and end states for the Follow Task.

IV.1.3.4 Follow Object

The Follow Object task required the swarm to follow a certain target throughout the environment. A target was placed at position ($d/2$, $d/4$). The swarm was generated with x and y values less than the respective values of the target. The direction vectors of each swarm agent were generated, such that they were within thirty degrees of the vector from the agent to the target. The target followed a randomly generated movement pattern throughout the environment for 60 timesteps. The agents followed the target, and upon trial completion the network efficiency and orientation error were measured. The simulation time of 60 timesteps was chosen to allow the target to complete four random segments of 15 timesteps through the environment, so that the target was facing a new direction and also preventing the agents from being accidentally in the correct position. A demonstration of potential start and end states for the Follow Object task are presented in Figure IV.5. The circle agents in the start state are concentrated in the lower left-hand corner, and the star target object is at the upper right corner of the rectangle, within which the agents are generated. The end state has the target at the endpoint of the path, and the agents arrayed behind the target. Some agents may not successfully follow the target. Triangle obstacles are distributed randomly throughout the environment.

IV.1.3.5 Disperse / Rally

The Rally and Disperse tasks required the agents move closer or further away from other agents in the swarm, respectively. The Disperse task began with the agents' positions randomly generated, such that each agent

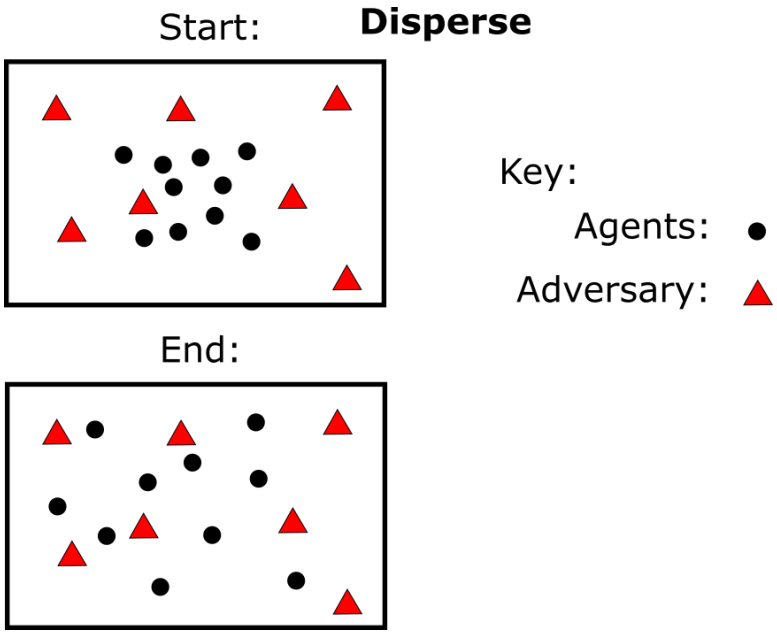

Figure IV.6: Example start and end states for the Disperse Task.

was within the radius of repulsion of at least one neighbor. A demonstration of potential start and end states of the Disperse task are presented in Figure IV.6. The triangle obstacles are randomly distributed throughout the environment. The circle agents are generated in a cluster at the start state, and are expected to spread throughout the environment prior to the end state. The trials ran for 90 timesteps, at which point the average nearest neighbor distance was recorded.

The Rally task began with the agents' positions randomly generated, such that each agent was outside of the radius of repulsion of all neighbors, but within the range of attraction of at least one neighbor. A demonstration of a potential start state and end state of the Rally task is presented in Figure IV.7. The start state has the circle agents spread throughout the environment. The agents move closer together as demonstrated in the end state. The triangle obstacles are distributed randomly throughout the environment. The trial lasted for 90 timesteps, at which point the average nearest neighbor distance was recorded.

IV.1.3.6 Maintain Group / Flocking

The Flocking task expected the swarm to maintain a basic swarming behavior in which the swarm's overall state was relatively unchanged over time. The swarm was randomly distributed throughout the environment, with the number of possible obstacles as defined in Chapter IV.1.2. The trial lasted for 90 timesteps, after which the difference in orientation and center of gravity were measured. Potential start and end states for the Flocking task are presented in Figure IV.8. The start state has the triangle obstacles and circle agents randomly distributed throughout the environment. The agents flock, as represented in the end state.

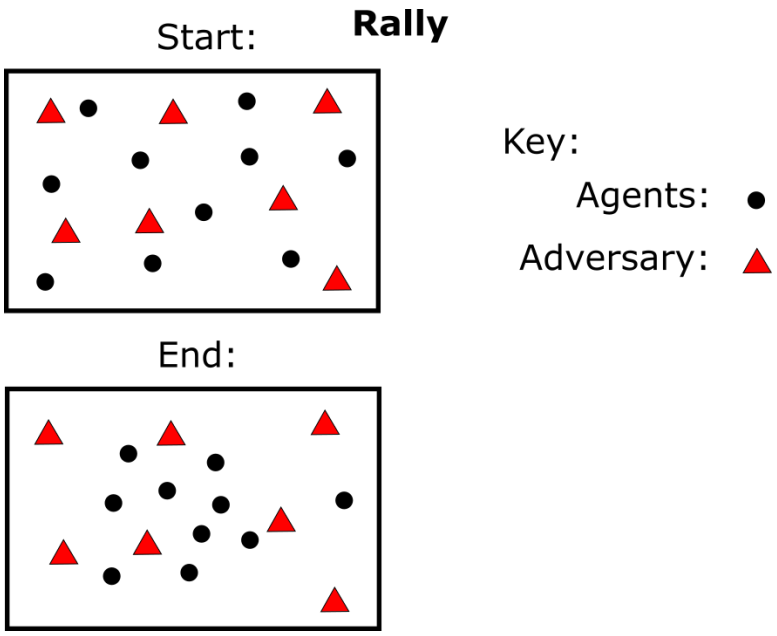

Figure IV.7: Example start and end states for the Rally Task.

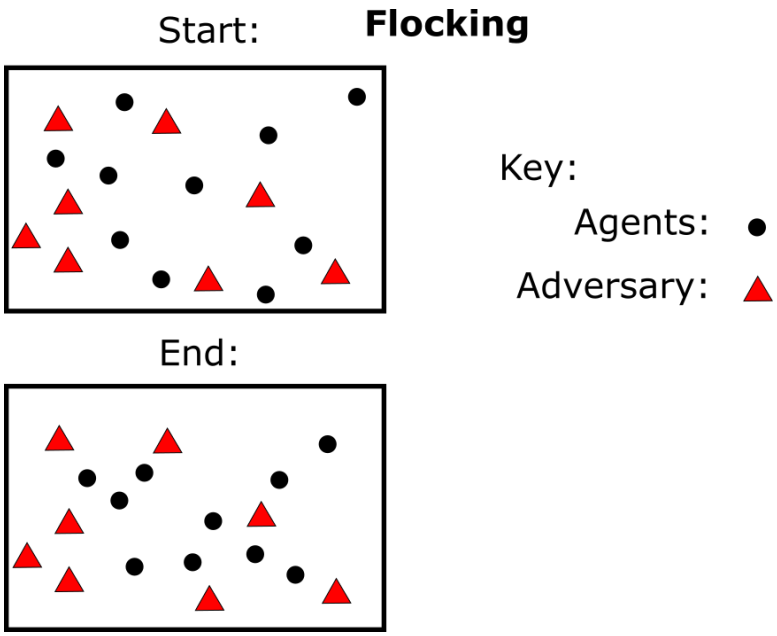

Figure IV.8: Example start and end states for the Maintain Group / Flocking Task.

IV.1.4 Metrics

This Thesis required a concrete assessment of each trial's endpoint in order to compare the independent trials. A specific metric or set of metrics was chosen for each task from a set of potential swarm metrics in order to optimally assess the task's results (Manning et al., 2015).

IV.1.4.1 Go to Location

The metric for the Go To Location task is the percentage of agents that reach the goal location (Parrish et al., 2002). The most successful trial has the highest percentage of agents that reach the goal location. The percentage of agents was determined by counting the number of agents that were within the task radius, and dividing by the total number of agents for the trial. The algorithm used to calculate the metric is formally defined in Algorithm 6.

Algorithm 6 The algorithm for the Percent Reached metric.

PercentReached[Objects o_i]

```
1: Create integer numReached and set to 0
2: for all o_i do
3:     if (o_i) is an Agent then
4:         if (o_i) is within the goal area then
5:             increment numReached by 1
6:         end if
7:     end if
8: end for
9: return (numReached)/(numAgents)
```

IV.1.4.2 Search / Monitor

The Search task metric is the percentage of objectives found (Walker et al., 2012). The most successful trial has the highest percent of goals found. This metric was calculated by totaling the number of goals that were discovered by the swarm, and dividing by the total number of goals. The algorithm used to calculate the metric is formally defined in Algorithm 7.

Algorithm 7 The algorithm for the Percent Found metric.

PercentFound[Objects o_i]

```
1: Create integer numFound and set to 0
2: for all o_i do
3:    if (o_i) is an Goal then
4:       if (o_i) is within the goal area then
5:          increment numFound by 1
6:       end if
7:    end if
8: end for
9: return (numFound)/(numGoals)
```

The metric for the Monitor task was the total environmental coverage (Walker et al., 2012). Total coverage was calculated by determining the maximum range at which an agent can sense another object, and then marking as covered the integer points (x, y) within that radius from the agent. When the area covered by all agents was marked, the total coverage was calculated by counting the number of covered points and dividing the sum by the total size of the environment. The most successful trial has the highest total coverage, as a swarm with higher total coverage will be able to sense objects within a larger part of the environment and respond to these objects. The algorithm used to calculate the metric is formally defined in Algorithm 8.

Algorithm 8 The algorithm that determines the Total Coverage of the swarm

TotalCoverage[Objects o_i]

```
1: Create empty list of points coveredPoints
2: for all o_i do
3:    if (o_i) is an Agent then
4:       set double maxRange = o_i's maximum range
5:       for all points p where p.distance(o_i.position) < maxRange do
6:          add p to coveredPoints
7:       end for
8:    end if
9: end for
10: Remove all duplicates from coveredPoints
11: return (coveredPoints.size)/(totalPoints)
```

IV.1.4.3 Avoid Object

The avoidance metric was the expanse of the group as the swarm moves away from the adversary (Parrish et al., 2002). The expanse of a swarm is a measurement of the dispersion of the swarm averaged over the number of agents in the swarm. Dispersion is calculated by computing the mean squared differences of each agent from the center of gravity of the swarm in both the x and y directions. These mean squared differences are averaged over the entire number of agents and summed to determine the expanse of the swarm. A lower expanse means that the agents are clustered more closely as one group, and so the most successful trial has the lowest expanse. The algorithm used to calculate expanse is formally defined in Algorithm 9, which relies upon the Center of Gravity and Dispersions defined in Algorithms 10 and 11, respectively.

Algorithm 9 The algorithm that determines the expanse of the swarm

Expanse[Objects o_i]

1: Set double dispersionTemp = Dispersion(o_i)
2: **return** $(dispersionTemp/numAgents)$

Algorithm 10 The algorithm that determines the center of gravity of the swarm

CenterOfGravity[Objects o_i]

1: Create doubles xTotal, yTotal; set them to 0
2: **for** all o_i **do**
3: **if** (o_i) is an Agent **then**
4: xTotal += o_i.Position.x
5: yTotal += o_i.Position.y
6: **end if**
7: **end for**
8: Double xReturn = xTotal / numAgents
9: Double yReturn = yTotal / numAgents
10: **return** $(xReturn, yReturn)$

Algorithm 11 The algorithm that determines the dispersion of the swarm

Dispersion[Objects o_i]

1: Set point p(xCOG, yCOG) = CenterOfGravity(o_i)
2: Create doubles xDifferenceSq, yDifferenceSq; set them to 0
3: **for** all o_i **do**
4: **if** (o_i) is an Agent **then**
5: xDifferenceSq += (o_i.Position.x - xCOG)^2
6: yDifferenceSq += (o_i.Position.y - yCOG)^2
7: **end if**
8: **end for**
9: **return** $(xDifferenceSq + yDifferenceSq)$

IV.1.4.4 Follow Object

The Follow Object task's metrics are the orientation error (Spears et al., 2004) and the network efficiency (Mersch et al., 2013; Strandburg-Peshkin et al., 2013; Attanasi et al., 2013). The network efficiency measures the spread of information through the swarm. A random swarm agent is designated as informed at the beginning of the trial. Any other agent that interacts with an informed agent is also marked as informed. The timestep at which each agent is first informed is recorded. The network efficiency is the number of timesteps required to inform 90% of the swarm's agents. The orientation error is measured as a percentage of agents with a heading within 30 degrees of the target at the end of the trial. This metric is calculated by counting the number of agents with a heading within 30 degrees of the target's heading and dividing by the total number of agents. The algorithm used to calculate Network Efficiency is formally defined in Algorithm 12, while the algorithm used to compute the percent within 30 degrees is established in Algorithm 13. A higher value for the network efficiency means that information takes a higher amount of time to propagate through the swarm, and thus the swarm has a lower efficiency. A higher value for the percent within 30 degrees means that there are more agents following the target, and thus the swarm has lower orientation error. Higher efficiency and lower orientation error means that the swarm is both able to pass along information regarding the target and stay oriented with the target, which is desirable. Thus, the most successful trial has the lowest orientation error (and the highest percent within 30 degrees) as well as the highest efficiency (and the lowest efficiency values).

Algorithm 12 The algorithm for the Network Efficiency metric.

NetworkEfficiency[Objects o_i]

```
Create an empty set of integers myTimesteps
for all o_i do
    if (o_i) is an Agent then
        add o_i.timestepInformed to myTimesteps
    end if
end for
Sort myTimesteps from lowest to highest
return myTimesteps.at(round(0.9 * numAgents))
```

Algorithm 13 The algorithm that determines the percentage of the swarm within 30 degrees of the target

PercentWithin30Degrees[Objects o_i, Target t]

```
Create integer numWithin30Degrees
for all o_i do
    if (o_i) is an Agent then
        if |o_i.θ - t.θ| < 30 then
            increment numWithin30Degrees by 1
        end if
    end if
end for
return (numWithin30Degrees)/(numAgents)
```

IV.1.4.5 Disperse / Rally

The metric for the Disperse and Rally tasks is the average nearest neighbor distance (Parrish et al., 2002; Krause et al., 2000). The most successful swarm in the Rally task has the lowest nearest neighbor distance, as this indicates that the swarm is able to come together more effectively. The most successful swarm in the Disperse task has the greatest nearest neighbor distance, as this indicates that the swarm is able to spread through the environment. The nearest neighbor distance is calculated by finding the single nearest neighbor to each agent, and taking the distance between the agent and that neighbor. The distances are averaged over the entire swarm. The algorithm used to calculate the metric is formally defined in Algorithm 14.

Algorithm 14 The algorithm for the Nearest Neighbor metric.

NearestNeighbor[Objects o_i]

```
1: Create double array distances with size = number of agents; initialize the values to maximum value
2: for all o_i do
3:    for all o_j do
4:       if (o_i.distance o_j <distances[i] then
5:          Set distances[i] to o_i.distance(o_j)
6:       end if
7:       if (o_i.distance o_j <distances[j] then
8:          Set distances[j] to o_i.distance(o_j)
9:       end if
10:   end for
11: end for
12: Create a double totalDistance and set to 0.0
13: for all o_i do
14:   if o_i is an Agent then
15:      add distances[i] to totalDistance
16:   end if
17: end for
18: return (totalDistance)/(numAgents)
```

IV.1.4.6 Maintain Group / Flocking

The metrics for Flocking were the magnitude of the changes in index of dispersion and center of gravity over time (Leca et al., 2003). The center of gravity is a point computed by averaging the *x* and *y* positions for each agent. The magnitude of the change in center of gravity is the distance from the center of gravity at the end of the trial from the center of gravity at the beginning of the trial. The method for determining the center of gravity is formally defined in Algorithm 10. The swarm dispersion is calculated by computing the mean squared differences of each agent from the swarm's center of gravity in both the *x* and *y* directions. The mean squared differences are summed to obtain the swarm's dispersion. The change in dispersion is calculated by determining the difference between the dispersion at the beginning of the trial and the dispersion at the end of the trial using the method defined in Algorithm 11. The absolute value of the change in dispersion determines the magnitude of the change in dispersion. A lower magnitude of change in center of gravity means that the swarm has not moved far from its original position. A lower magnitude of change in dispersion means the

Task	Hypothesis	Description
Go To Location	H_{GTL}	$PercentReached_{Visual} > PercentReached_{Topo} > PercentReached_{Metric}$
Search	H_{S1}	$PercentFound_{Visual} > PercentFound_{Topo}$
	H_{S2}	$PercentFound_{Visual} > PercentFound_{Metric}$
Monitor	H_M	$TotalCoverage_{Visual} > TotalCoverage_{Metric} > TotalCoverage_{Topo}$
Avoid Object	H_{A1}	$Expanse_{Visual} < Expanse_{Metric}$
	H_{A2}	$Expanse_{Topo} < Expanse_{Metric}$
Follow Object	H_{F1}	$Efficiency_{Visual} > Efficiency_{Topo} > Efficiency_{Metric}$
	H_{F2}	$Error_{Visual} < Error_{Topo} < Error_{Metric}$
Disperse	H_{D1}	$NearestNeighbor_{Metric} > NearestNeighbor_{Visual}$
	H_{D2}	$NearestNeighbor_{Metric} > NearestNeighbor_{Topo}$
Rally	H_{R1}	$NearestNeighbor_{Visual} < NearestNeighbor_{Metric}$
	H_{R2}	$NearestNeighbor_{Topo} < NearestNeighbor_{Metric}$
Maintain Group	H_{MG1}	$\Delta Dispersion_{Visual} > \Delta Dispersion_{Topo}$
	H_{MG2}	$\Delta Dispersion_{Metric} > \Delta Dispersion_{Topo}$
	H_{MG3}	$\Delta COG_{Visual} > \Delta COG_{Topo}$
	H_{MG4}	$\Delta COG_{Metric} > \Delta COG_{Topo}$

Table IV.3: Summary of hypotheses by task.

swarm has not expanded or contracted rapidly. Thus, the model with the lowest change in index of dispersion and center of gravity over time represents the most successful in maintaining group location. The magnitude of the changes in index of dispersion and center of gravity will be referred to as the change in dispersion and the change in center of gravity for the sake of efficency.

IV.1.5 Hypotheses

IV.1.5.1 Go to Location

The hypothesis (H_{GTL}) for the Go To Location task is that the visual model will have a significantly higher percentage of agents reaching the goal area, followed by the topological model, with the metric model having the lowest percentage of agents reaching the goal location. The metric model has clearly defined endpoints as to where an agent will be in the zone of attraction; thus, if the straggler becomes too far displaced from the swarm, it will be unable to rejoin the swarm (Couzin et al., 2002). However, the topological and visual models have the potential to perform an attracting movement far outside the zone of orientation; thus it is possible that a straggler can rejoin the swarm. For example, the closest five or six agents to an agent that is separated from the main swarm, may be part of that main swarm. The main swarm would then have an attractive effect on the topological model agent when the swarm will otherwise be outside of the metric model agent's radius of attraction (Ballerini et al., 2008). The ability to sense distant agents allows the topological agent to sense the swarm and eventually return to it. The visual method permits a similar behavior. The objects within a visual model agent's field of view may be in a situation similar to that described for the topological model.

The objects that the visual model agent can sense may be outside of the radius of attraction, and thus out of the range of the metric agent, which means visual agents have a higher likelihood of returning to the swarm than metric agents. More objects are within the visual model agent's field of view, on average, than the fixed topological number (Strandburg-Peshkin et al., 2013), which means that the visual model agent has a larger number of attractive inputs from the main group. The higher amount of attraction means the visual model agent has a higher likelihood of returning to the main swarm than the topological model agent. Thus, the visual model results in fewer stragglers than the topological model, which performs better than the metric model.

IV.1.5.2 Search / Monitor

The hypotheses for the Search task are that the visual model will detect significantly more objects, than either the topological model (H_{S1}) or the metric model (H_{S2}) . The metric model is unable to sense the targets outside of the zone of attraction, which results in less effective searching (Couzin et al., 2002). Similarly, the topological model only focuses on the closest agents or targets and has a less effective search capability (Ballerini et al., 2008). The visual model is only bounded by the associated field of view and line of sight. Thus, it can better locate targets (Strandburg-Peshkin et al., 2013).

The Monitor task's hypothesis (H_M) is that the visual model will provide significantly larger total coverage, with the metric model providing the second largest coverage, and the topological metric providing the lowest coverage. The reasoning behind this hypothesis is that the visual model can recognize objects located outside of the radius of attraction, thus it can provide better coverage than the metric or topological models (Strandburg-Peshkin et al., 2013). The metric model responds to objects within the radius of attraction only, which is usually more constrained and results in less coverage than the visual model (Couzin et al., 2002). However, the metric model is more responsive than the topological model, which can only sense the closest objects (Ballerini et al., 2008).

IV.1.5.3 Avoid Object

The hypotheses for the Avoid task are that the topological model (H_{A1}) and the visual model (H_{A2}) will both have a significantly smaller expanse than the metric model, which will have the highest expanse, and perform with the lowest efficacy. The topological model has been shown to have better performance in staying together after encountering an adversary (Ballerini et al., 2008), and the visual model acts in a manner similar to the topological model (Strandburg-Peshkin et al., 2013).

IV.1.5.4 Follow Object

The first hypothesis (H_{F1}) is that the visual model will have significantly higher efficiency, followed by the topological model, with the metric model resulting in the lowest efficiency and performance. The second hypothesis (H_{F2}) is that the visual model will have significantly lower error, with the topological model having higher error and the metric model resulting in the highest error. These hypotheses are formulated based on the logic that the visual model agents are more capable of reacting to the target object, as most of the outer agents and some interior agents will have a line of sight to the target (Strandburg-Peshkin et al., 2013). The topological model agents on the edge of the swarm closest to the target will likely have the target as one of their closest objects, where the metric model may be unable to sense the target as it may be outside of the radius of attraction (Couzin et al., 2002).

IV.1.5.5 Disperse / Rally

The Disperse task's hypotheses are that the metric model will have significantly higher nearest neighbor distances, greater than either the topological (H_{D1}) or the visual (H_{D2}) models. The hypotheses for the Rally task are that the topological (H_{R1}) and visual (H_{R2}) models both have lower nearest neighbor distances than the metric model. The metric model is limited in range to the radius of attraction, while the topological and visual models are not (Strandburg-Peshkin et al., 2013). This limitation in range means that agents spread further apart than the radius of attraction in the topological and visual models will be sensed in those models and cause an attractive effect while the metric model agents cannot sense at that range. The additional attractive forces imply that the swarm will coalesce more quickly with the topological and visual models, which will not be the case with the metric model. Thus, the visual and topological models rally to a similar distance, with the metric model performing at the lowest efficiency. The metric model in the dispersion task can respond to all agents within the radius of repulsion, while the topological and visual models are limited to the closest n agents and those within the field of view, respectively (Strandburg-Peshkin et al., 2013). The metric model agents can experience a greater repulsive force, and the swarm will have a greater nearest neighbor distance, while both the topological model and visual model swarms will have a significantly smaller distance (Couzin et al., 2002).

IV.1.5.6 Maintain Group / Flocking

The Flocking task's hypotheses are that the topological model will have a significantly lower change in Index of Dispersion and Center of Gravity over a set period of time, and both the visual model's change in Dispersion (H_{MG1}) and Center of Gravity (H_{MG3}) and the metric model's change in Dispersion (H_{MG2}) and Center of Gravity (H_{MG4}) will have a significantly lower values than the topological model. The logic behind

the hypotheses is that the limited number of interactions that the topological model performs (Strandburg-Peshkin et al., 2013) will prevent disturbances from spreading rapidly across the swarm. The topological model requires a response from a small set of agents (Ballerini et al., 2008) while the visual and metric models respond to a much larger subset of the swarm. Thus, any disturbances in the swarm affect only a small number of local agents in the topological model, which is less likely to effect the position and dispersion of the swarm than either of the visual or metric models.

IV.2 Results

One trial was executed for each combination of the parameters used for each task. That is, for each given number of agents, set of radii values, and model type, a single trial was completed. The topological and visual models required additional parameters (c and *maxVisRange*, respectively), which required additional trials. Different tasks required fewer or more trials, depending on the associated required parameters. The parameters required for each task are detailed in Tables IV.1 and IV.2. The Avoid tasks only used one obstacle in the environment, and thus needed 2,160 trials. The Search task required the number of goals, thus requiring 32,832 trials.

The Avoid trials were distributed as: metric = 270 trials, topological = 1080 trials, and visual = 810 trials. The Search task had its 32,832 trials distributed as: metric = 4,104 trials, topological = 16,416 trials, and visual = 12,312 trials. All other tasks required 8,208 trials. The standard number of trials per model for all tasks were distributed among the communication models based on the model's required parameters: metric = 1026 trials, topological = 4104 trials, and visual = 3078 trials. The number of topological model trials was four times the number of metric model trials in every task due to the extra parameter c, and the number of visual model trials was three times the number of metric model trials due to *maxVisRange*.

The large number of trials per task meant that a Shapiro-Wilk test is unable to determine the normality of the data. The use of QQ-plots to determine the normality was similarly inconclusive. Thus, the analysis used the non-parametric Kruskal-Wallis and Wilcoxon Rank-Sum tests to determine significant differences between trials of the three models.

A full summary of the results is shown in Table IV.4. All figures provide the mean and the standard error of the presented results.

IV.2.1 Go to Location

There were a total of 8,208 trials for the Go To Location task, decomposed by model: metric = 1,026 trials, topological = 4,104 trials, and visual = 3,078 trials. The metric was the percentage of agents that reached the goal area, *PercentReached*. The mean *PercentReached* for the metric model was 13.60%, with a standard

Task	Result
Go To Location	$PercentReached_{Visual} < PercentReached_{Topo}$ $PercentReached_{Metric} < PercentReached_{Topo}$ No significant difference between $PercentReached_{Metric}$ and $PercentReached_{Visual}$
Search	$PercentFound_{Topo} > PercentFound_{Visual}$ No significant difference between $PercentFound_{Metric}$ and $PercentFound_{Visual}$ No significant difference between $PercentFound_{Metric}$ and $PercentFound_{Topo}$
Monitor	$TotalCoverage_{Topo} > TotalCoverage_{Visual} > TotalCoverage_{Metric}$
Avoid Object	$Expanse_{Visual} < Expanse_{Topo}$ $Expanse_{Metric} < Expanse_{Topo}$ No significant difference between $Expanse_{Metric}$ and $Expanse_{Visual}$
Follow Object	$Efficiency_{Visual} < Efficiency_{Topo} < Efficiency_{Metric}$ $Error_{Visual} < Error_{Topo} < Error_{Metric}$
Disperse	$NearestNeighbor_{Topo} > NearestNeighbor_{Visual}$ $NearestNeighbor_{Topo} > NearestNeighbor_{Metric}$ No significant difference between $NearestNeighbor_{Metric}$ and $NearestNeighbor_{Visual}$
Rally	$NearestNeighbor_{Visual} > NearestNeighbor_{Topo} > NearestNeighbor_{Metric}$
Maintain Group	$\Delta Dispersion_{Metric} > \Delta Dispersion_{Visual} > \Delta Dispersion_{Topo}$ $\Delta COG_{Visual} > \Delta COG_{Topo}$ $\Delta COG_{Metric} > \Delta COG_{Topo}$

Table IV.4: Summary of the results of the analyses conducted.

deviation (std. dev.) of 21.70%. The mean *PercentReached* for the topological model was 14.00% (std. dev. = 21.57%), while the mean *PercentReached* for the visual model was 13.64% (std. dev. = 21.59%).

A Kruskal-Wallis test indicated that there was a significant impact of model type (p = 0.0447, $\chi^2(2)$ = 6.21). The Wilcoxon Rank-Sum test provided pairwise comparisons of the models and determined that the topological model had a significantly higher *PercentReached* than both the visual (p = 0.0488, z = 6,483,746) and the metric models (p = 0.0438, z = 2,021,637). There was no significant difference between the metric and the visual models. The distributions for each model are illustrated in Figure IV.9. These results imply that the topological model has a significantly higher percentage of agents reaching the goal area than both the visual and metric models.

The data was further analyzed by the different parameters. The means and standard deviations for the Go To Location task analyzed by the number of agents are provided in Table IV.5. The descriptive statistics are visualized in Figure IV.10. The Kruskal-Wallis test found no significant affect of the model type on the *PercentReached* when analyzed by number of agents.

The means and standard deviations for the Go To Location task analyzed by the number of obstacles are provided in Table IV.6. The descriptive statistics are visualized in Figure IV.10. The Kruskal-Wallis test did not find any significant affect of the model type on the *PercentReached* analyzed by number of obstacles.

The means and standard deviations for the Go To Location task analyzed by the radius of repulsion are

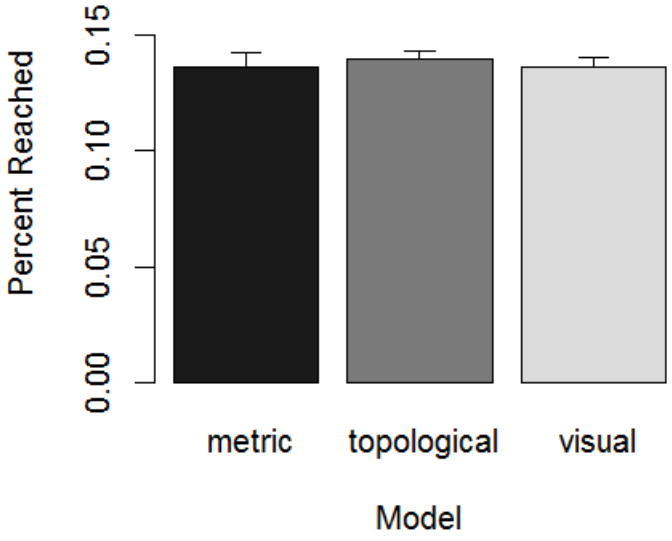

Figure IV.9: The distributions for each model in the Go To Location task.

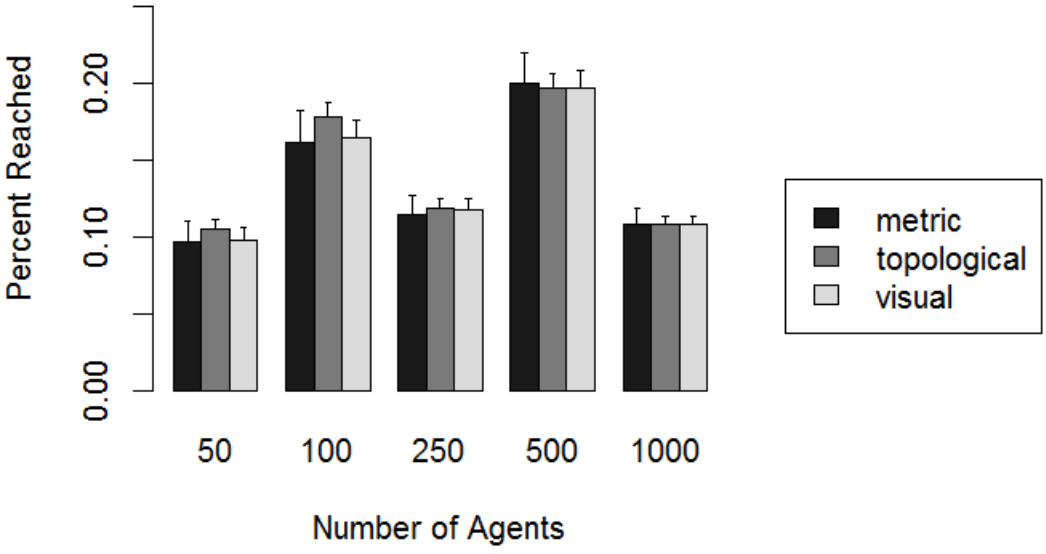

Figure IV.10: The distributions of PercentReached by number of agents and model.

Number of Agents	Metric Mean (Std. Dev.)	Topological Mean (Std. Dev.)	Visual Mean (Std. Dev.)
50	9.72% (17.63%)	10.52% (17.74%)	9.84% (17.53%)
100	16.17% (25.90%)	17.78% (25.14%)	16.46% (25.68%)
250	11.51% (17.70%)	11.95% (17.47%)	11.81% (17.32%)
500	20.04% (28.18%)	19.71% (28.14%)	19.69% (28.12%)
1000	10.90% (16.26%)	10.91% (16.42%)	10.86% (16.33%)

Table IV.5: The means and standard deviations of the Go To Location task by number of agents.

Number of Obstacles	Metric Mean (Std. Dev.)	Topological Mean (Std. Dev.)	Visual Mean (Std. Dev.)
0	13.68% (22.13%)	14.01% (21.96%)	13.63% (21.92%)
25	13.61% (22.01%)	14.09% (21.83%)	13.73% (21.91%)
50	13.70% (21.90%)	14.42% (21.73%)	13.84% (21.82%)
100	14.17% (21.81%)	14.17% (21.67%)	14.13% (21.61%)
250	10.92% (16.45%)	10.92% (16.48%)	10.89% (16.42%)

Table IV.6: The means and standard deviations of the Go To Location task by number of obstacles.

presented in Table IV.7. The descriptive statistics are visualized in Figure IV.12. The Kruskal-Wallis test did not find any significant affect of the model type on the *PercentReached* in the trials where the radius of repulsion was greater than 25. The Kruskal-Wallis test found highly significant affects of the model type on the *PercentReaced* when the radius of orientation was equal to 5 ($p < 0.01$, $\chi^2(2) = 10.34$) and 25 ($p < 0.001$, $\chi^2(2) = 31.75$). The Wilcoxon Rank-Sum test found that in trials where the radius of repulsion was equal to 5, the topological model had a significantly higher *PercentReached* than the visual ($p < 0.01$, $z =$ 998,845) and metric ($p = 0.0287$, $z = 301{,}703.5$) models. The Wilcoxon Rank-Sum test found that when the radius of repulsion was equal to 25, the topological model had a significantly higher *PercentReached* than the visual ($p < 0.001$, $z = 554{,}572.5$) and metric ($p < 0.001$, $z = 141{,}399$) models. That is, the topological model performed significantly better than the visual and metric models with the radius of repulsion equal to 5 or 25.

Radius of Repulsion	Metric Mean (Std. Dev.)	Topological Mean (Std. Dev.)	Visual Mean (Std. Dev.)
5	0.07% (0.18%)	0.16% (0.68%)	0.09% (0.21%)
25	4.90% (4.41%)	5.84% (4.20%)	4.97% (3.45%)
50	19.31% (6.13%)	19.82% (6.03%)	19.47% (5.96%)
100	63.85% (15.54%)	63.89% (15.28%)	63.73% (15.42%)

Table IV.7: The means and standard deviations of the Go To Location task by radius of repulsion.

The means and standard deviations for the Go To Location task analyzed by the radius of orientation are provided in Table IV.8. The descriptive statistics are visualized in Figure IV.13. The Kruskal-Wallis test found no significant affect of model type on the *PercentReached* in the trials where the radius of orientation

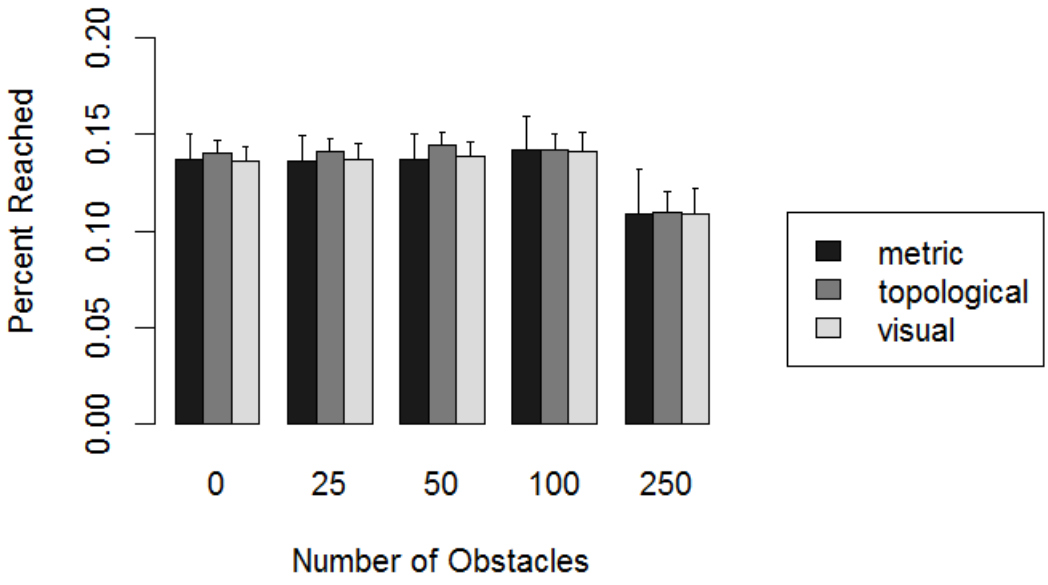

Figure IV.11: The distributions of PercentReached by number of obstacles and model.

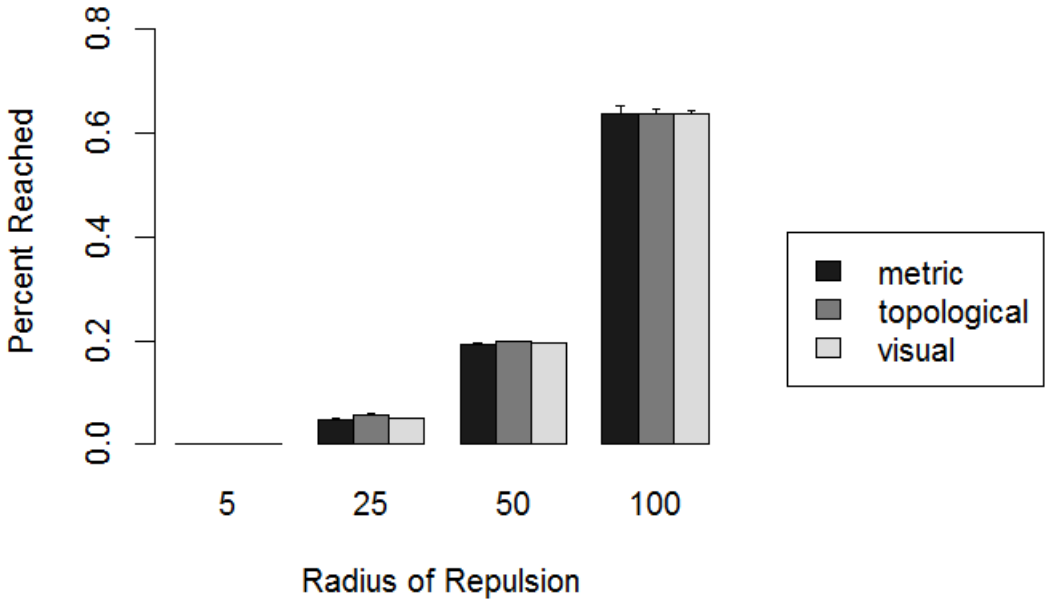

Figure IV.12: The distributions of PercentReached by radius of repulsion and model.

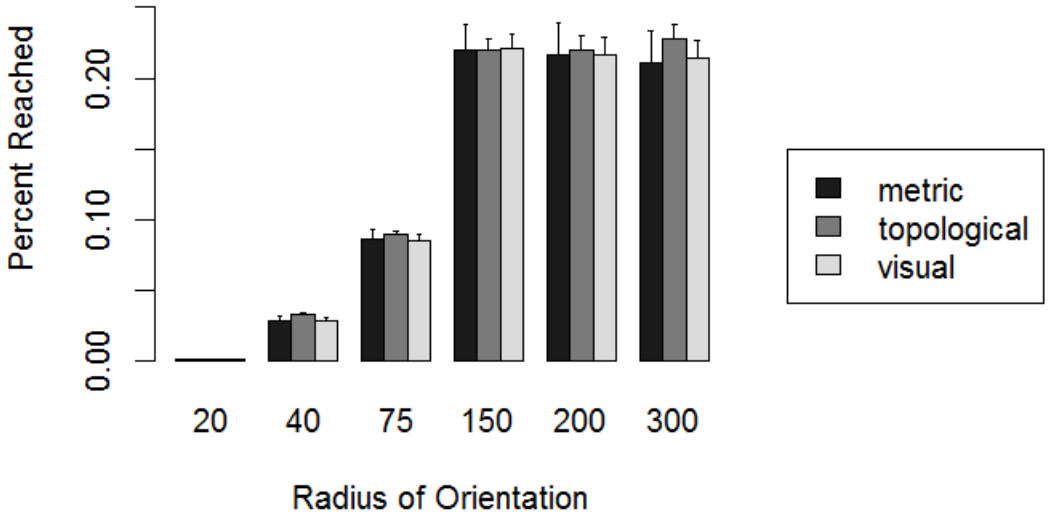

Figure IV.13: The distributions of PercentReached by radius of orientation and model.

was less than 300. The Kruskal-Wallis test found a significant affect of the model type on the *PercentReaced* in the trials where the radius of orientation was equal to 300 (p = 0.0283, $\chi^2(2)$ = 7.13). The Wilcoxon Rank-Sum test determined that when the radius of orientation was equal to 300, the topological model had a significantly higher *PercentReached* than the visual (p = 0.0223, z = 149,898.5) and metric (p = 0.0471, z = 41,420) models. That is, the topological model performed significantly better than the visual and metric models with the radius of orientation equal to 300.

Radius of Orientation	**Metric Mean (Std. Dev.)**	**Topological Mean (Std. Dev.)**	**Visual Mean (Std. Dev.)**
20	0.12% (0.24%)	0.13% (0.24%)	0.13% (0.27%)
40	2.85% (3.99%)	3.31% (4.11%)	2.93% (3.68%)
75	8.67% (9.43%)	8.94% (9.22%)	8.59% (9.31%)
150	22.01% (26.63%)	21.95% (26.57%)	22.07% (26.54%)
200	21.71% (26.82%)	21.99% (26.59%)	21.68% (26.61%)
300	21.11% (27.21%)	22.79% (26.46%)	21.39% (26.83%)

Table IV.8: The means and standard deviations of the Go To Location task by radius of orientation.

The means and standard deviations for the Go To Location task analyzed by the radius of attraction are presented in Table IV.9. The descriptive statistics are visualized in Figure IV.14. The Kruskal-Wallis test found no significant affect of model type on the *PercentReached* when analyzed by radius of attraction.

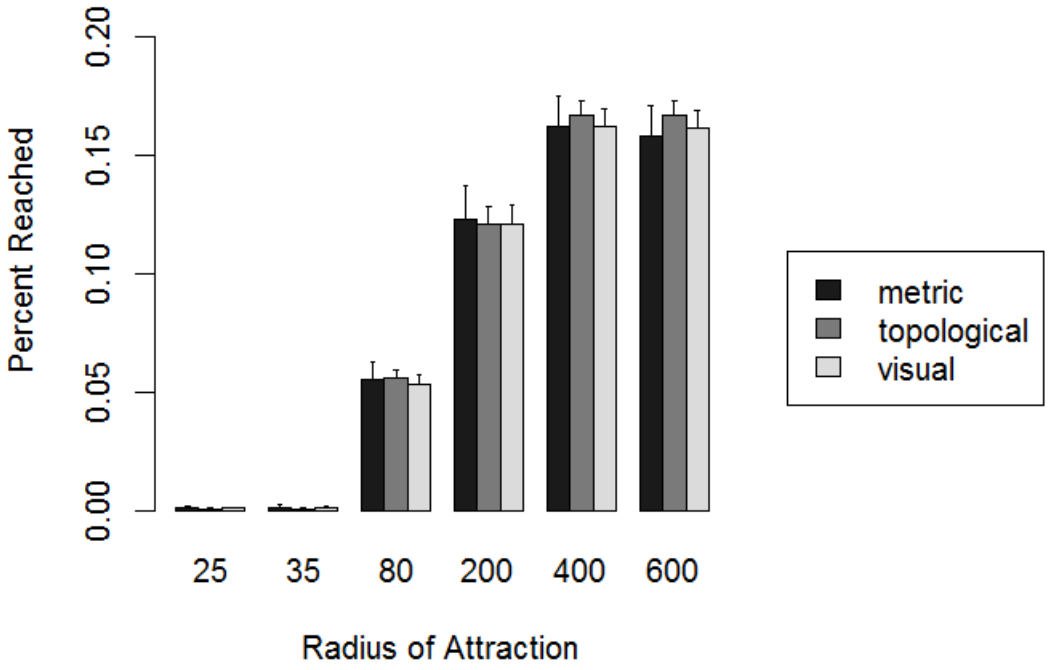

Figure IV.14: The distributions of PercentReached by radius of attraction and model.

Radius of Attraction	Metric Mean (Std. Dev.)	Topological Mean (Std. Dev.)	Visual Mean (Std. Dev.)
25	0.16% (0.23%)	0.13% (0.24%)	0.14% (0.29%)
35	0.19% (0.33%)	0.13% (0.24%)	0.19% (0.35%)
80	5.6% (7.93%)	5.62% (7.81%)	5.35% (7.77%)
200	12.33% (19.57%)	12.14% (19.54%)	12.10% (19.62%)
400	16.21% (23.68%)	16.67% (23.52%)	16.24% (23.53%)
600	15.85% (23.82%)	16.71% (23.45%)	16.16% (23.53%)

Table IV.9: The means and standard deviations of the Go To Location task by radius of attraction.

IV.2.2 Search / Monitor

The Search task had a total of 32,832 trials, decomposed by model: metric = 4,104 trials, topological = 16,416 trials, and visual = 12,312 trials. The metric for the search task was the percentage of goals found, *PercentFound*. The metric model trials had a mean *PercentFound* of 72.85% (std. dev. = 33.13%). The topological model resulted in a mean *PercentFound* of 73.94% (std. dev. = 32.44%), while the mean for the visual model was 72.69% (std. dev. = 32.65%). The distributions of this data are visualized in Figure IV.15.

The Kruskal-Wallis test found a significant affect of model type ($p < 0.001$, $\chi^2(2) = 16.67$). The Wilcoxon Rank-Sum test determined that the swarm using the topological model had a significantly higher *PercentFound* (i.e., identified significantly more goals), than the visual model ($p < 0.001$, z = 103,800,609). The topological and metric models and the visual and metric models comparisons were not significantly different. These analyses imply that the visual model found a lower percentage of goals than the topological model.

The means and standard deviations for the Search task, analyzed by the number of agents, are reported in Table IV.10. The descriptive statistics are visualized in Figure IV.16. The Kruskal-Wallis test found no significant difference based on model type for the *PercentFound*hwen analyzing the results by the number of agents for 50, 100, or 1,000 agents. The Kruskal-Wallis test found a highly significant affect of the model type on *PercentFound* when the number of agents was 250 ($p = 0.0159$, $\chi^2(2) = 8.28$) or 500 ($p < 0.001$, $\chi^2(2) = 29.59$). The Wilcoxon Rank-Sum test found that, when the number of agents was 250, the topological model resulted in a significantly higher mean *PercentFound* than the visual model ($p < 0.01$, z = 4,661,256). That is, for trials with 250 agents, the topological model outperformed the visual model. The Wilcoxon Rank-Sum test for 1,000 agents determined that the topological model had a significantly higher *PercentFound* than both the visual model ($p < 0.001$, z = 4,786,319) and the metric model ($p < 0.001$, z = 1,376,854). This analysis implies that the topological model performs significantly better than both the visual and metric models. Although the data was not statistically significant, it is interesting to note that the metric model trials had a lower mean percentage of goals found than the visual model for 500 or 1,000 agents.

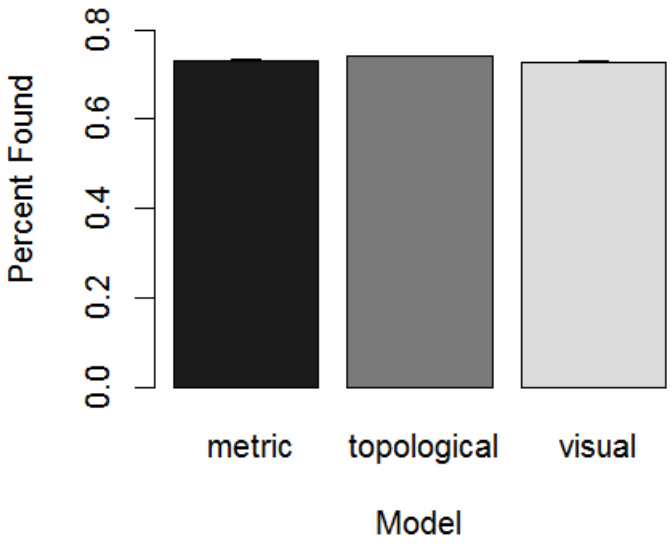

Figure IV.15: The distributions for each model in the Search task.

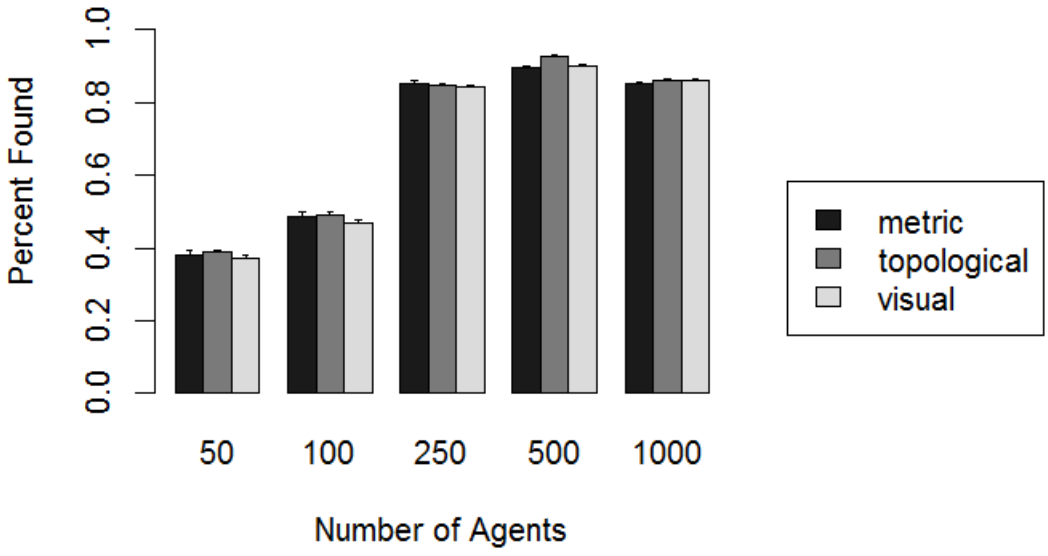

Figure IV.16: The distributions of PercentFound by number of agents and model.

Number of Agents	Metric Mean (Std. Dev.)	Topological Mean (Std. Dev.)	Visual Mean (Std. Dev.)
50	38.17% (35.72%)	38.87% (35.43%)	37.34% (34.70%)
100	48.46% (39.37%)	49.04% (38.60%)	46.92% (38.26%)
250	85.15% (20.72%)	84.85% (19.95%)	84.22% (19.96%)
500	89.64% (16.53%)	92.76% (10.73%)	90.20% (14.07%)
1000	85.02% (18.51%)	86.15% (17.42%)	86.13% (17.17%)

Table IV.10: The means and standard deviations of the Search task by number of agents.

The means and standard deviations for the Search task analyzed by the number of obstacles are presented in Table IV.11. The descriptive statistics are visualized in Figure IV.17. The Kruskal-Wallis test found no significant affect of the model type on the *PercentFound* when analyzing the results by number of obstacles, when the number of obstacles was 0, 50, or 250. The Kruskal-Wallis test found a significant affect of the model type on *PercentFound* when the number of obstacles was 25 (p = 0.0201, $\chi^2(2)$ = 7.82) and 100 (p = 0.0320, $\chi^2(2)$ = 6.88). The Wilcoxon Rank-Sum test found that the topological model had a significantly higher mean percentage when the number of obstacles was 25 ($p < 0.01$, z = 7,256,544) and 100 (p = 0.0181, z = 2,617,933). Although the results were not significant, the trials in which there were 50, 100, or 250 obstacles all demonstrated that there was a higher mean *PercentFound* for the visual model when compared to the metric model.

Number of Obstacles	Metric Mean (Std. Dev.)	Topological Mean (Std. Dev.)	Visual Mean (Std. Dev.)
0	70.44% (33.61%)	71.16% (33.22%)	69.53% (33.71%)
25	69.57% (35.27%)	70.64% (34.39%)	68.64% (68.64%)
50	68.01% (36.59%)	68.94% (35.99%)	68.69% (35.35%)
100	86.42% (18.89%)	88.28% (16.55%)	86.86% (17.45%)
250	84.79% (18.60%)	86.28% (16.73%)	86.26% (16.51%)

Table IV.11: The means and standard deviations of the Search task by number of obstacles.

The means and standard deviations for the Search task analyzed by the number of goals are provided in Table IV.11. The descriptive statistics are visualized in Figure IV.17. The Kruskal-Wallis test found no significant affect of the model type on the *PercentFound* when analyzing the results by number of goals, when the number of goals was 5, 25, or 50. The Kruskal-Wallis test found a significant affect of the model type on *PercentFound* when the number of goals was 5 ($p < 0.001$, $\chi^2(2) = 20.04$). The Wilcoxon Rank-Sum test determined that the topological model had a significantly higher mean percentage than both the metric ($p < 0.001$, z = 6,608,783) and visual (p = 0.0103, z = 2,021,771) models for the trials where the number of obstacles was 5. That is, the metric and visual models performed worse than the topological model when the number of goals was 5.

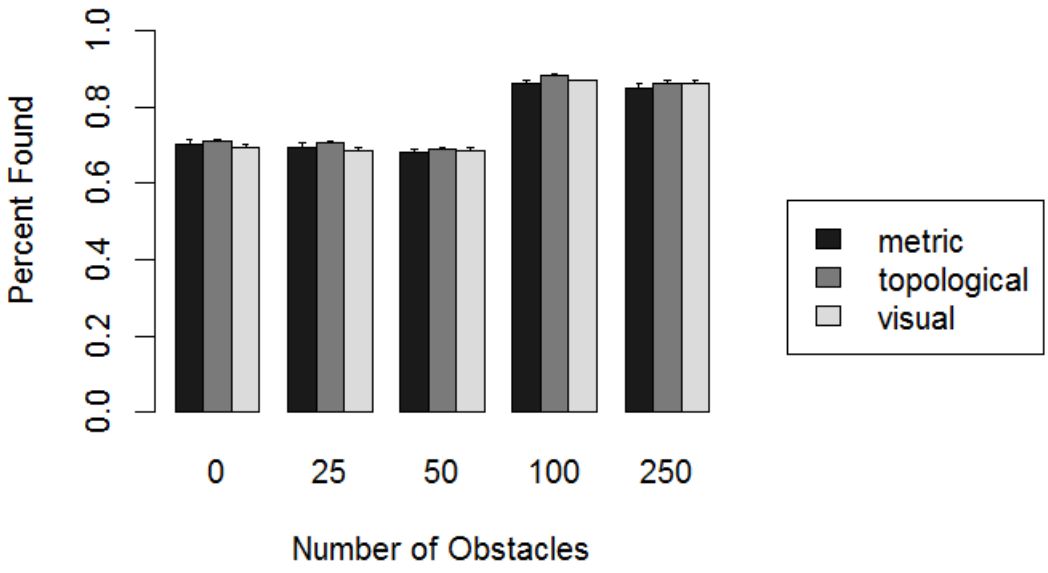

Figure IV.17: The distributions of PercentFound by number of obstacles and model.

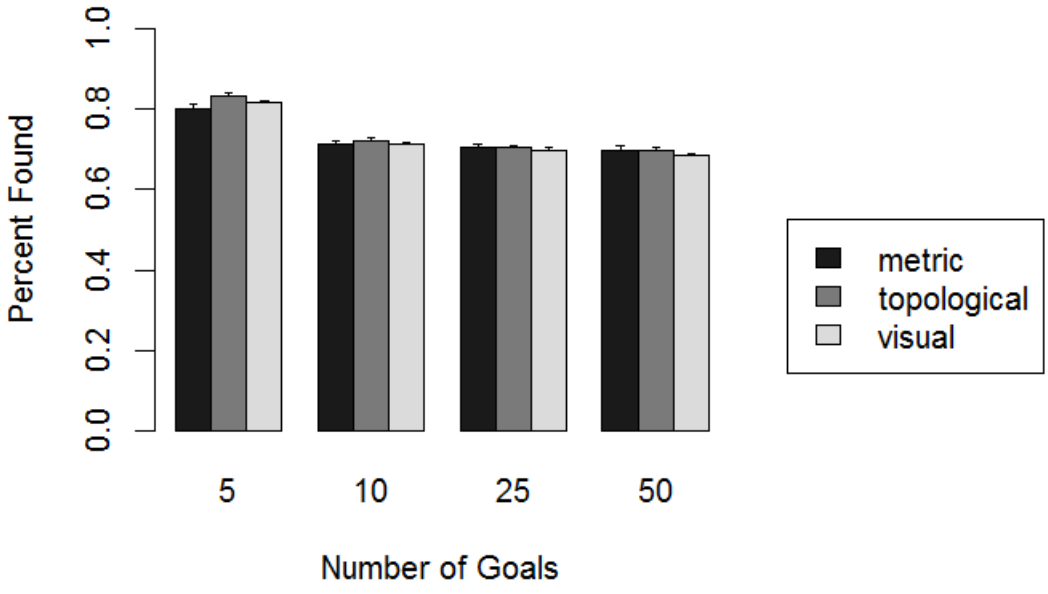

Figure IV.18: The distributions of PercentFound by number of goals and model.

Number of Goals	Metric Mean (Std. Dev.)	Topological Mean (Std. Dev.)	Visual Mean (Std. Dev.)
5	80.16% (35.33%)	83.30% (33.18%)	81.45% (33.76%)
10	71.11% (32.23%)	72.17% (31.16%)	71.09% (31.25%)
25	70.44% (31.48%)	70.46% (31.19%)	69.79% (31.28%)
50	69.69% (32.31%)	69.82% (32.33%)	68.42% (32.65%)

Table IV.12: The means and standard deviations of the Search task by number of goals.

The means and standard deviations for the Search task analyzed by the radius of repulsion are reported in Table IV.13. The descriptive statistics are visualized in Figure IV.19. The Kruskal-Wallis test did not find a significant affect of the model type on the *PercentFound* when the results were analyzed by radius of repulsion, when the radius of repulsion was 50 or 100. The Kruskal-Wallis test found a significant affect of the model type on *PercentFound* when the radius of repulsion was 5 (p = 0.0475, $\chi^2(2)$ = 6.09) and 25 ($p < 0.01$, $\chi^2(2)$ = 10.88). The Wilcoxon Rank-Sum test found that the topological model had a significantly higher mean percentage than the visual model when the radius of repulsion was 5 (p = 0.0289, z = 15,648,480) and 25 ($p < 0.01$, z = 8,120,798). Although the results were not significant, the trials in which the radius of repulsion was 5 demonstrated that there was a higher mean *PercentFound* for the visual model when compared to the metric model.

Radius of Repulsion	Metric Mean (Std. Dev.)	Topological Mean (Std. Dev.)	Visual Mean (Std. Dev.)
5	63.72% (35.00%)	65.46% (34.56%)	64.27% (34.40%)
25	72.85% (32.57%)	74.25% (31.63%)	72.36% (32.08%)
50	80.66% (28.91%)	81.30% (28.15%)	80.29% (28.66%)
100	87.96% (25.22%)	87.14% (25.92%)	86.72% (26.09%)

Table IV.13: The means and standard deviations of the Search task by radius of repulsion.

The means and standard deviations for the Search task analyzed by the radius of orientation are provided in Table IV.14. The descriptive statistics are visualized in Figure IV.20. The Kruskal-Wallis test found no significant affect of the model type on the *PercentFound* when the results were analyzed by radius of orientation when the radius of orientation was 40 or 300. The Kruskal-Wallis test found a significant affect of the model type on *PercentFound* when the radius of orientation was 20 ($p < 0.001$, $\chi^2(2)$ = 21.01), 75 ($p < 0.01$, $\chi^2(2)$ = 12.24), 150 (p = 0.0158, $\chi^2(2)$ = 8.29), or 200 (p = 0.0476, $\chi^2(2)$ = 6.09). The Wilcoxon Rank-Sum test found a significant difference when the radius of orientation was equal to 20 between the metric and the visual models ($p < 0.01$, z = 282,626), and between the metric and topological models ($p < 0.001$, z = 358,249.5). These results imply that when the radius of orientation was equal to 20, the metric model found a higher percentage of agents than either the metric or the visual models. The Wilcoxon Rank-Sum test found a significant difference between the topological and visual models when the radius of orientation equals 75 (p

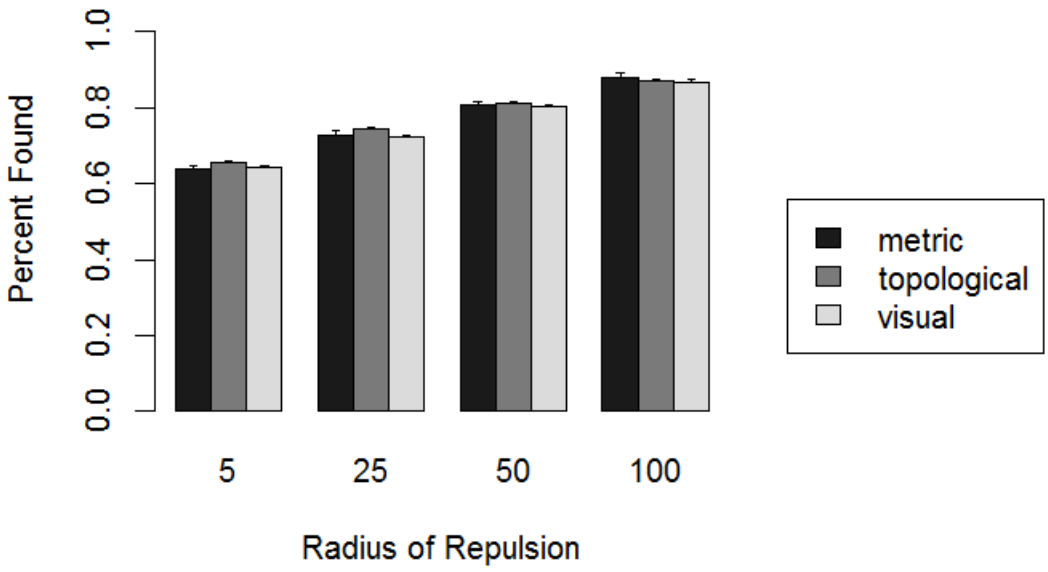

Figure IV.19: The distributions of PercentFound by radius of repulsion and model.

< 0.001, $z = 5{,}246{,}490$), which means that when the radius of orientation equaled 75, the topological model outperformed the visual model. The Wilcoxon Rank-Sum test found that the visual model has a significantly lower *PercentFound* than the topological model ($p < 0.01$, $z = 5{,}192{,}409$) when the radius of orientation was equal to 150. That is, the metric model outperformed the visual model when the radius of orientation was equal to 150. The trials with the radius of orientation equal to 200 were found by the Wilcoxon Rank-Sum test to have topological model means that were significantly higher than both the metric model means ($p = 0.0480$, $z = 705{,}371.5$) and the visual model means ($p = 0.0436$, $z = 2{,}289{,}062$). That is, the topological model outperformed both the metric and visual models.

Radius of Orientation	**Metric Mean (Std. Dev.)**	**Topological Mean (Std. Dev.)**	**Visual Mean (Std. Dev.)**
20	37.02% (29.02%)	44.03% (31.56%)	41.49% (30.11%)
40	54.62% (31.22%)	54.04% (31.86%)	53.22% (31.26%)
75	69.46% (30.04%)	70.72% (29.11%)	69.05% (29.33%)
150	84.14% (27.24%)	84.98% (26.99%)	83.82% (27.07%)
200	88.03% (26.30%)	88.49% (25.52%)	87.27% (26.63%)
300	90.91% (24.29%)	89.99% (24.32%)	89.76% (25.01%)

Table IV.14: The means and standard deviations of the Search task by radius of orientation.

The means and standard deviations for the Search task analyzed by the radius of attraction are presented

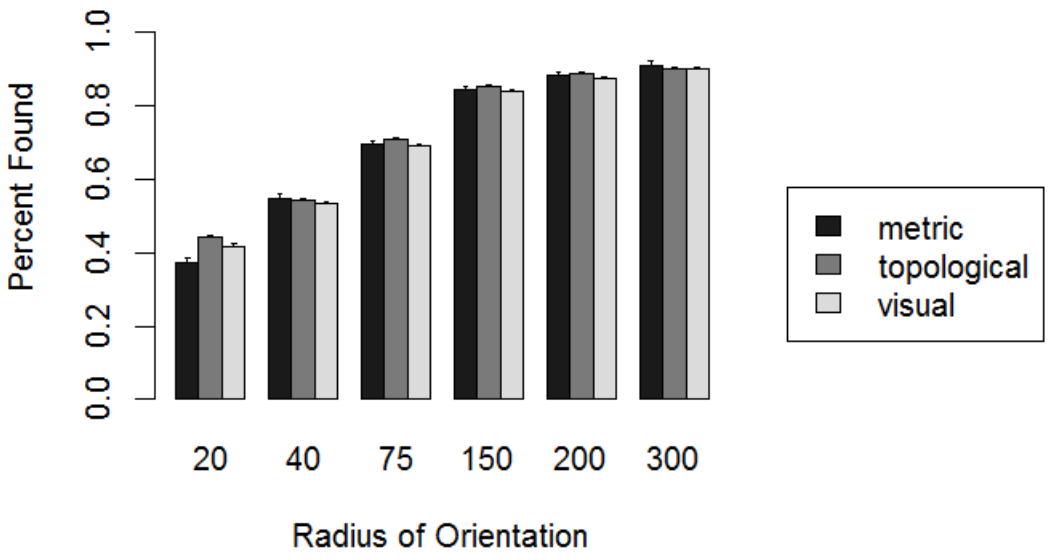

Figure IV.20: The distributions of PercentFound by radius of orientation and model.

in Table IV.15. The descriptive statistics are visualized in Figure IV.21. The Kruskal-Wallis test found no significant affect of the model type on the *PercentFound* when the results were analyzed by radius of attraction, when the radius of attraction was 80. The Kruskal-Wallis test found a significant affect of the model type on *PercentFound* when the radius of orientation was 25 ($p < 0.001$, $\chi^2(2) = 32.94$), 35 ($p < 0.01$, $\chi^2(2) = 10.26$), 80 ($p = 0.0456$, $\chi^2(2) = 6.1772$), 200 ($p = 0.0476$, $\chi^2(2) = 6.09$), 400 ($p = 0.0109$, $\chi^2(2) = 9.0457$), and 600 ($p < 0.01$, $\chi^2(2) = 11.19$). The Wilcoxon Rank-Sum test found a significant difference when the radius of attraction is equal to 25 between all possible pairwise model combinations. The signficiance results are included in Table IV.16. This analysis means that when the radius of attraction was equal to 25, the topological model finds a higher percentage of agents than either the metric or the visual models, and the topological model finds a higher percentage of agents than the metric model. The Wilcoxon Rank-Sum test found a significant difference between the topological and visual models when the radius of attraction equaled 35 ($p < 0.01$, z =8,929), which means that when the radius of attraction was equal to 35, the topological model outperformed the metric model. The Wilcoxon Rank-Sum test found that the metric model has a significantly higher mean *PercentFound* than the topological model ($p = 0.0173$, $z = 1{,}219{,}119$) and the visual model ($p = 0.0217$, $z = 914{,}147.5$) when the radius of attraction equaled 200. That is, the metric model outperforms the visual model and the topological model when the radius of attraction equaled

200. The trials when the radius of attraction was equal to 400 were found by the Wilcoxon Rank-Sum test to have topological model means that are significantly higher than both the metric model means ($p = 0.0180$, z = 3,594,143) and the visual model means ($p = 0.0137$, z = 11,546,567). That is, the topological model outperforms both the metric and visual models. The Wilcoxon Rank-Sum test found the topological model to have a significantly higher mean *PercentFound* than the visual model ($p < 0.001$, z =11,655,251), which means that the topological model performs significantly better than the visual model.

Radius of Attraction	**Metric Mean (Std. Dev.)**	**Topological Mean (Std. Dev.)**	**Visual Mean (Std. Dev.)**
25	21.26% (16.18%)	44.01% (31.66%)	35.82% (27.57%)
35	33.58% (23.82%)	43.95% (31.78%)	39.41% (28.93%)
80	61.54% (31.90%)	60.67% (32.30%)	60.16% (32.09%)
200	72.75% (32.54%)	70.14% (32.64%)	70.49% (32.07%)
400	76.29% (32.54%)	78.82% (30.86%)	77.72% (31.00%)
600	78.29% (30.75%)	78.92% (30.64%)	76.96% (31.62%)

Table IV.15: The means and standard deviations of the Search task by radius of attraction.

Pairing	**Significance**	**z-Value**
Metric-Visual	$p < 0.001$	6,211.5
Metric-Topological	$p < 0.001$	6675.5
Topological-Visual	$p = 0.0110$	39,106.5

Table IV.16: The significance results from the Wilcoxon Rank-Sum Test for the Search task when the radius of attraction equals 25.

A total of 8,208 trials were conducted for the Monitor task: 1,026 metric model trials, 4,104 trials using the topological model, and 3,078 trials under the visual model. The metric for the Monitor task was the percent of the environment covered (i.e., within sensor range of an agent), *PercentCoverage*. The metric model had a mean *PercentCoverage* of 88.78% (std. dev. = 23.30%). The mean *PercentCoverage* for the topological model was 98.41% (std. dev. = 1.77%), while the visual model had a mean *PercentCoverage* of 95.03% (std. dev. = 16.42%). The Percent Coverage data is visualized in Figure IV.22.

The Kruskal-Wallis test found a strong affect of model on *PercentCoverage* ($p < 0.001$, $\chi^2(2) = 2{,}190.99$). The Wilcoxon Rank-Sum test found highly significant differences between all pairings, as presented in Table IV.17. These results show that the percent coverage for the visual model was significantly higher than either of the other two models, and that the topological model had a significantly higher *PercentCoverage* than the metric model.

The means and standard deviations of the Monitor results grouped by number of agents are reported in Table IV.18. The descriptive statistics are visualized in Figure IV.23. The Kruskal-Wallis test found a highly significant impact of the model type on *PercentCoverage* for each subgroup by number of agents,

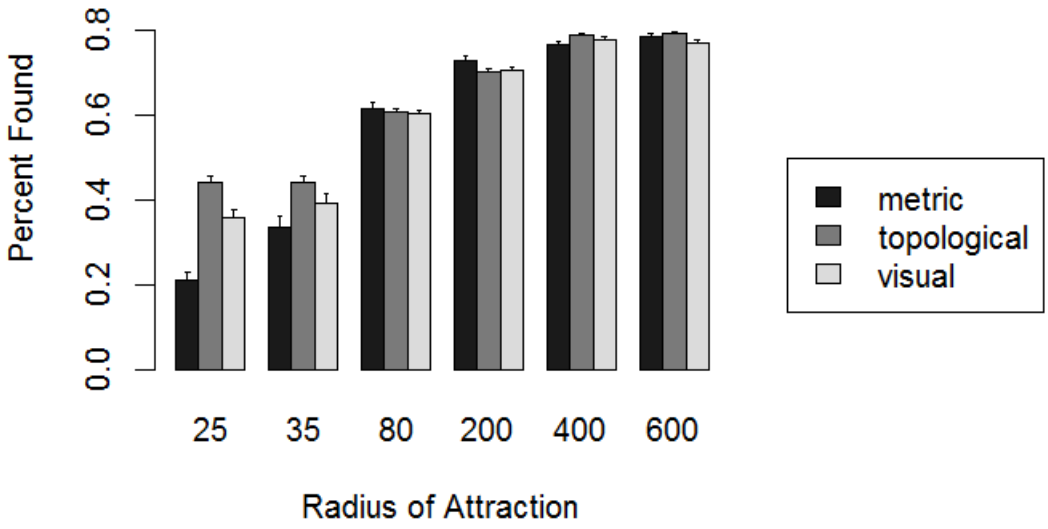

Figure IV.21: The distributions of PercentFound by radius of attraction and model.

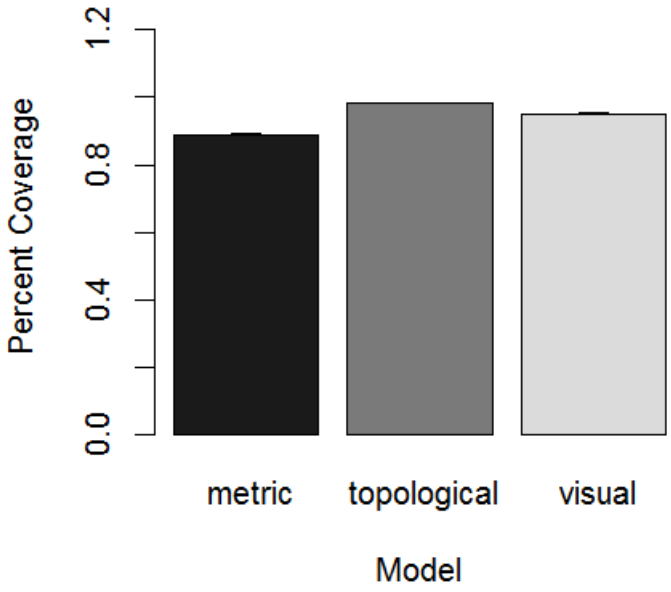

Figure IV.22: The distributions for each model in the Monitor task

Pairing	Significance	z-Value
Metric-Visual	$p < 0.001$	839,495
Metric-Topological	$p < 0.001$	2,315,698
Topological-Visual	$p < 0.001$	2,327,127

Table IV.17: The significance results from the Wilcoxon Rank-Sum Test for the Monitor task.

as detailed in Table IV.19. The Wilcoxon Rank-Sum test found that for trials with 50 agents, there was a highly significant difference between the metric and topological models ($p < 0.001$, z = 67,220), the metric and visual models ($p < 0.001$, z = 31,386.5), and the topological and visual models ($p < 0.001$, z = 59,997). The Wilcoxon Rank-Sum test found that for trials with 100 agents, there was a highly significant difference between the metric and topological models ($p < 0.001$, z = 68,443.5), the metric and visual models ($p < 0.001$, z = 20,312), and the topological and visual models ($p < 0.001$, z = 44,440). The Wilcoxon Rank-Sum test found that for trials with 250 agents, there was a highly significant difference between the metric and visual models ($p < 0.001$, z = 32,720), and the topological and visual models ($p < 0.001$, z = 114,025). The Wilcoxon Rank-Sum test found that for trials with 500 agents, there was a highly significant difference between the metric and visual models ($p < 0.001$, z = 30,214.5), and the topological and visual models ($p < 0.001$, z = 101,976.5). The Wilcoxon Rank-Sum test found that for trials with 1000 agents, there was a highly significant difference between the metric and topological models ($p < 0.01$, z = 160,591), the metric and visual models ($p < 0.001$, z = 53,102), and the topological and visual models ($p < 0.001$, z = 154,513.5). These analyses indicate that for all possible number of agents, the topological model had a significantly higher coverage and better performance than the visual model, and that the metric model had a significantly lower coverage and worse performance than the visual model. All trials with 50,100, or 1000 agents also indicate that the topological model has a significantly higher *PercentCoverage* and better performance than the metric model.

Number of Agents	Metric Mean (Std. Dev.)	Topological Mean (Std. Dev.)	Visual Mean (Std. Dev.)
50	87.35% (25.74%)	97.31% (2.06%)	94.17% (18.22%)
100	90.70% (20.83%)	96.94% (2.50%)	96.10% (14.40%)
250	87.37% (24.57%)	98.62% (1.14%)	94.28% (17.49%)
500	90.92% (20.09%)	98.75% (1.08%)	96.31% (13.93%)
1000	87.91% (24.45		

Table IV.18: The means and standard deviations of the Monitor task by number of agents.

The means and standard deviations of the Monitor results grouped by number of obstacles are provided in Table IV.20. The descriptive statistics are visualized in Figure IV.24. The Kruskal-Wallis test found a highly significant impact of the model type on *PercentCoverage* for each subgroup by number of obstacles,

Number of Agents	Significance	$\chi^2(2)$
50	$p < 0.001$	329.61
100	$p < 0.001$	464.76
250	$p < 0.001$	417.69
500	$p < 0.001$	493.76
1000	$p < 0.001$	607.85

Table IV.19: The significance results from the Kruskal-Wallis Test for the Monitor task by number of agents.

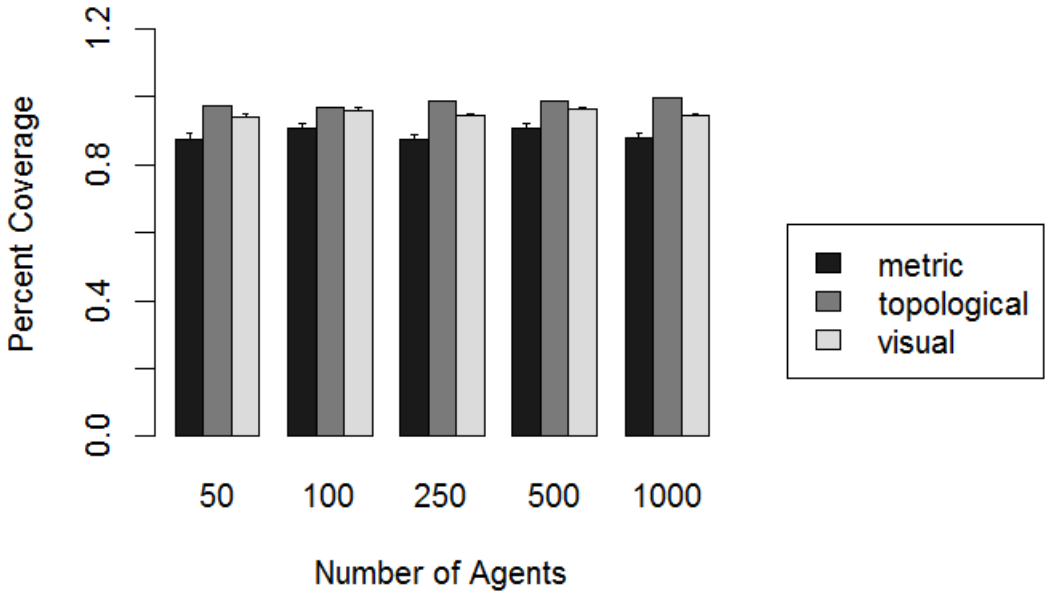

Figure IV.23: The distributions of PercentCoverage by number of agents and model.

as detailed in Table IV.21. The Wilcoxon Rank-Sum test found that for trials with 0 obstacles, there was a highly significant difference between the metric and visual models ($p < 0.001$, z = 56,568.5), and the topological and visual models ($p < 0.001$, z = 186,444). The Wilcoxon Rank-Sum test found that for trials with 25 obstacles, there was a significant difference between the metric and topological models (p = 0.0147, z = 159,773), the metric and visual models ($p < 0.001$, z = 60,035.5), and the topological and visual models ($p < 0.001$, z = 159,349.5). The Wilcoxon Rank-Sum test found that for trials with 50 obstacles, there was a highly significant difference between the metric and topological models ($p < 0.001$, z = 173,714.5), the metric and visual models ($p < 0.001$, z = 60,946.5), and the topological and visual models ($p < 0.001$, z = 144,441). The Wilcoxon Rank-Sum test found that for trials with 100 obstacles, there was a highly significant difference between the metric and visual models ($p < 0.001$, z = 19,303) and the topological and visual models ($p <$

0.001, z = 54,310). The Wilcoxon Rank-Sum test found that for trials with 250 obstacles, there was a highly significant difference between the metric and topological models ($p < 0.01$, z = 7,325.5), the metric and visual models ($p < 0.001$, z = 2,123.5), and the topological and visual models ($p < 0.001$, z = 5,625). These analyses indicate that for all possible number of obstacles, the topological model had a significantly higher coverage and better performance than the visual model, and that the metric model had a significantly lower coverage and worse performance than the visual model. All trials with 25, 50, or 250 obstacles also indicate that the topological model has a significantly higher *PercentCoverage* and better performance than the metric model.

Number of Obstacles	**Metric Mean (Std. Dev.)**	**Topological Mean (Std. Dev.)**	**Visual Mean (Std. Dev.)**
0	88.54% (23.39%)	98.39% (2.01%)	94.90% (16.56%)
25	88.77% (23.34%)	98.54% (1.38%)	95.03% (16.43%)
50	88.99% (23.22%)	97.95% (2.10%)	95.18% (16.28%)
100	89.01% (23.08%)	98.66% (1.27%)	95.14% (16.22%)
250	88.29% (24.52%)	99.37% (00.66%)	94.68% (17.19%)

Table IV.20: The means and standard deviations of the Monitor task by number of obstacles.

Number of Obstacles	**Significance**	$\chi^2(2)$
0	$p < 0.001$	493.57
25	$p < 0.001$	577.69
50	$p < 0.001$	643.04
100	$p < 0.001$	371.55
250	$p < 0.001$	136.33

Table IV.21: The significance results from the Kruskal-Wallis Test for the Monitor task by number of obstacles.

The means and standard deviations for the monitor results grouped by radius of repulsion are provided in Table IV.22. The descriptive statistics are visualized in Figure IV.25. The Kruskal-Wallis test found a highly significant impact of the model type on *PercentCoverage* for each subgroup by radius of repulsion, as detailed in Table IV.23. The Wilcoxon Rank-Sum test found that for trials with radius of repulsion equal to 5, there was a highly significant difference between the metric and visual models ($p < 0.001$, z = 106,090.5), the metric and topological models ($p < 0.001$, z = 272,440.5), and the topological and visual models ($p < 0.001$, z = 430,039). The Wilcoxon Rank-Sum test found that for trials with radius of repulsion equal to 25, there was a highly significant difference between the metric and topological models ($p < 0.001$, z = 189,636), the metric and visual models ($p < 0.001$, z = 55,982.5), and the topological and visual models ($p < 0.001$, z = 157,497.5). The Wilcoxon Rank-Sum test found that for trials with radius of repulsion equal to 50, there was a highly significant difference between the metric and topological models ($p < 0.001$, z = 117,715.5), the metric and visual models ($p < 0.001$, z = 41,816), and the topological and visual models ($p < 0.001$,

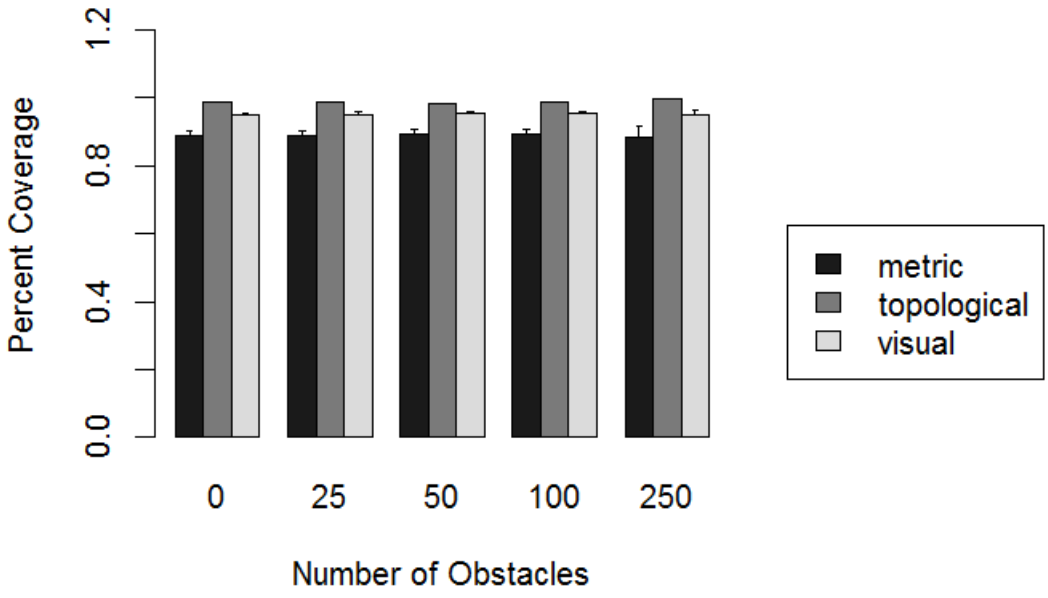

Figure IV.24: The distributions of PercentCoverage by number of obstacles and model.

z = 73,767). These analyses indicate that for trials with the radius of repulsion equal to 5, 25, or 50, the topological model has a significantly higher *PercentCoverage* and better performance than both the visual and metric models, and the metric model has a significantly lower *PercentCoverage* and worse performance than the visual model. The Wilcoxon Rank-Sum test found that for trials with radius of repulsion equal to 100, there was a highly significant difference between the metric and topological models ($p < 0.001$, z = 49,543.5), the metric and visual models ($p < 0.001$, z = 21,146), and the topological and visual models ($p < 0.001$, z = 39,956.5). That is, for trials with radius of repulsion equal to 100, the visual model has a significantly higher *PercentCoverage* and better performance than the metric and topological models, and the metric model has higher *PercentCoverage* than the topological model.

Radius of Repulsion	**Metric Mean (Std. Dev.)**	**Topological Mean (Std. Dev.)**	**Visual Mean (Std. Dev.)**
5	81.04% (30.27%)	98.01% (1.95%)	91.00% (22.79%)
25	90.83% (18.61%)	98.14% (1.75%)	96.50% (11.81%)
50	94.06% (15.03%)	98.96% (1.05%)	97.72% (9.31%)
100	99.34% (2.09%)	99.32% (1.56%)	99.78% (1.24%)

Table IV.22: The means and standard deviations of the Monitor task by radius of repulsion.

The means and standard deviations for the Monitor task results grouped by radius of orientation are

Radius of Repulsion	Significance	$\chi^2(2)$
5	$p < 0.001$	703.42
25	$p < 0.001$	713.43
50	$p < 0.001$	581.98
100	$p < 0.001$	324.49

Table IV.23: The significance results from the Kruskal-Wallis Test for the Monitor task by radius of repulsion.

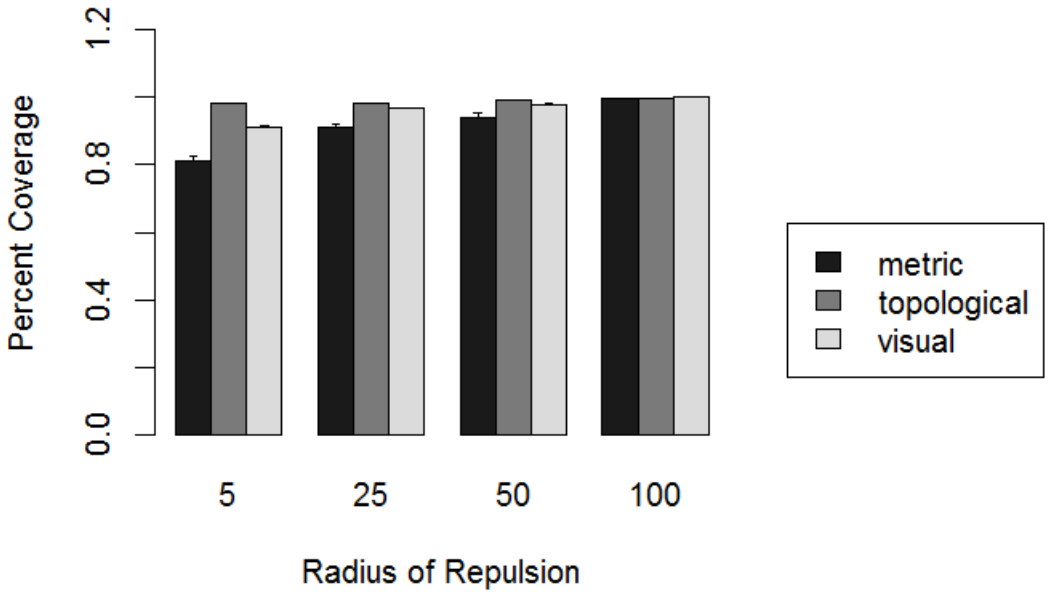

Figure IV.25: The distributions of PercentCoverage by radius of repulsion and model.

presented in Table IV.24. The descriptive statistics are visualized in Figure IV.26. The Kruskal-Wallis test found a highly significant impact of the model type on *PercentCoverage* for each subgroup by radius of orientation, as detailed in Table IV.25. The Wilcoxon Rank-Sum test found that for trials with radius of orientation equal to 20, there was a highly significant difference between the metric and topological models ($p < 0.001$, z = 13,870.5), the metric and visual models ($p < 0.001$, z = 10,342), and the topological and visual models ($p < 0.001$, z = 60,338). The Wilcoxon Rank-Sum test found that for trials with radius of orientation equal to 40, there was a highly significant difference between the metric and topological models ($p < 0.001$, z = 39,690), the metric and visual models ($p < 0.001$, z = 16,218.5), and the topological and visual models ($p < 0.001$, z = 68,097.5). The Wilcoxon Rank-Sum test found that for trials with radius of orientation equal to 75, there was a highly significant difference between the metric and topological models ($p < 0.01$, z = 92,493), the metric and visual models ($p < 0.001$, z = 39,610), and the topological and visual

models ($p < 0.001$, $z = 150{,}537$). These analyses indicate that for trials where the radius of orientation is equal to 20, 40, or 75, the topological model has a significantly higher *PercentCoverage* and better performance than both the metric and visual models, and the visual model has a significantly higher *PercentCoverage* than the metric model. The Wilcoxon Rank-Sum test for a radius of orientation equal to 150 found a highly significant difference between the metric and topological models ($p < 0.001$, $z = 120{,}594$), the metric and visual models ($p < 0.001$, $z = 39{,}460.5$) and the topological and visual models ($p < 0.001$, $z = 83{,}348.5$). That is, the trials where the radius of orientation was equal to 150, the visual model had a significantly higher *PercentCoverage* and better performance than both the metric and topological models, and the topological model has higher *PercentCoverage* than the metric model. The Wilcoxon Rank-Sum test found that when the radius of orientation equaled 200, there was a highly significant difference between the metric and topological models ($p < 0.001$, $z = 72{,}051.5$), the metric and visual models ($p < 0.001$, $z = 18{,}650.5$), and the topological and visual models ($p < 0.001$, $z = 13{,}887.5$). The Wilcoxon Rank-Sum test found that for trials with radius of orientation equal to 300, there was a highly significant difference between the metric and topological models ($p < 0.001$, $z = 65{,}354$), the metric and visual models ($p < 0.001$, $z = 18{,}351.5$), and the topological and visual models ($p < 0.001$, $z = 29{,}249.5$). These analyses mean that for trials where the radius of orientation is 200 or 300, the visual model has a significantly higher *PercentCoverage* and better performance than both the metric and topological models, and the metric model has higher *PercentCoverage* than the topological model.

Radius of Orientation	**Metric Mean (Std. Dev.)**	**Topological Mean (Std. Dev.)**	**Visual Mean (Std. Dev.)**
20	58.03% (40.15%)	97.96% (1.93%)	77.37% (34.71%)
40	83.04% (24.18%)	97.92% (1.79%)	93.36% (16.23%)
75	84.63% (22.27%)	98.03% (1.77%)	93.97% (14.95%)
150	97.64% (3.43%)	98.47% (1.89%)	99.46% (1.72%)
200	99.60% (0.90%)	98.95% (1.26%)	99.98% (0.12%)
300	99.70% (0.69%)	99.18% (1.38%)	99.97% (0.16%)

Table IV.24: The means and standard deviations of the Monitor task by radius of orientation.

Radius of Orientation	**Significance**	$\chi^2(2)$
20	$p < 0.001$	89.32
40	$p < 0.001$	232.89
75	$p < 0.001$	345.19
150	$p < 0.001$	650.26
200	$p < 0.001$	716.13
300	$p < 0.001$	563.01

Table IV.25: The significance results from the Kruskal-Wallis Test for the Monitor task by radius of orientation.

The means and standard deviations for the Monitor task results grouped by radius of attraction are reported

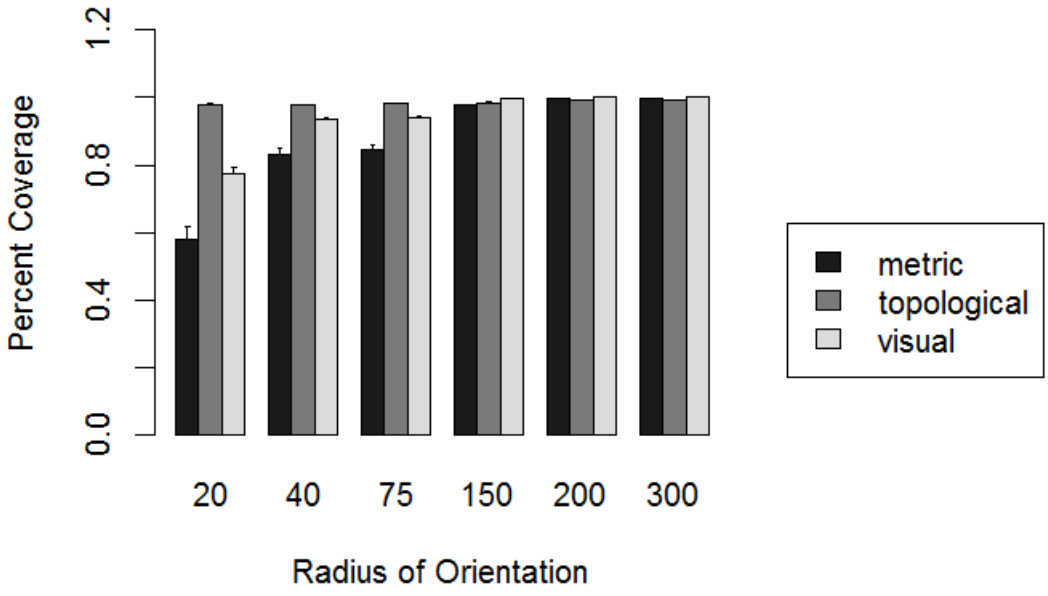

Figure IV.26: The distributions of PercentCoverage by radius of orientation and model.

in Table IV.26. The descriptive statistics are visualized in Figure IV.27. The Kruskal-Wallis test found a highly significant impact of the model type on *PercentCoverage* for each subgroup by number of agents, as detailed in Table IV.27. The Wilcoxon Rank-Sum test found that for trials with radius of attraction equal to 25, there was a highly significant difference between the metric and topological models ($p < 0.001$, $z = 0$), the metric and visual models ($p < 0.001$, $z = 174$) and the topological and visual models ($p < 0.01$, $z = 2{,}888$). The Wilcoxon Rank-Sum test found that for trials with radius of attraction equal to 35, there was a highly significant difference between the metric and topological models ($p < 0.001$, $z = 0$), the metric and visual models ($p < 0.001$, $z = 182$) and the topological and visual models ($p < 0.01$, $z = 2{,}888$). The Wilcoxon Rank-Sum test when the radius of attraction was equal to 80 found a highly significant difference between the metric and topological models ($p < 0.001$, $z = 0$), the metric and visual models ($p < 0.001$, $z = 6{,}436$) and the topological and visual models ($p < 0.001$, $z = 102{,}830.5$). The Wilcoxon Rank-Sum test with radius of attraction equal to 200 determined that a highly significant difference existed between the metric and topological models ($p < 0.001$, $z = 11{,}914.5$), the metric and visual models ($p < 0.001$, $z = 12{,}979$) and the topological and visual models ($p < 0.001$, $z = 132{,}951$). These analyses indicate that for trials where the radius of attraction is equal to 25, 35, 80, or 200, the topological model has a significantly higher *PercentCoverage* and better performance than both the metric and visual models, and the visual model has a

significantly higher *PercentCoverage* than the metric model. The Wilcoxon Rank-Sum results for a radius of attraction equal to 400 found a highly significant difference between the metric and topological models ($p <$ 0.001, z = 339,180.5), the metric and visual models ($p < 0.001$, z = 69,672) and the topological and visual models ($p < 0.001$, z = 86.451.5). The Wilcoxon Rank-Sum test found that for trials with radius of attraction equal to 600, there was a highly significant difference between the metric and topological models ($p < 0.001$, z = 391,903), the metric and visual models ($p < 0.001$, z = 89,775) and the topological and visual models ($p < 0.001$, z = 44,118). These analyses indicate that for trials with a radius of attraction is equal to 400 or 600, the visual model has a significantly higher *PercentCoverage* and better performance than both the metric and topological models, and the metric model has a significantly higher *PercentCoverage* than the topological model.

Radius of Attraction	**Metric Mean (Std. Dev.)**	**Topological Mean (Std. Dev.)**	**Visual Mean (Std. Dev.)**
25	6.67% (2.10%)	97.87% (2.04%)	42.70% (41.48%)
35	12.06% (3.65%)	98.00% (1.93%)	49.07% (37.94%)
80	44.86% (9.75%)	97.97% (1.79%)	76.87% (24.30%)
200	92.08% (4.01%)	98.18% (1.86%)	97.96% (3.51%)
400	99.50% (0.75%)	98.55% (1.74%)	99.96% (0.16%)
600	99.69% (0.81%)	98.59% (1.66%)	1.00% (0.00%)

Table IV.26: The means and standard deviations of the Monitor task by radius of attraction.

Radius of Attraction	**Significance**	$\chi^2(2)$
25	$p < 0.001$	47.62
35	$p < 0.001$	47.20
80	$p < 0.001$	280.90
200	$p < 0.001$	430.11
300	$p < 0.001$	1,498.75
600	$p < 0.001$	1,860.44

Table IV.27: The significance results from the Kruskal-Wallis Test for the Monitor task by radius of attraction.

IV.2.3 Avoid Object

The Avoid task had a total of 2160 trials: metric = 270 trials, topological = 1,080 trials, and visual = 810 trials. The resulting metric value for the Avoid task was the expanse, measured in units squared. The mean expanse for the metric trials was 440,312.2 units^2 (std. dev. = 554,458.8 units^2). The topological trials had a mean expanse of 537,337.2 units^2 (std. dev = 608,850.1 units^2). The visual model trials had a mean expanse of 409,926.9 units^2 (std. dev. = 504,317.5 units^2). These means and standard errors are visualized in Figure IV.28.

The Kruskal-Wallis test found a highly significant affect of model on expanse ($p < 0.001$, $\chi^2(2) = 61.96$). The Wilcoxon Rank-Sum test found a highly significant difference between the the topological and visual

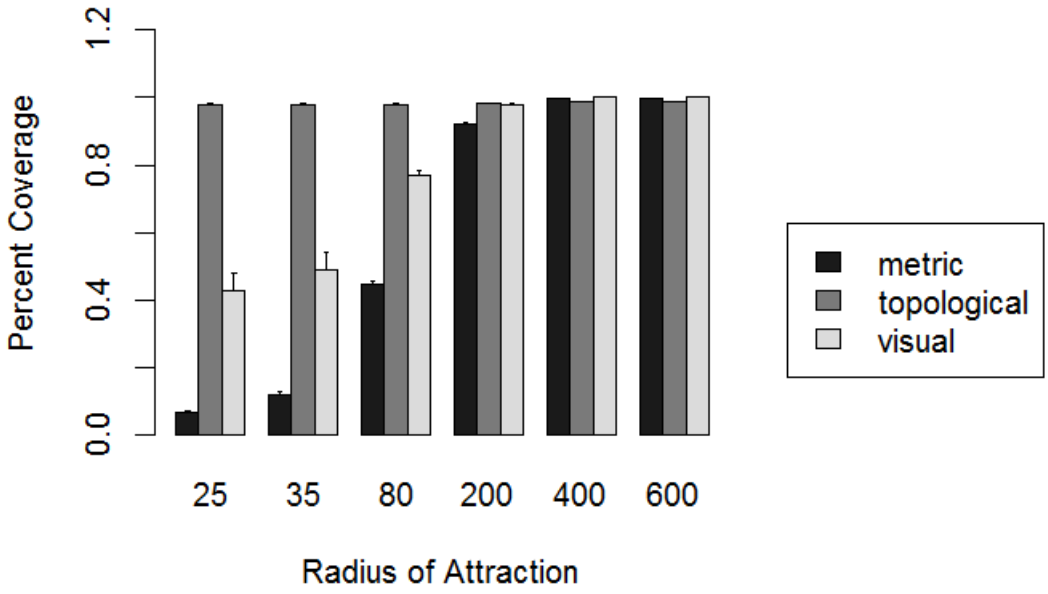

Figure IV.27: The distributions of PercentCoverage by radius of attraction and model.

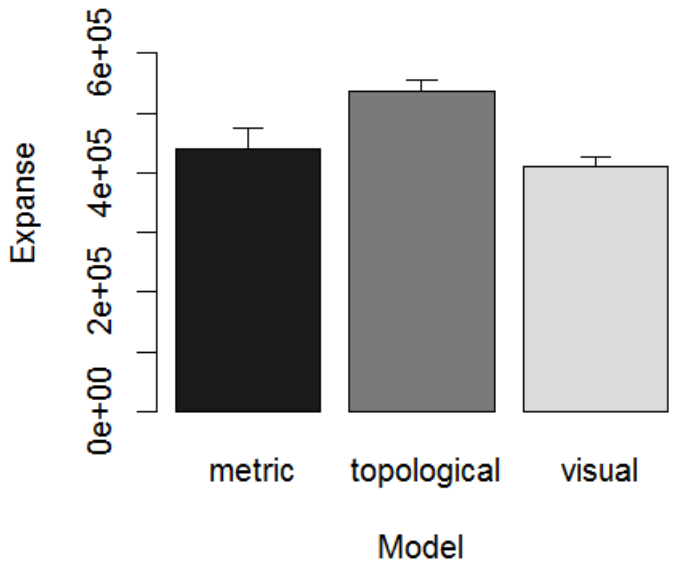

Figure IV.28: The distributions for each model in the Avoid task.

models ($p < 0.001$, z = 523,154) and the topological and metric models ($p < 0.001$, z = 117,576). No significant difference was found between the visual and metric models. This analysis demonstrates that the expanse of the topological model was significantly higher than that of both the metric and visual models.

The means and standard deviations by number of agents are presented in Table IV.28. The descriptive statistics are visualized in Figure IV.29. The Kruskal-Wallis test found a significant affect of the model type on expanse by number of agents; the results are provided in Table IV.29. The Wilcoxon Rank-Sum test for the trials with 50 agents found that there was a highly significant difference between the metric and topological models ($p < 0.001$, z = 3,584), between the metric and visual models ($p < 0.01$, z = 3,308), and the topological and visual models ($p < 0.001$, z = 21,600). The Wilcoxon Rank-Sum test for the trials with 100 agents found that there was a highly significant difference between the metric and topological models ($p < 0.001$, z = 2,713), between the metric and visual models (p = 0.0203, z = 3,451), and the topological and visual models ($p < 0.001$, z = 25,677). These analyses mean that the topological model had a significantly higher mean expanse than the visual and metric models, and the metric model had a significantly lower mean expanse than the visual model in trials with 50 or 100 agents. The Wilcoxon Rank-Sum test for the trials with 250 agents found that there was a highly significant difference between the metric and topological models ($p < 0.001$, z = 3,148) and between the topological and visual models ($p < 0.001$, z = 24,925). The Wilcoxon Rank-Sum test for the trials with 500 agents found that there was a highly significant difference between the metric and topological models ($p < 0.001$, z = 2,377) and between the topological and visual models ($p < 0.001$, z = 29,087). That is, the topological model performed signficantly better than the metric and visual models with 250 or 500 agents. The Wilcoxon Rank-Sum test for the trials with 1000 agents found that there was a highly significant difference between the metric and topological models ($p < 0.001$, z = 3,462), between the metric and visual models (p = 0.0428, z = 5,180), and between the topological and visual models ($p < 0.001$, z = 26,643). This analysis means that for the trials where there were 1000 agents, the topological model performed worse than the metric and visual models due to a higher mean expanse, and the visual model performed better than the metric model due to a lower expanse.

Number of Agents	**Metric Mean (Std. Dev.)**	**Topological Mean (Std. Dev.)**	**Visual Mean (Std. Dev.)**
50	56,004.37 (33189.77)	78,299.28 (23188.93)	68,614.19 (21744.25)
100	57,993.01 (38,551.4)	94,454.55 (27,510.92)	71,448.41 (24,758.35)
250	294,259.6 (113,405.2)	390,863.2 (83,540.75)	315,140.8 (102,205.9)
500	307,334.4 (122,095.4)	437,009.9 (91,754.03)	293,959.2 (118,815.6)
1000	1,485,970 (277,095)	1,686,059 (278,527.4)	1,300,472 (446,413.2)

Table IV.28: The means and standard deviations of the Avoid task by number of agents.

A similar analysis was conducted for the results grouped by the radii of attraction, orientation, and re-

Number of Agents	Significance	$\chi^2(2)$
50	$p < 0.001$	28.69
100	$p < 0.001$	78.19
250	$p < 0.001$	61.55
500	$p < 0.001$	135.10
1000	$p < 0.001$	81.53

Table IV.29: The significance results from the Kruskal-Wallis Test for the Avoid task by number of agents.

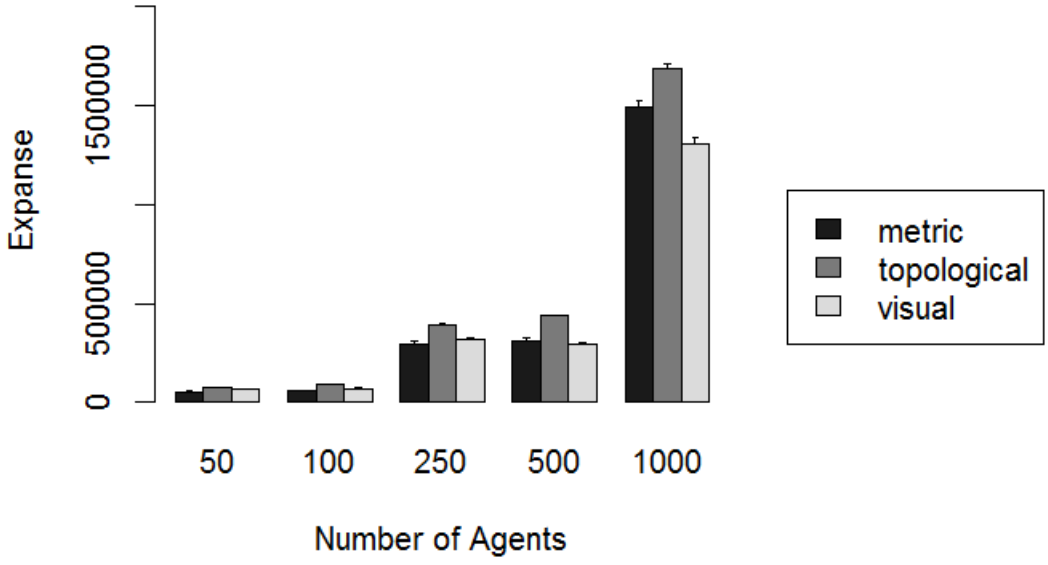

Figure IV.29: The distributions for each model in the Avoid task by number of agents.

pulsion. The means and standard deviations for the results grouped by radius of repulsion are reported in Table IV.30, and the descriptive statistics are visualized in Figure IV.30. The Kruskal-Wallis test found a significant affect of the model type on the expanse for each of the subgroups, with significance as detailed in Table IV.31. The Wilcoxon Rank-Sum test for the trials with the radius of repulsion equal to 5 found that there was a highly significant difference between the metric and topological models ($p < 0.01$, z = 17,612) and between the topological and visual models ($p < 0.001$, z = 82,245). The Wilcoxon Rank-Sum test for the trials with the radius of repulsion equal to 25 found that there was a highly significant difference between the metric and topological models ($p < 0.001$, z = 8,338) and between the topological and visual models ($p < 0.001$, z = 42,049). The Wilcoxon Rank-Sum test for the trials with the radius of repulsion equal to 50 found that there was a highly significant difference between the metric and topological models ($p < 0.01$, z

= 4,547) and between the topological and visual models ($p < 0.001$, z = 21,738). These results imply that when the radius of repulsion equaled 5, 25 or 50, the topological model had a significantly higher expanse and thus performed worse than the metric and visual models. The Wilcoxon Rank-Sum test for the trials with the radius of repulsion equal to 100 found a significant difference between the topological and visual models ($p < 0.01$, z = 8,923), indicating that the topological model had a significantly higher expanse, and worse performance, with respect to the task than the visual model.

Radius of Repulsion	**Metric Mean (Std. Dev.)**	**Topological Mean (Std. Dev.)**	**Visual Mean (Std. Dev.)**
5	419,497.3 (580,161.4)	505,886.8 (593,135.9)	354,684.4 (474,285.4)
25	411,736.3 (531,628)	543,671.6 (614,945.2)	387,298.1 (478,835.7)
50	442,152.5 (520,387.9)	546,288.6 (610,290.2)	441,205.6 (497,198.5)
100	561,099.3 (582,504.3)	604,047.9 (639,640.2)	574,992.4 (613,348.8)

Table IV.30: The means and standard deviations of the Avoid task by radius of repulsion.

Radius of Repulsion	**Significance**	$\chi^2(2)$
5	$p < 0.001$	34.12
25	$p < 0.001$	28.23
50	$p < 0.001$	15.40
100	$p = 0.0117$	8.89

Table IV.31: The significance results from the Kruskal-Wallis Test for the Avoid task by radius of repulsion.

The means and standard deviations for the results grouped by radius of orientation are provided in Table IV.32. The descriptive statistics are visualized in Figure IV.31. The Kruskal-Wallis test found no significant affect by model type on expanse when the radius of orientation was equal to 20, 40, or 75. The Kruskal-Wallis test found a significant affect of the model type on expanse when the radius of orientation was equal to 150 ($p < 0.01$, $\chi^2(2) = 13.42$), 200 ($p < 0.001$, $\chi^2(2) = 20.34$), or 300 ($p < 0.001$, $\chi^2(2) = 38.12$). The Wilcoxon Rank-Sum test found a significant difference for radius of orientation equal to 150 between the metric and topological models ($p = 0.0254$, z = 5,856) and the visual and topological models ($p < 0.001$, z = 25,821). The Wilcoxon Rank-Sum test found a significant difference in trials with radius of orientation equal to 200 between the metric and topological models ($p < 0.01$, z = 2,313) and the visual and topological models ($p < 0.001$, z = 12,439). The Wilcoxon Rank-Sum test found a significant difference in trials with radius of orientation equal to 300 between the metric and topological models ($p < 0.001$, z = 1,924) and the visual and topological models ($p < 0.001$, z = 13,429). These analyses imply that when the radius of orientation was equal to 150, 200, or 300, the topological model had a significantly higher expanse and lower performance relative to the task than both the metric and visual models.

The means and standard deviations for the results grouped by radius of attraction are presented in Table IV.33. The descriptive statistics are visualized in Figure IV.32. The Kruskal-Wallis test found no significant

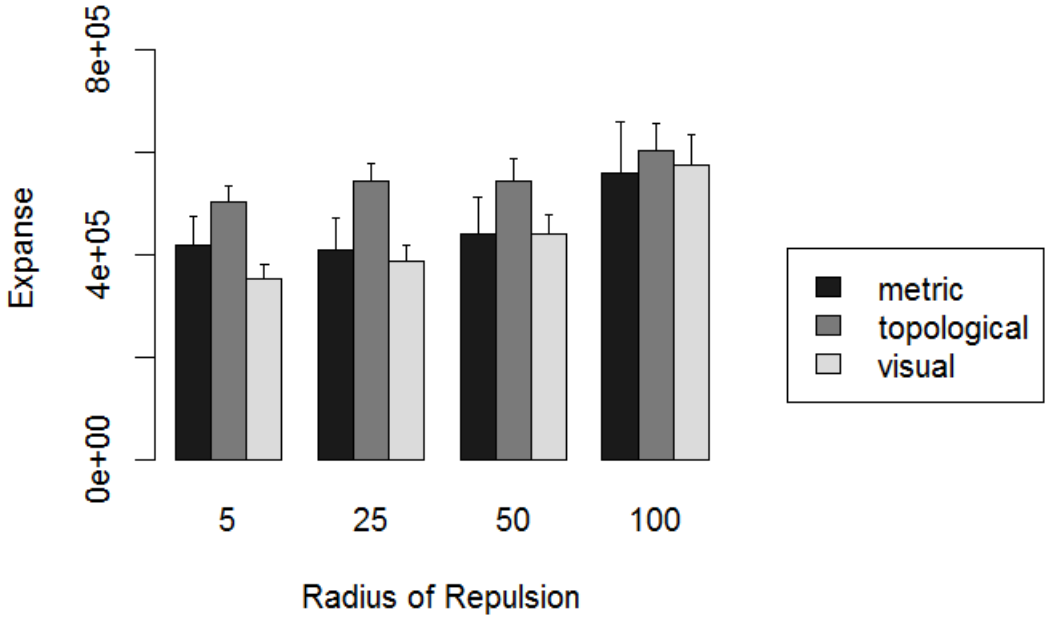

Figure IV.30: The distributions for each model in the Avoid task by radius of repulsion.

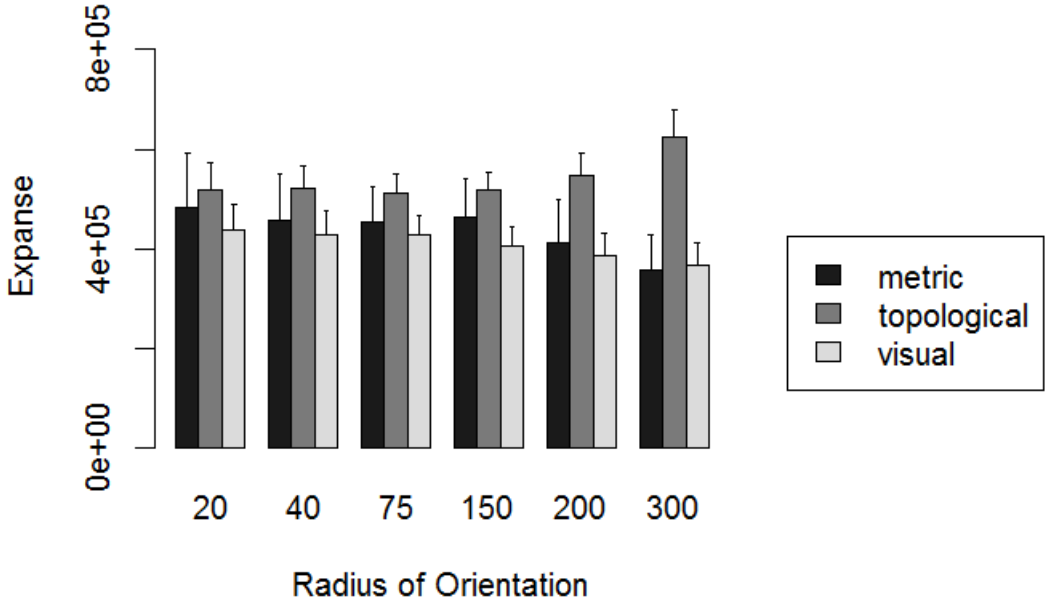

Figure IV.31: The distributions of expanse by radius of orientation and model.

Radius of Orientation	Metric Mean (Std. Dev.)	Topological Mean (Std. Dev.)	Visual Mean (Std. Dev.)
20	484,925.6 (585,212.6)	520,252.5 (595,978.7)	437,101.7 (512,542.8)
40	459,072.4 (577,606.1)	520,563.1 (598,694.1)	430,150.2 (515,227)
75	454,234.6 (556,578.3)	512,261.1 (617,367.5)	428,946.1 (516,295.4)
150	465,029.6 (594,652.3)	517,658 (580,664.3)	407,633.7 (508,409.1)
200	413,300.9 (553,563.2)	546,069.4 (593,726.9)	385,673.2 (490,532.1)
300	357,143.6 (459,514.4)	625,325.2 (670,228.1)	368,487.3 (482,582.8)

Table IV.32: The means and standard deviations of the Avoid task by radius of orientation.

affect of the model type on expanse in the trials where the radius of attraction was equal to 25, 35, or 80. The Kruskal-Wallis test found a significant affect of the model type on expanse when the radius of attraction was equal to 200 (p = 0.0372, $\chi^2(2)$ = 6.58), 400 ($p < 0.001$, $\chi^2(2)$ = 33.42), or 600 ($p < 0.001$, $\chi^2(2)$ = 42.05). The Wilcoxon Rank-Sum test found a significant difference for a radius of attraction equal to 200 between the visual and topological models (p = 0.0118, z = 17,360), indicating that the topological model had a significantly higher expanse and performed less effectively than the visual model. The Wilcoxon Rank-Sum test found a significant difference for a radius of attraction equal to 400 between the metric and topological models ($p < 0.001$, z = 12,202) and the visual and topological models ($p < 0.001$, z = 60,707). This analysis indicates that when the radius of attraction was equal to 400, the topological model had a significantly higher mean expanse and performed worse than the metric and visual models. The Wilcoxon Rank-Sum test found a significant difference in trials with radius of attraction equal to 600 between the metric and topological models ($p < 0.001$, z = 11,065), the metric and visual models (p = 0.0282, z = 10,273), and the visual and topological models ($p < 0.001$, z = 61,049). These analyses imply that when the radius of attraction equaled 600, the topological model had a significantly higher expanse and lower performance relative to the task than both the metric and visual models, and that the metric model had a significantly lower expanse and higher performance than the visual model.

Radius of Attraction	Metric Mean (Std. Dev.)	Topological Mean (Std. Dev.)	Visual Mean (Std. Dev.)
25	542,778.2 (660,826.5)	521,021.8 (608,943.5)	468,528.2 (550,152.6)
35	546,382.1 (649,677.6)	521,757.9 (610,805.8)	465,022.7 (546,166.8)
80	527,356.1 (587,783.6)	519,266.8 (622,439)	471,620.8 (553,198.5)
200	500,912.3 (595,592.8)	512,150.5 (587,831.2)	426,807.1 (516,184.8)
400	432,963 (555,577.1)	548,818.2 (611,474.2)	402,351 (500,749.1)
600	373,394.8 (513,439.5)	547,644.1 (616,598.5)	381,243.8 (480,998.3)

Table IV.33: The means and standard deviations of the Avoid task by radius of attraction.

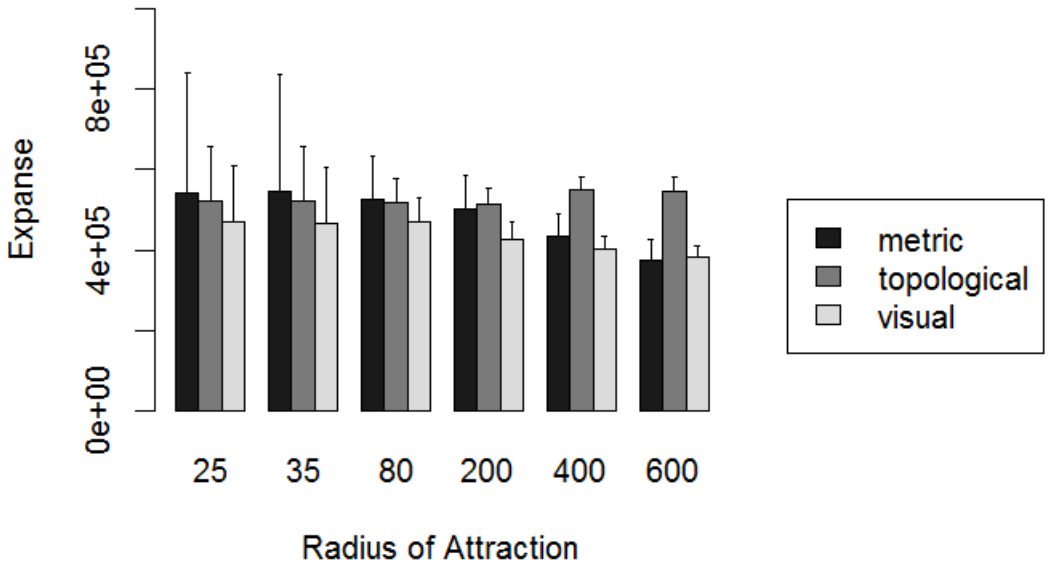

Figure IV.32: The distributions of expanse by radius of attraction and model.

IV.2.4 Follow Object

The Follow task had 8,208 trials in total, decomposed by model: metric = 1,026 trials, topological = 4,104 trials, and visual = 3,078 trials. The metrics for the Follow Object task were network efficiency, measured by the number of timesteps that it took 90% of the agents to become informed, and the percent of agents that had a heading within 30 degrees of the target's heading. The metric model had a mean network efficiency of 8.87 timesteps, (std. dev. = 11.11 timesteps). The mean network efficiency for the topological model was 11.44 timesteps (std. dev. = 7.26 timesteps), while the visual model mean network efficiency was 15.60 timesteps (std. dev. = 12.87 timesteps). The network efficiency data distributions for each model can be viewed in Figure IV.33. The Kruskal-Wallis test found a highly significant affect of the model type on network efficiency ($p < 0.001$, $\chi^2(2) = 515.47$). The Wilcoxon Rank-Sum test found highly significant differences between all three pairings, as presented in Table IV.34. The results imply that the metric model resulted in a significantly faster time for information propagation (and better network efficiency) than both the topological and visual models. The topological model has a significantly faster time for information propagation (and better efficiency) than the visual model.

The means and standard deviations by number of agents are presented in Table IV.35. The descriptive

Pairing	Significance	z-Value
Metric-Visual	$p < 0.001$	859,688
Metric-Topological	$p < 0.001$	1,394,966
Topological-Visual	$p < 0.001$	5,386,823

Table IV.34: The significance results from the Wilcoxon Rank-Sum Test for the Follow task using the network efficiency metric.

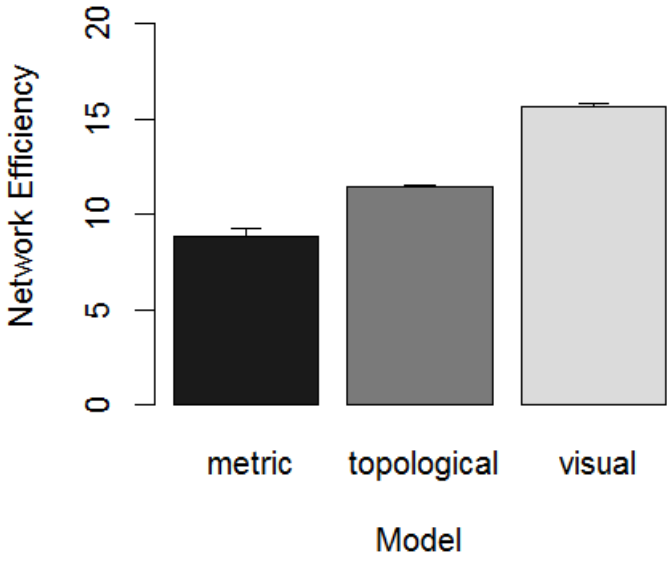

Figure IV.33: The distributions of network efficiency for each model in the Follow task.

statistics separated by number of agents are displayed in Figure IV.34. The Kruskal-Wallis test found a significant affect of the model type on network efficiency for each of the subgroups, with significance as detailed in Table IV.36. The Wilcoxon Rank-Sum test for 50 agents found that there was a highly significant difference between the metric and visual models ($p < 0.001$, z = 24,186.5), and between the topological and visual models ($p < 0.001$, z = 98,986). These results indicate that with 50 agents, the visual model had a significantly slower time for information propagation, and lower efficiency, than the metric and topological models. The Wilcoxon Rank-Sum test for the trials with 100 agents found that there was a highly significant difference between the metric and topological models ($p < 0.001$, z = 34,643), the metric and visual models ($p < 0.001$, z = 19,260.5), and the topological and visual models ($p < 0.001$, z = 113,568.5). The Wilcoxon Rank-Sum test for the trials with 250 agents found that there was a highly significant difference between the metric and topological models ($p < 0.001$, z = 62,053), the metric and visual models ($p < 0.001$, z =

35,492.5), and the topological and visual models ($p < 0.001$, z = 210,729.5). These analyses indicate that for the trials with 250 or 100 agents, the metric model had a significantly faster time for propagation and a higher efficiency than both the topological and metric models, and the topological model had a faster time for propagation and higher efficiency than the visual model. The Wilcoxon Rank-Sum test for the trials with 500 agents found that there was a highly significant difference between the metric and topological models ($p < 0.001$, z = 42,768) and the metric and visual models ($p < 0.001$, z = 29,054.5). The Wilcoxon Rank-Sum test for the trials with 1000 agents found that there was a highly significant difference between the metric and topological models ($p < 0.001$, z = 79,907) and the metric and visual models ($p < 0.001$, z = 61,481). That is, for trials with 500 or 1000 agents, the metric model had a significantly faster time for propagation and better efficiency than the topological and visual models. The data contained partial evidence that the topological model had a faster time for propagation (and better network efficiency) than the metric model. The trials with 50 agents showed that the metric model had a higher mean time of 9.51 timesteps (std. dev. = 11.19 timesteps) than the topological model's mean of 8.29 (std. dev. = 6.28). This difference was not significant.

Number of Agents	**Metric Mean (Std. Dev.)**	**Topological Mean (Std. Dev.)**	**Visual Mean (Std. Dev.)**
50	9.52 (11.19)	8.29 (6.28)	13.89 (12.28)
100	8.13 (11.08)	9.77 (7.07)	14.83 (11.87)
250	8.51 (11.05)	9.53 (5.77)	15.53 (13.56)
500	8.30 (10.85)	13.60 (8.23)	15.11 (10.82)
1000	9.66 (11.32)	14.14 (6.68)	17.54 (14.42)

Table IV.35: The means and standard deviations of the Follow task by number of agents for Network Efficiency.

Number of Agents	**Significance**	$\chi^2(2)$
50	$p < 0.001$	130.32
100	$p < 0.001$	132.04
250	$p < 0.001$	154.76
500	$p < 0.001$	180.20
1000	$p < 0.001$	141.43

Table IV.36: The significance results from the Kruskal-Wallis Test for the Follow task by number of agents for Network Efficiency.

The means and standard deviations by number of obstacles are provided in Table IV.37. The descriptive statistics separated by number of obstacles are displayed in Figure IV.35. The Kruskal-Wallis test found a significant affect of the model type on network efficiency for each of the subgroups, with significance as detailed in Table IV.38. The Wilcoxon Rank-Sum test for the trials with zero obstacles found that there was a highly significant difference between the metric and topological models ($p < 0.001$, z = 99,892), the metric and visual models ($p < 0.001$, z = 59,845), and the topological and visual models ($p < 0.001$, z

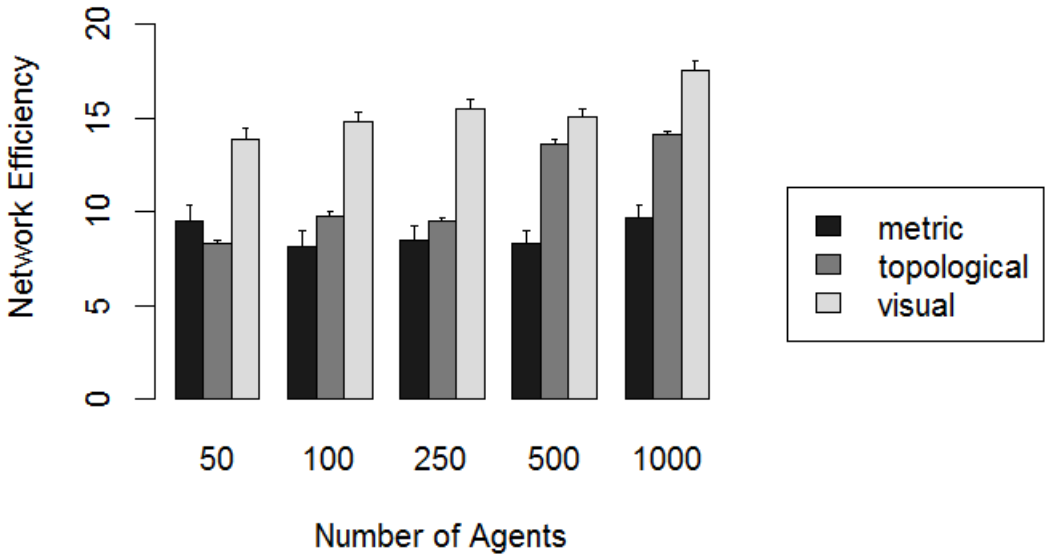

Figure IV.34: The distributions of Network Efficiency by number of agents and model.

= 363,914). The Wilcoxon Rank-Sum test for the trials with 25 obstacles found that there was a highly significant difference between the metric and topological models ($p < 0.001$, z = 99,050), the metric and visual models ($p < 0.001$, z = 58,836.5), and the topological and visual models ($p < 0.001$, z = 362,710). The Wilcoxon Rank-Sum test for the trials with 50 obstacles found that there was a highly significant difference between the metric and topological models ($p < 0.001$, z = 99,967), the metric and visual models ($p < 0.001$, z = 60,268), and the topological and visual models ($p < 0.001$, z = 361,890). The Wilcoxon Rank-Sum test for the trials with 100 obstacles found that there was a highly significant difference between the metric and topological models ($p < 0.001$, z = 30,949), the metric and visual models ($p < 0.001$, z = 20,538), and the topological and visual models ($p < 0.01$, z = 143,362.5). These results indicate that with 0, 25, 50, or 100 obstacles, the metric model had significantly faster mean information propagation time and higher efficiency than both the topological and visual models, and the visual model had slower mean information propagation time and lower efficiency than the topological model. The Wilcoxon Rank-Sum test for the trials with 250 obstacles found that there was a highly significant difference between the metric and topological models ($p < 0.001$, z = 3,241) and the metric and visual models ($p < 0.001$, z = 2,552). These results imply with 250 obstacles, the metric model had significantly faster mean information propagation time and higher efficiency than both the topological and visual models.

Number of Obstacles	Metric Mean (Std. Dev.)	Topological Mean (Std. Dev.)	Visual Mean (Std. Dev.)
0	8.72 (11.10)	10.92 (7.20)	15.12 (12.61)
25	8.71 (11.03)	10.99 (7.20)	15.37 (12.82)
50	8.97 (11.20)	11.16 (7.17)	15.72 (12.89)
100	8.88 (11.11)	12.62 (7.49)	15.95 (12.75)
250	9.87 (11.39)	14.19 (6.69)	17.56 (14.45)

Table IV.37: The means and standard deviations of the Follow task by number of obstacles for Network Efficiency.

Number of Obstacles	Significance	$\chi^2(2)$
0	$p < 0.001$	136.90
25	$p < 0.001$	142.13
50	$p < 0.001$	137.52
100	$p < 0.001$	88.54
500	$p < 0.001$	26.52

Table IV.38: The significance results from the Kruskal-Wallis Test for the Follow task by number of obstacles for Network Efficiency.

Similar evidence was discovered when the data was analyzed by the radii of repulsion, orientation, and attraction. The means and standard deviations for radius of repulsion are presented in Table IV.39. The descriptive statistics separated by radius of repulsion are displayed in Figure IV.36. The Kruskal-Wallis test found a significant affect of the model type on network efficiency for each of the subgroups, with significance as detailed in Table IV.40. The Wilcoxon Rank-Sum test when the radius of repulsion was equal to 5 found that there was a highly significant difference between the metric and topological models ($p < 0.001$, z = 127,153.5) and the metric and visual models ($p < 0.001$, z = 103,085). That is, for trials when the radius of repulsion equaled 5, the topological model had a signficantly faster mean time for information propagation and better efficiency than the metric model, and the metric model had a significantly faster mean time for information propagation and better efficiency than the visual model. The Wilcoxon Rank-Sum test for a radius of repulsion equal to 25 found that there was a highly significant difference between the metric and topological models ($p < 0.001$, z = 24,907) and the metric and visual models ($p < 0.001$, z = 13,488.5). Thus, when the radius of repulsion equaled 25, the metric model had a significantly faster time for information propagation and better efficiency than both the visual and topological models. The Wilcoxon Rank-Sum test where the radius of repulsion was equal to 50 found that there was a highly significant difference between the metric and topological models ($p < 0.001$, z = 65,521.5), the metric and visual models ($p < 0.001$, z = 19,365.5), and the topological and visual models ($p < 0.001$, z = 148,770.5). The Wilcoxon Rank-Sum test for a radius of repulsion equal to 100 found that there was a highly significant difference between the metric and topological models ($p < 0.001$, z = 9,608), the metric and visual models ($p < 0.001$, z = 1,341.5), and

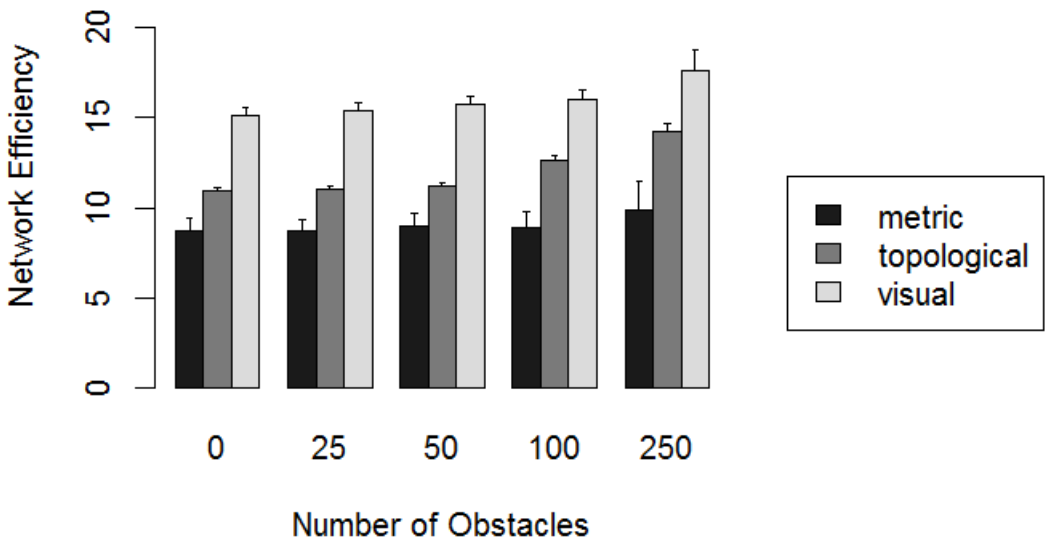

Figure IV.35: The distributions of Network Efficiency by number of obstacles and model.

the topological and visual models ($p < 0.001$, z = 63,795). These analyses indicate that when the radius of repulsion equaled 50 or 100, the metric model had a faster time for information propagation and better efficiency than the topological and visual models, and the topological model had a faster time for information propagation and better efficiency than the visual model.

Radius of Repulsion	**Metric Mean (Std. Dev.)**	**Topological Mean (Std. Dev.)**	**Visual Mean (Std. Dev.)**
5	8.35 (16.83)	6.65 (3.28)	13.63 (18.12)
25	11.15 (2.88)	19.34 (5.32)	19.46 (5.10)
50	10.62 (4.41)	13.59 (6.36)	19.37 (7.83)
100	2.77 (0.83)	5.53 (2.38)	7.33 (2.54)

Table IV.39: The means and standard deviations of the Follow task by radius of repulsion for Network Efficiency.

The means and standard deviations for the Follow task results for network efficiency grouped by radius of orientation are presented in Table IV.41. The descriptive statistics are visualized in Figure IV.37. The Kruskal-Wallis test found a highly significant impact of the model type on network efficiency for each subgroup by radius of orientation, as detailed in Table IV.42. The Wilcoxon Rank-Sum test found that when the radius of orientation was equal to 20, there was a highly significant difference between the metric and visual models

Radius of Repulsion	Significance	$\chi^2(2)$
5	$p < 0.001$	366.30
25	$p < 0.001$	561.53
50	$p < 0.001$	312.64
100	$p < 0.001$	337.90

Table IV.40: The significance results from the Kruskal-Wallis Test for the Follow task by radius of repulsion for Network Efficiency.

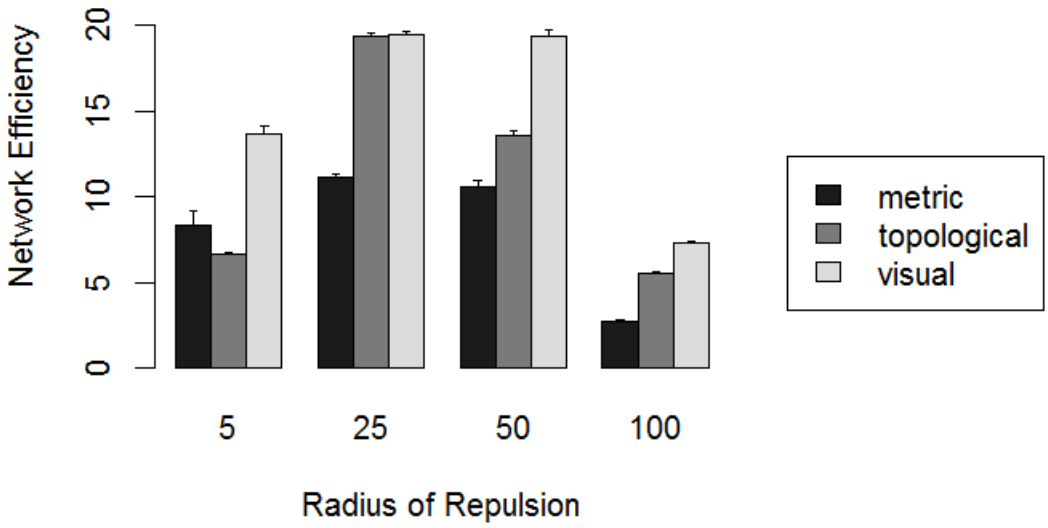

Figure IV.36: The distributions of Network Efficiency by radius of repulsion and model.

($p < 0.01$, z = 16,269.5) and the topological and visual models (p = 0.0472, z = 71,642.5). That is, when the radius of orientation was 20, the metric model had a signficantly slower time for information propagation and a lower efficiency than the visual model, and the visual model had a significantly slower propagation time and lower efficiency than the topological model. The Wilcoxon Rank-Sum test found that when the radius of orientation was equal to 40, there was a highly significant difference between the metric and topological models ($p < 0.001$, z = 27,872.5), the metric and visual models ($p < 0.001$, z = 18,114), and the topological and visual models ($p < 0.01$, z = 124,457.5). The Wilcoxon Rank-Sum test found that when the radius of orientation was equal to 75, there was a highly significant difference between the metric and topological models ($p < 0.001$, z = 67,380.5), the metric and visual models ($p < 0.001$, z = 38,652), and the topological and visual models ($p < 0.001$, z = 252,092.5). The Wilcoxon Rank-Sum test found that when the radius of

orientation was equal to 150, there was a highly significant difference between the metric and topological models ($p < 0.001$, z = 59,862), the metric and visual models ($p < 0.001$, z = 36,524), and the topological and visual models ($p < 0.001$, z = 275,167). The Wilcoxon Rank-Sum test found that when the radius of orientation was equal to 200, there was a highly significant difference between the metric and topological models ($p < 0.001$, z = 25,738.5), the metric and visual models ($p < 0.001$, z = 14,279.5), and the topological and visual models ($p < 0.001$, z = 116,760.5). The Wilcoxon Rank-Sum test found that when the radius of orientation was equal to 300, there was a highly significant difference between the metric and topological models ($p < 0.001$, z = 25,277.5), the metric and visual models ($p < 0.001$, z = 14,826.5), and the topological and visual models ($p < 0.001$, z = 121,227.5). These analyses imply that when the radius of orientation was greater than 20, the metric model had a significantly faster propagation time and higher efficiency than the visual and topological models, and the visual model had a significantly slower propagation time and lower efficiency than the topological model. An interesting note is that when the radius of orientation was equal to 20, the mean for the topological model was higher than the mean for the metric model. However, the Wilcoxon Rank-Sum test did not find a significant difference between the two models when the radius of orientation was equal to 20.

Radius of Orientation	**Metric Mean (Std. Dev.)**	**Topological Mean (Std. Dev.)**	**Visual Mean (Std. Dev.)**
20	22.11 (26.95)	5.71 (2.30)	18.00 (22.47)
40	7.55 (4.97)	12.17 (7.18)	15.69 (12.54)
75	9.02 (5.72)	13.36 (7.10)	17.77 (12.00)
150	6.54 (4.48)	11.65 (7.46)	14.05 (10.14)
200	6.21 (4.03)	11.51 (7.29)	14.46 (10.23)
300	6.18 (4.09)	11.75 (7.61)	13.93 (9.46)

Table IV.41: The means and standard deviations of the Follow task by radius of orientation for Network Efficiency.

Radius of Orientation	**Significance**	$\chi^2(2)$
20	$p < 0.01$	9.31
40	$p < 0.001$	82.14
75	$p < 0.001$	145.27
150	$p < 0.001$	148.57
200	$p < 0.001$	121.07
300	$p < 0.001$	113.73

Table IV.42: The significance results from the Kruskal-Wallis Test for the Follow Task task by radius of orientation for Network Efficiency.

The means and standard deviations for the Follow task results for network efficiency grouped by radius of attraction are presented in Table IV.43. The descriptive statistics are visualized in Figure IV.38. The Kruskal-Wallis test found a highly significant impact of the model type on network efficiency for each subgroup by

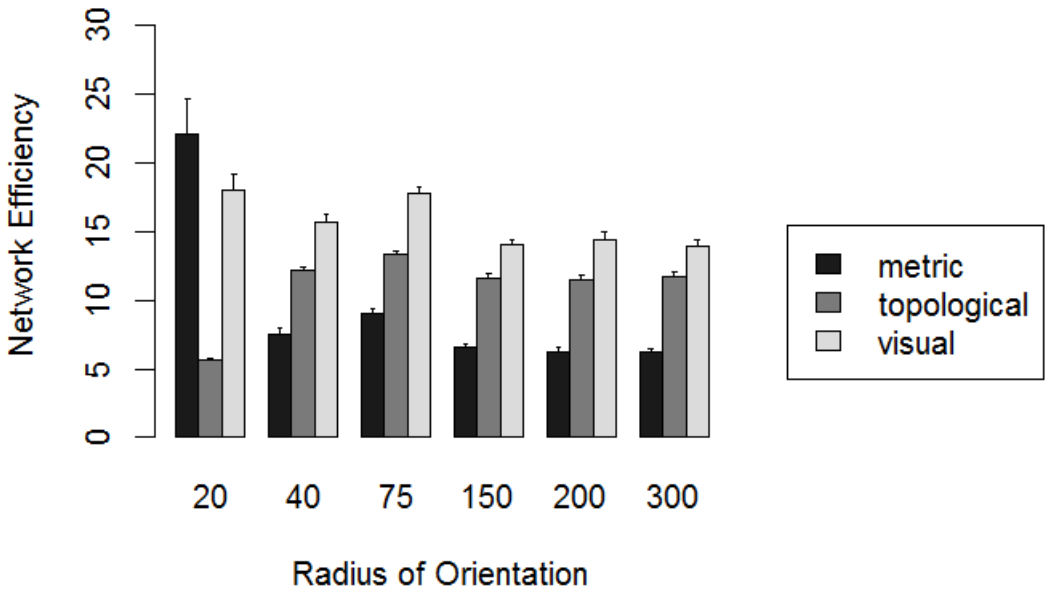

Figure IV.37: The distributions of Network Efficiency by radius of orientation and model.

radius of attraction, as detailed in Table IV.44. The Wilcoxon Rank-Sum test found that when the radius of attraction was equal to 25, there was a highly significant difference between the metric and topological models ($p < 0.001$, z = 1,444), the metric and visual models ($p < 0.001$, z = 788.5), and the topological and visual models ($p < 0.001$, z = 1,174.5). The Wilcoxon Rank-Sum test found that when the radius of attraction was equal to 35, there was a highly significant difference between the metric and topological models ($p < 0.001$, z = 1,444), the metric and visual models ($p < 0.01$, z = 741), and the topological and visual models ($p < 0.001$, z = 1,137). These results indicate that when the radius of attraction was 25 or 35, the topological model had a faster propagation time and higher efficiency than both the metric and the visual models and the metric model had a slower propagation time and lower efficiency than the visual model. The Wilcoxon Rank-Sum test found that when the radius of attraction was equal to 80, there was a highly significant difference between the metric and visual models ($p < 0.001$, z = 11,843) and the topological and visual models ($p < 0.001$, z = 51,528). That is, when the radius of attraction equaled 80, the visual model had a significantly slower time for propagation and lower efficiency than both the metric and topological models. The Wilcoxon Rank-Sum test found that when the radius of attraction was equal to 200, there was a highly significant difference between the metric and topological models ($p < 0.001$, z = 43,376) and the metric and visual models ($p < 0.001$, z = 31,650.5). This analysis implies that when the radius of attraction equaled 200, the metric

model had a significantly faster propagation time and higher efficiency than both the visual and topological models. The Wilcoxon Rank-Sum test found that when the radius of attraction was equal to 400, there was a highly significant difference between the metric and topological models ($p < 0.001$, z = 130,378.5), the metric and visual models ($p < 0.001$, z = 81,804.5), and the topological and visual models ($p < 0.001$, z = 635,728). The Wilcoxon Rank-Sum test found that when the radius of attraction was equal to 600, there was a highly significant difference between the metric and topological models ($p < 0.001$, z = 123,950), the metric and visual models ($p < 0.001$, z = 71,048.5), and the topological and visual models ($p < 0.001$, z = 589,897). These results imply that when the radius of attraction was equal to 400 or 600, the metric model had a significantly faster information propagation time and higher efficiency than both the topological and visual models, and the visual model had a slower information propagation time and lower efficiency than the topological model.

Radius of Attraction	**Metric Mean (Std. Dev.)**	**Topological Mean (Std. Dev.)**	**Visual Mean (Std. Dev.)**
25	60 (0)	5.67 (2.30)	35.79 (27.00)
35	60 (0)	5.68 (2.29)	40.68 (26.61)
80	10.55 (6.41)	11.71 (7.12)	20.34 (14.97)
200	7.16 (5.25)	11.73 (7.32)	11.92 (8.05)
400	6.36 (4.22)	11.56 (7.24)	13.53 (9.24)
600	6.08 (3.99)	11.71 (7.41)	15.63 (12.07)

Table IV.43: The means and standard deviations of the Follow task by radius of attraction for Network Efficiency.

Radius of Attraction	**Significance**	$\chi^2(2)$
25	$p < 0.01$	52.75
35	$p < 0.001$	53.03
80	$p < 0.001$	80.20
200	$p < 0.001$	82.80
400	$p < 0.001$	224.29
600	$p < 0.001$	289.08

Table IV.44: The significance results from the Kruskal-Wallis Test for the Follow Task task by radius of orientation for Network Efficiency.

The mean percentage of agents within thirty degrees of the target for the metric model was 15.13% (std. dev. = 7.32%), the topological model had a mean of 17.70% (std. dev. = 9.94%), and the visual model mean was 17.96% (std. dev. = 7.68%). The Kruskal-Wallis test indicated that there was a highly significant affect of the model type on percentage within 30 degrees ($p < 0.001$, $\chi^2(2) = 153.13$). The Wilcoxon Rank-Sum test found highly significant differences between all three pairings, as presented in Table IV.77. These results imply that the visual model had a significantly higher percentage of agents following the target, (and lower error) than the topological and metric model. The topological model had a significantly higher percentage of

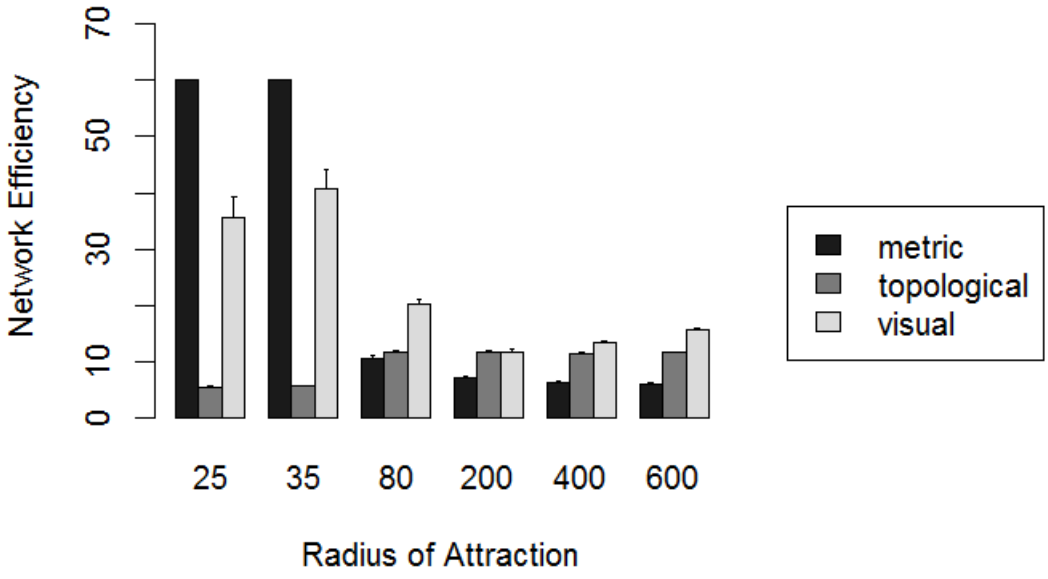

Figure IV.38: The distributions of Network Efficiency by radius of attraction and model.

agents following the target (and lower error) than the metric model.

Pairing	**Significance**	***z*-Value**
Metric-Visual	$p < 0.001$	1,162,784
Metric-Topological	$p < 0.001$	1,747,481
Topological-Visual	$p < 0.001$	5,819,213

Table IV.45: The significance results from the Wilcoxon Rank-Sum Test for the Follow task using the percentage of agents within 30 degrees metric.

The means and standard deviations by number of agents are presented in Table IV.46. The descriptive statistics separated by number of agents are displayed in Figure IV.40. The Kruskal-Wallis test found a significant affect of the model type on percent within 30 degrees for each of the subgroups, with significance as detailed in Table IV.47. The Wilcoxon Rank-Sum test for 50 agents found that there was a highly significant difference and between the topological and visual models ($p < 0.01$, $z = 142{,}818$). These results indicate that with 50 agents, the visual model had a significantly higher percentage of agents within 30 degrees, and less heading error than the topological model. The Wilcoxon Rank-Sum test for 100 agents found that there was a highly significant difference between the metric and visual models ($p < 0.001$, $z = 29{,}904$) and the topological and visual models ($p < 0.001$, $z = 138{,}967.5$). That is, when there were 100 agents, the visual model had a

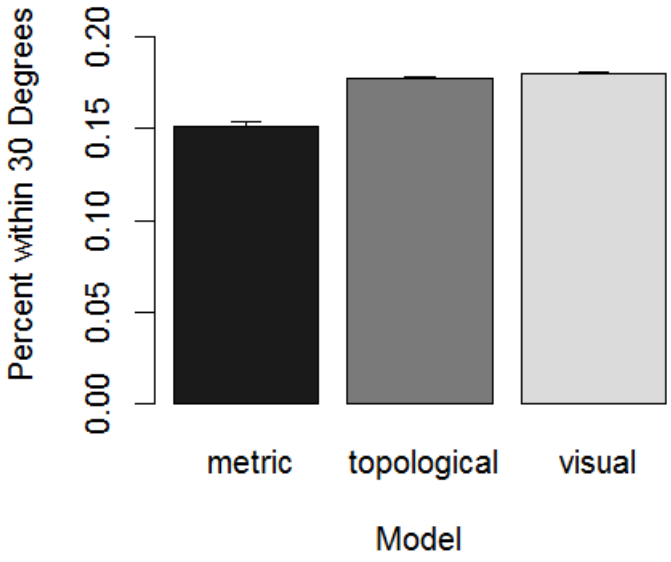

Figure IV.39: The distributions of percentage of agents within 30 degrees for each model in the Follow task.

significantly higher percentage of agents within 30 degrees and less heading error than the topological and metric models. The Wilcoxon Rank-Sum test for the trials with 250 agents found that there was a significant difference between the metric and topological models ($p < 0.001$, $z = 78{,}352.5$), the metric and visual models ($p < 0.001$, $z = 51{,}889$), and the topological and visual models ($p = 0.0312$, $z = 261{,}834.5$). This result implies that with 250 agents, the metric model had a significantly lower percentage of agents within 30 degrees and more heading error than the topological and visual models, and the visual model had significantly higher percentage of agents within 30 degrees and less efficiency error than the topological model. The Wilcoxon Rank-Sum test for the trials with 500 agents found that there was a significant difference between the metric and topological models ($p < 0.001$, $z = 59{,}879$), the metric and visual models ($p < 0.001$, $z = 40{,}415.5$), and the topological and visual models ($p = 0.0184$, $z = 260{,}135$). The Wilcoxon Rank-Sum test for the trials with 1000 agents found that there was a highly significant difference between the metric and topological models ($p < 0.001$, $z = 113{,}556$), the metric and visual models ($p < 0.001$, $z = 73{,}525.5$), and the topological and visual models ($p < 0.001$, $z = 397{,}103.5$). That is, for trials with 500 or 1000 agents, the metric model had a significantly lower percentage of agents within 30 degrees and a larger heading error than the visual and topological models, and the topological model had a higher percentage of agents within 30 degrees and less error than the visual model.

Number of Agents	Metric Mean (Std. Dev.)	Topological Mean (Std. Dev.)	Visual Mean (Std. Dev.)
50	17.04% (11.21%)	18.33% (15.52%)	19.38% (13.32%)
100	14.96% (7.38%)	17.79% (12.47%)	18.32% (9.45%)
250	15.36% (6.52%)	17.73% (9.29%)	17.98% (6.46%)
500	13.85% (6.31%)	17.74% (6.66%)	17.55% (4.56%)
1000	14.93% (5.17%)	17.22% (5.72%)	17.21% (3.49%)

Table IV.46: The means and standard deviations of the Follow task by number of agents for percentage of agents within 30 degrees.

Number of Agents	Significance	$\chi^2(2)$
50	$p = 0.0205$	7.77
100	$p < 0.001$	22.90
250	$p < 0.001$	28.50
500	$p < 0.001$	89.80
1000	$p < 0.001$	62.67

Table IV.47: The significance results from the Kruskal-Wallis Test for the Follow task by number of agents for percentage of agents within 30 degrees.

The percentage of agents within 30 degrees means and standard deviations from when the data was grouped by number of obstacles are provided in Table IV.48. The descriptive statistics separated by number of obstacles are displayed in Figure IV.41. The Kruskal-Wallis test found a significant affect of the model type on percentage of agents within 30 degrees for each of the subgroups, with significance as detailed in Table IV.49. The Wilcoxon Rank-Sum test for the trials with zero obstacles found that there was a highly significant difference between the metric and topological models ($p < 0.001$, z = 124,934), the metric and visual models ($p < 0.001$, z = 79,906.5), and the topological and visual models ($p < 0.001$, z = 391,291). The Wilcoxon Rank-Sum test for the trials with 25 obstacles found that there was a highly significant difference between the metric and topological models ($p < 0.01$, z = 129,792), the metric and visual models ($p < 0.001$, z = 83,992.5), and the topological and visual models ($p < 0.001$, z = 388,897.5). These results imply that when there were zero or 25 obstacles, the metric model had a significantly lower percentage of agents within 30 degrees and higher error than the topological and visual models, and the topological model had a lower percentage of agents within 30 degrees and higher error than the visual model. The Wilcoxon Rank-Sum test for the trials with 50 obstacles found that there was a highly significant difference between the metric and topological models ($p < 0.001$, z = 116,112.5), the metric and visual models ($p < 0.001$, z = 79,553), and the topological and visual models ($p = 0.0478$, z = 414,161.5). That is, when there were 50 obstacles, the metric model had a significantly lower percentage of agents within 30 degrees and larger error than the topological and visual models, and the topological model had a higher percentage of agents within 30 degrees and less error than the visual model. The Wilcoxon Rank-Sum test for the trials with 100 obstacles found that there

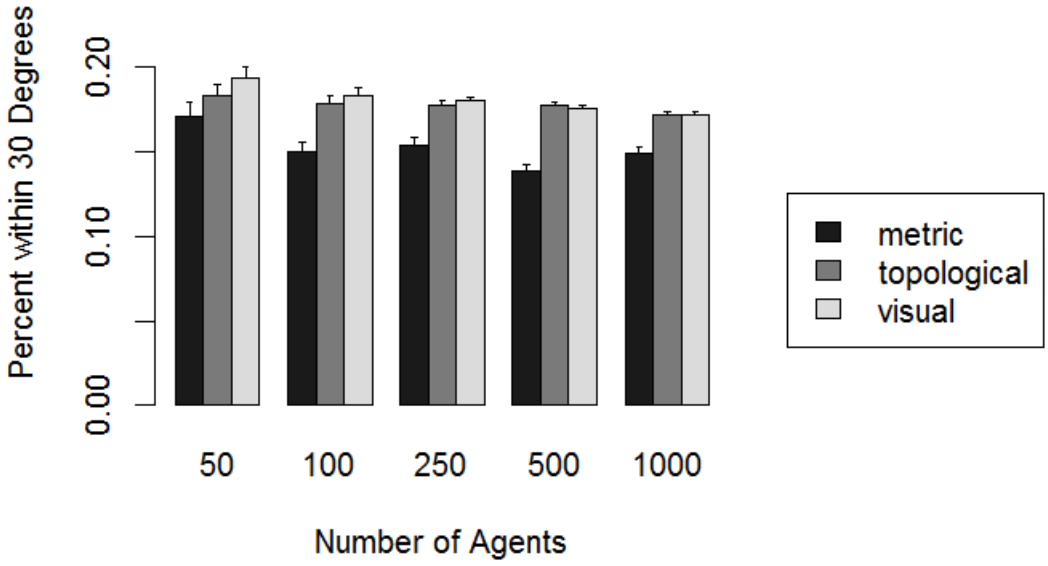

Figure IV.40: The distributions of percentage of agents within 30 degrees by number of agents and model.

was a highly significant difference between the metric and topological models ($p < 0.001$, $z = 39{,}621.5$) and the metric and visual models ($p < 0.001$, $z = 27{,}536.5$). The Wilcoxon Rank-Sum test for the trials with 250 obstacles found that there was a highly significant difference between the metric and topological models ($p < 0.01$, $z = 4{,}501$) and the metric and visual models ($p < 0.01$, $z = 3{,}219$). These results imply that when there were 100 or 250 obstacles, the metric model had a significantly lower percentage of agents within 30 degrees and larger error than the topological and visual models.

Number of Obstacles	**Metric Mean (Std. Dev.)**	**Topological Mean (Std. Dev.)**	**Visual Mean (Std. Dev.)**
0	14.75% (6.58%)	17.75% (11.79%)	18.10% (8.24%)
25	15.61% (9.18%)	16.88% (9.63%)	17.99% (8.35%)
50	15.01% (6.70%)	18.48% (10.44%)	18.32% (8.48%)
100	15.18% (6.68%)	17.70% (6.69%)	17.35% (4.35%)
250	15.08% (4.70%)	17.63% (5.71%)	17.14% (3.75%)

Table IV.48: The means and standard deviations of the Follow task by number of obstacles for percentage of agents within 30 degrees.

The means and standard deviations by radius of repulsion are presented in Table IV.50. The descriptive statistics separated by radius of repulsion are displayed in Figure IV.42. The Kruskal-Wallis test found no significant affect of the model type on percentage of agents within 30 degrees when the radius of repulsion

Number of Obstacles	Significance	$\chi^2(2)$
0	$p < 0.001$	43.75
25	$p < 0.001$	36.13
50	$p < 0.001$	42.73
100	$p < 0.001$	31.94
500	$p = 0.0131$	8.67

Table IV.49: The significance results from the Kruskal-Wallis Test for the Follow task by number of obstacles for percentage of agents within 30 degrees.

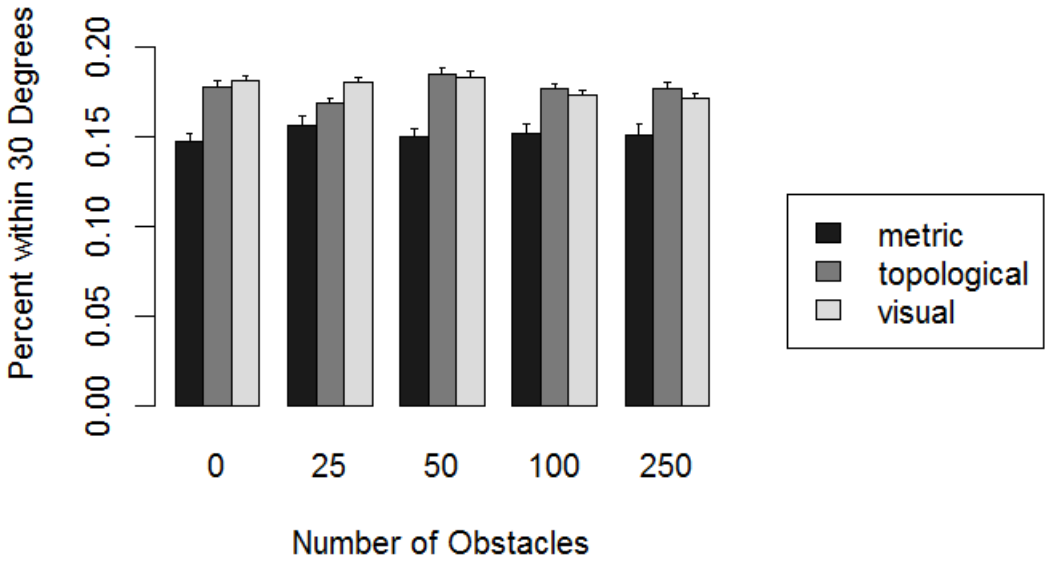

Figure IV.41: The distributions of percentage of agents within 30 degrees by number of obstacles and model.

was 25. The Kruskal-Wallis test found a significant affect of the model type on percentage of agents within 30 degrees when the radius of repulsion was 5, 50, or 100, with significance as detailed in Table IV.51. The Wilcoxon Rank-Sum test when the radius of repulsion was equal to 5 found that there was a highly significant difference between the metric and topological models ($p < 0.001$, z = 219,159.5) and the metric and visual models ($p < 0.001$, z = 151,959). That is, when the radius of repulsion equaled 5, the metric model had a significantly lower percentage of agents within 30 degrees and higher orientation error than the topological and visual models. The Wilcoxon Rank-Sum test where the radius of repulsion was equal to 50 found that there was a highly significant difference between the metric and visual models (p= 0.0179, z = 58,366.5) and the topological and visual models ($p < 0.001$, z = 220,476). This result indicates that when the radius of repulsion was equal to 5, the visual model had a significantly higher percentage of agents within 30 degrees

and less orientation error than the topological and metric models. The Wilcoxon Rank-Sum test for a radius of repulsion equal to 100 found that there was a highly significant difference between the metric and topological models ($p < 0.001$, z = 27,800), the metric and visual models ($p < 0.001$, z = 9,209.5), and the topological and visual models ($p < 0.001$, z = 52,053). That is, when the radius of repulsion equaled 100, the visual model had a significantly higher percentage of agents within 30 degrees and less orientation error than the topological and metric models, and the metric model had significantly lower percentage of agents within 30 degrees and larger orientation error than the topological model.

Radius of Repulsion	**Metric Mean (Std. Dev.)**	**Topological Mean (Std. Dev.)**	**Visual Mean (Std. Dev.)**
5	13.23% (9.81%)	18.95% (14.00%)	18.12% (10.75%)
25	17.27% (4.79%)	18.01% (7.28%)	17.67% (5.86%)
50	17.06% (4.27%)	16.87% (4.07%)	17.84% (3.53%)
100	13.23% (4.16%)	14.61% (4.37%)	18.28% (3.83%)

Table IV.50: The means and standard deviations of the Follow task by radius of repulsion for percentage of agents within 30 degrees.

Radius of Repulsion	**Significance**	$\chi^2(2)$
5	$p < 0.001$	116.81
25	Not Significant	N/A
50	$p < 0.001$	312.64
100	$p < 0.001$	227.86

Table IV.51: The significance results from the Kruskal-Wallis Test for the Follow task by radius of repulsion for percentage of agents within 30 degrees.

The means and standard deviations for the Follow task results for percentage of agents within 30 degrees grouped by radius of orientation are presented in Table IV.52. The descriptive statistics are visualized in Figure IV.43. The Kruskal-Wallis test found a highly significant impact of the model type on percentage of agents within 30 degrees for each subgroup by radius of orientation, as detailed in Table IV.53. The Wilcoxon Rank-Sum test found that when the radius of orientation was equal to 20, there was a highly significant difference between the metric and visual models ($p < 0.001$, z = 14,472.5) and the metric and topological models ($p < 0.001$, z = 19,061.5). These results imply that when the radius of orientation was 20, the metric model had a significantly lower percentage of agents within 30 degrees and higher error than the topological and visual models. The Wilcoxon Rank-Sum test found that when the radius of orientation was equal to 75, there was a highly significant difference between the metric and topological models ($p < 0.001$, z =85,328), the metric and visual models ($p < 0.01$, z = 68,902), and the topological and visual models ($p < 0.01$, z = 339,344.5). That is, when the radius of orientation was 75, the topological model had a significantly higher percentage of agents within 30 degrees and less orientation error than the metric and visual models, and the

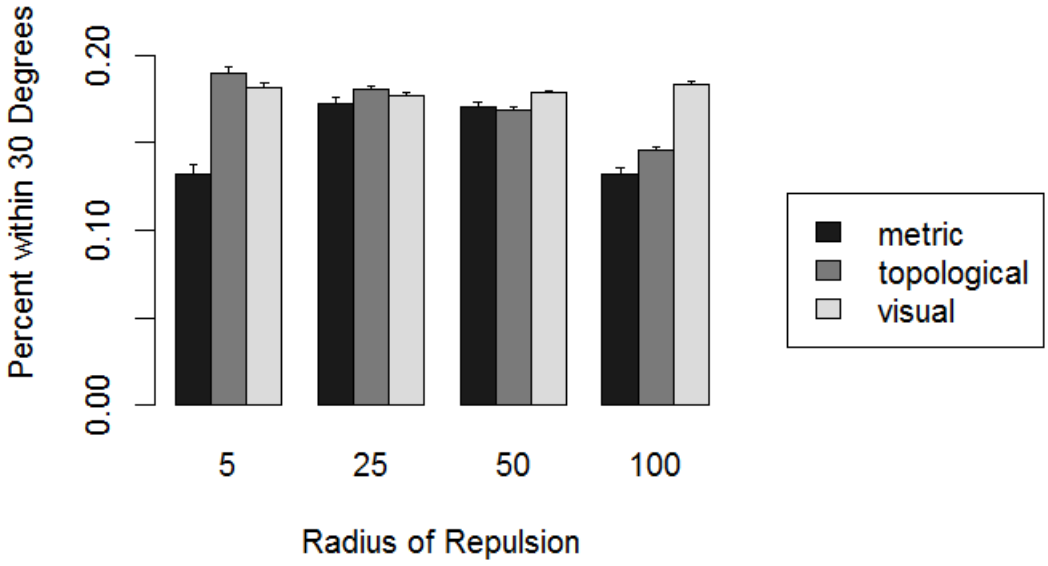

Figure IV.42: The distributions of percentage of agents within 30 degrees by radius of repulsion and model.

metric model had a lower percentage of agents within 30 degrees and higher orientation error than the visual model. The Wilcoxon Rank-Sum test found that when the radius of orientation was equal to 40, there was a significant difference between the metric and topological models ($p = 0.0206$, $z = 40{,}603.5$), the metric and visual models ($p < 0.001$, $z = 27{,}343.5$), and the topological and visual models ($p = 0.0138$, $z = 126{,}413.5$). The Wilcoxon Rank-Sum test found that when the radius of orientation was equal to 150, there was a highly significant difference between the metric and topological models ($p < 0.01$, $z = 89{,}514.5$), the metric and visual models ($p < 0.001$, $z = 53{,}273.5$), and the topological and visual models ($p < 0.001$, $z = 263{,}561.5$). The Wilcoxon Rank-Sum test found that when the radius of orientation was equal to 200, there was a highly significant difference between the metric and topological models ($p < 0.01$, $z = 39{,}842.5$), the metric and visual models ($p < 0.001$, $z = 24{,}883$), and the topological and visual models ($p < 0.01$, $z = 122{,}711.5$). The Wilcoxon Rank-Sum test found that when the radius of orientation was equal to 300, there was a highly significant difference between the metric and topological models ($p < 0.001$, $z = 36{,}330.5$), the metric and visual models ($p < 0.001$, $z = 19{,}870$), and the topological and visual models ($p < 0.001$, $z = 108{,}396.5$). These results imply that when the radius of orientation was 40, 150, 200, or 200, the metric model had a significantly lower percentage of agents within 30 degrees and higher orientation error than the topological and visual models, and the topological model had a lower percentage of agents within 30 degrees and higher

orientation error than the visual model.

Radius of Orientation	Metric Mean (Std. Dev.)	Topological Mean (Std. Dev.)	Visual Mean (Std. Dev.)
20	15.11% (4.65%)	17.72% (4.85%)	17.13% (4.71%)
40	15.27% (4.75%)	16.96% (6.35%)	17.25% (4.62%)
75	16.93% (8.74%)	19.52% (10.14%)	17.39% (6.19%)
150	14.30% (7.10%)	16.92% (10.92%)	17.78% (7.79%)
200	14.65% (6.76%)	16.91% (11.36%)	18.02% (8.82%)
300	14.03% (8.99%)	17.66% (11.82%)	20.36% (11.27%)

Table IV.52: The means and standard deviations of the Follow task by radius of orientation for percentage of agents within 30 degrees.

Radius of Orientation	Significance	$\chi^2(2)$
20	$p < 0.001$	20.65
40	$p < 0.001$	16.27
75	$p < 0.001$	22.32
150	$p < 0.001$	56.92
200	$p < 0.001$	26.85
300	$p < 0.001$	74.02

Table IV.53: The significance results from the Kruskal-Wallis Test for the Follow Task task by radius of orientation for percentage of agents within 30 degrees.

The means and standard deviations for the Follow task results for percentage of agents within 30 degrees grouped by radius of attraction are presented in Table IV.54. The descriptive statistics are visualized in Figure IV.44. The Kruskal-Wallis test found no significant affect of model type on percentage of agents within 30 degrees when the radius of attraction was 25, 35, or 80. The Kruskal-Wallis test found a highly significant impact of the model type on percentage of agents within 30 degrees when the radius of attraction was 200, 400, or 800, with significance as detailed in Table IV.55. The Wilcoxon Rank-Sum test found that when the radius of attraction was equal to 200, there was a highly significant difference between the metric and topological models ($p < 0.001$, z = 57,094.5) and the metric and visual models ($p < 0.001$, z = 39,656.5). That is, when the radius of attraction was 200, the metric model had a lower percentage of agents within 30 degrees and higher orientation error than the visual and topological models. The Wilcoxon Rank-Sum test found that when the radius of attraction was equal to 400, there was a highly significant difference between the metric and topological models ($p < 0.001$, z = 186,470), the metric and visual models ($p < 0.001$, z = 120,303.5), and the topological and visual models ($p < 0.001$, z = 639,670). The Wilcoxon Rank-Sum test found that when the radius of attraction was equal to 600, there was a highly significant difference between the metric and topological models ($p < 0.001$, z = 186,294.5), the metric and visual models ($p < 0.001$, z = 115,584), and the topological and visual models ($p < 0.001$, z = 617,825.5). These results imply that when the radius of attraction was 400 or 600, the metric model had a lower percentage of agents within 30

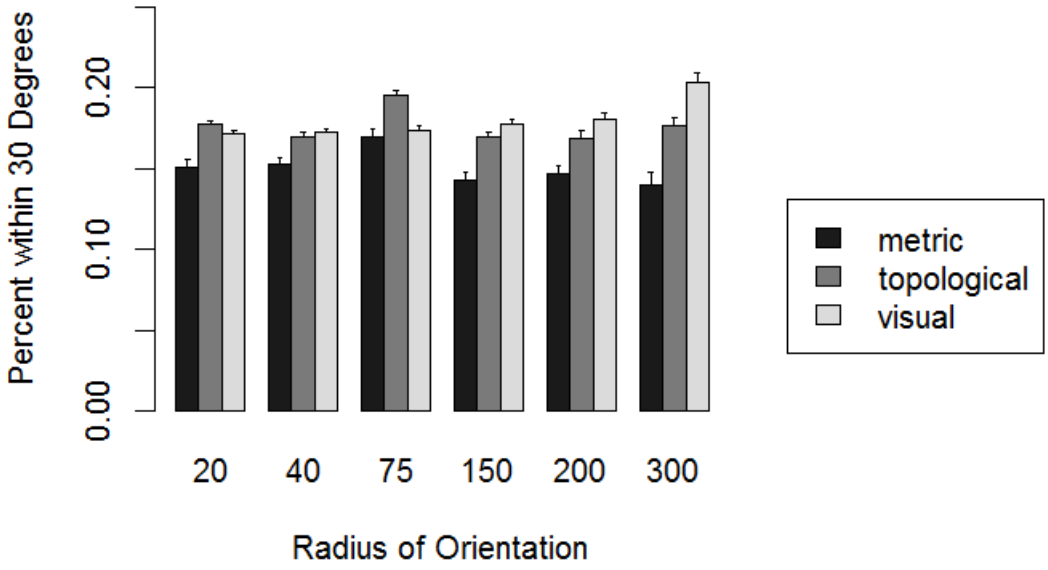

Figure IV.43: The distributions of percentage of agents within 30 degrees by radius of orientation and model.

degrees and higher orientation error than the visual and topological models and the visual model had a higher percentage of agents within 30 degrees and lower error than the topological model.

Radius of Attraction	**Metric Mean (Std. Dev.)**	**Topological Mean (Std. Dev.)**	**Visual Mean (Std. Dev.)**
25	15.07% (4.89%)	17.86% (4.96%)	16.92% (4.08%)
35	17.21% (4.61%)	16.87% (4.75%)	16.11% (6.22%)
80	19.49% (9.66%)	18.00% (8.73%)	17.83% (7.07%)
200	15.27% (6.71%)	18.59% (10.26%)	17.63% (5.88%)
400	14.53% (6.85%)	17.49% (10.03%)	18.07% (7.98%)
600	14.08% (6.90%)	17.36% (10.43%)	18.24% (8.60%)

Table IV.54: The means and standard deviations of the Follow task by radius of attraction for percentage of agents within 30 degrees.

IV.2.5 Disperse / Rally

The Disperse task ran 8,208 trials, distributed across models: metric = 1,026 trials, topological = 4,104 trials, and visual = 3,078 trials. The metric for the Disperse task was the average nearest neighbor distance, *NearestNeighbor*. The mean *NearestNeighbor* across the metric model was 22.31 units (std. dev. = 10.93 units). The topological model had a mean *NearestNeighbor* of 26.59 units (std. dev. = 9.69 units), while the

Radius of Attraction	Significance	$\chi^2(2)$
25	Not Significant	N/A
35	Not Significant	N/A
80	Not Significant	N/A
200	$p < 0.001$	28.62
400	$p < 0.001$	71.07
600	$p < 0.001$	88.02

Table IV.55: The significance results from the Kruskal-Wallis Test for the Follow Task task by radius of orientation for percentage of agents within 30 degrees.

visual model's mean *NearestNeighbor* was 24.16 units (std. dev. = 14.31 units). The distributions for these three models are illustrated in Figure IV.45.

The Kruskal-Wallis test indicated a highly significant affect of the model type on mean nearest neighbor distance ($p < 0.001$, $\chi^2(2) = 372.71$). The Wilcoxon Rank-Sum test found a highly significant difference between both the topological and visual models ($p < 0.001$, z = 7,777,349) and the topological and metric models ($p < 0.001$, z = 1,506,726). This result implies that the topological model had a significantly larger nearest neighbor distance and performed better than both the visual and metric models. No significant difference was found between the metric and visual models.

The means and standard deviations by number of agents are presented in Table IV.56. The descriptive statistics are visualized in Figure IV.46. The Kruskal-Wallis test found a significant affect of the model type on nearest neighbor distance when analyzed by the number of agents; the results are provided in Table IV.57. The Wilcoxon Rank-Sum test for the trials with 50 agents found that there was a significant difference between the metric and topological models ($p < 0.001$, z = 41,204), the metric and visual models ($p < 0.01$, z = 33,232), and the topological and visual models (p = 0.0164, z = 170,558). The Wilcoxon Rank-Sum test for the trials with 100 agents found that there was a significant difference between the metric and topological models ($p < 0.001$, z = 36,252), the metric and visual models ($p < 0.001$, z = 31,328), and the topological and visual models (p = 0.0245, z = 169,742). The Wilcoxon Rank-Sum test for the trials with 250 agents found that there was a highly significant difference between the metric and topological models ($p < 0.001$, z = 53,630), the metric and visual models (p = 0.0102, z = 61,822), and the topological and visual models ($p < 0.001$, z = 343,486). These analyses indicate that when there were 50, 100, or 250 agents, the topological model had a significantly larger nearest neighbor distance and better performance than the metric and visual models, and the visual model had a significantly larger nearest neighbor distance and better performance than the metric model. The Wilcoxon Rank-Sum test for the trials with 500 agents found that there was a highly significant difference between the metric and topological models ($p < 0.001$, z = 63,276) and the topological and visual models ($p < 0.001$, z = 367,073). These results indicate that when there were 500 agents, the

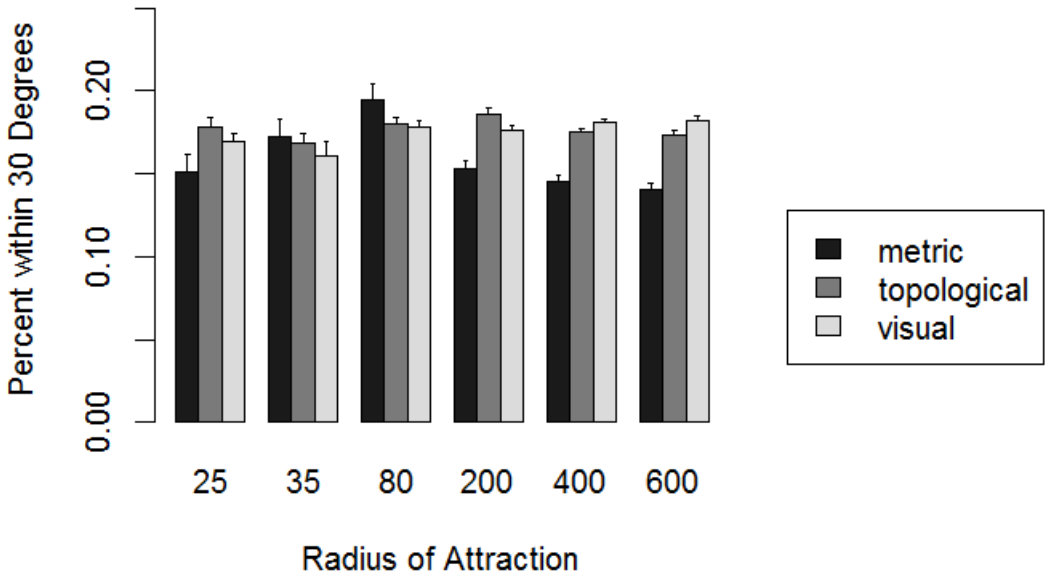

Figure IV.44: The distributions of percentage of agents within 30 degrees by radius of attraction and model.

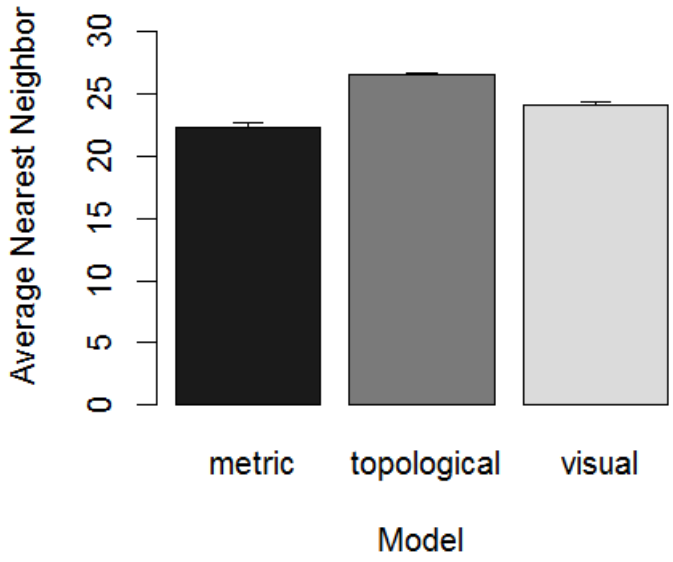

Figure IV.45: The distributions for each model in the Disperse task.

topological model had a significantly larger nearest neighbor distance and better performance than the metric and visual models. The Wilcoxon Rank-Sum test for the trials with 1000 agents found that there was a highly significant difference between the metric and topological models ($p < 0.001$, z = 102,033), the metric and visual models ($p < 0.01$, z = 135,883), and the topological and visual models ($p < 0.001$, z = 654,517). That is, when there were 1000 agents, the topological model had a significantly larger nearest neighbor distance and better performance than the metric and visual models, and the metric model had a significantly larger nearest neighbor distance and better performance than the visual model.

Number of Agents	**Metric Mean (Std. Dev.)**	**Topological Mean (Std. Dev.)**	**Visual Mean (Std. Dev.)**
50	28.93 (15.32)	33.65 (15.46)	31.19 (17.90)
100	24.24 (11.08)	29.48 (10.21)	28.08 (14.92)
250	20.26 (8.64)	25.75 (6.93)	24.89 (14.29)
500	19.21 (7.55)	23.18 (5.60)	21.32 (12.25)
1000	21.29 (9.77)	24.00 (6.00)	19.28 (9.99)

Table IV.56: The means and standard deviations of the Disperse task by number of agents.

Number of Agents	**Significance**	$\chi^2(2)$
50	$p < 0.001$	20.63
100	$p < 0.001$	35.19
250	$p < 0.001$	111.12
500	$p < 0.001$	127.84
1000	$p < 0.001$	353.26

Table IV.57: The significance results from the Kruskal-Wallis Test for the Disperse task by number of agents.

The means and standard deviations by number of obstacles are presented in Table IV.58. The descriptive statistics are visualized in Figure IV.47. The Kruskal-Wallis test found a significant affect of the model type on the nearest neighbor distance by number of obstacles; the results are provided in Table IV.59. The Wilcoxon Rank-Sum test for zero obstacles found that there was a highly significant difference between the metric and topological models ($p < 0.001$, z = 105,129) and the topological and visual models ($p < 0.001$, z = 528,643). The Wilcoxon Rank-Sum test for 25 obstacles found that there was a highly significant difference between the metric and topological models ($p < 0.001$, z = 104,618) and the topological and visual models ($p < 0.001$, z = 525,314). The Wilcoxon Rank-Sum test with 50 obstacles found that there was a highly significant difference between the metric and topological models ($p < 0.001$, z = 105,746) and the topological and visual models ($p < 0.001$, z = 522,084). The Wilcoxon Rank-Sum test for 100 obstacles found that there was a highly significant difference between the metric and topological models ($p < 0.001$, z = 35,694) and the topological and visual models ($p < 0.001$, z = 208,281). These results indicate that when there were 0, 25, 50, or 100 obstacles, the topological model had a significantly larger nearest neighbor distance and better performance

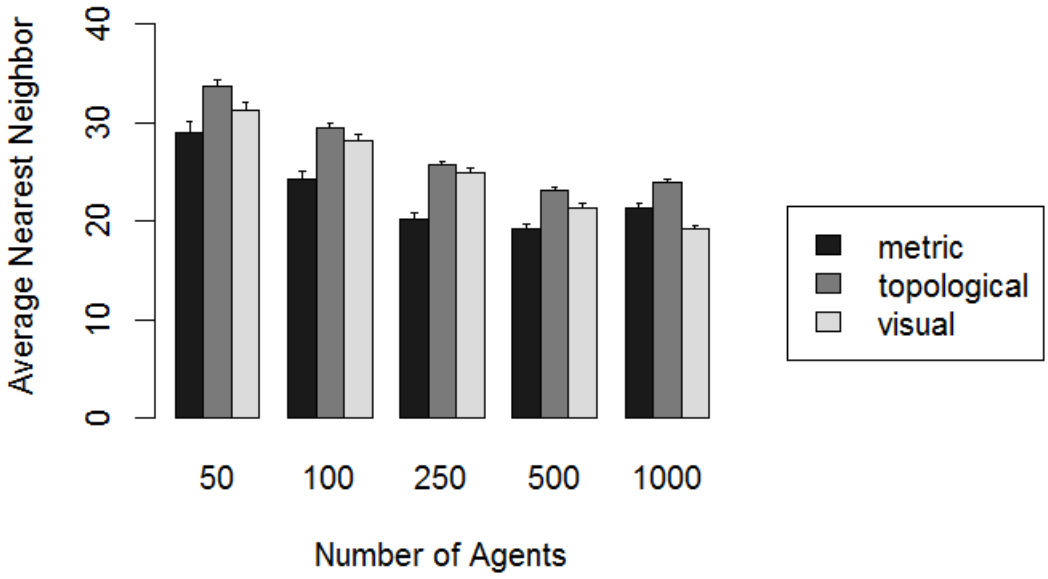

Figure IV.46: The distributions for each model in the Disperse task by number of agents.

than the visual and metric models. The Wilcoxon Rank-Sum test for 250 obstacles found that there was a significant difference between the metric and topological models ($p < 0.001$, $z = 3{,}940$), the metric and visual models ($p = 0.0193$, $z = 5{,}305$), and the topological and visual models ($p < 0.001$, $z = 26{,}247$). That is, when there were 250 obstacles, the topological model had a significantly larger nearest neighbor distance and better performance than the visual and metric models, and the metric model had a significantly larger nearest neighbor distance and better performance than the visual model.

Number of Obstacles	**Metric Mean (Std. Dev.)**	**Topological Mean (Std. Dev.)**	**Visual Mean (Std. Dev.)**
0	23.13 (11.95)	27.64 (11.02)	25.16 (15.22)
25	22.63 (10.88)	27.16 (10.09)	24.92 (14.68)
50	22.61 (11.16)	26.89 (9.84)	24.85 (14.47)
100	20.39 (8.92)	24.24 (6.27)	21.72 (12.39)
250	20.81 (9.64)	23.96 (5.94)	19.27 (9.85)

Table IV.58: The means and standard deviations of the Disperse task by number of obstacles.

A similar analysis was conducted for the results grouped by the radii of attraction, orientation, and repulsion. The means and standard deviations for the results grouped by radius of repulsion are reported in Table IV.60, and the descriptive statistics are visualized in Figure IV.48. The Kruskal-Wallis test found a signifi-

Number of Obstacles	Significance	$\chi^2(2)$
0	$p < 0.001$	85.07
25	$p < 0.001$	82.46
50	$p < 0.001$	77.48
100	$p < 0.001$	100.78
250	$p < 0.001$	71.86

Table IV.59: The significance results from the Kruskal-Wallis Test for the Disperse task by number of obstacles.

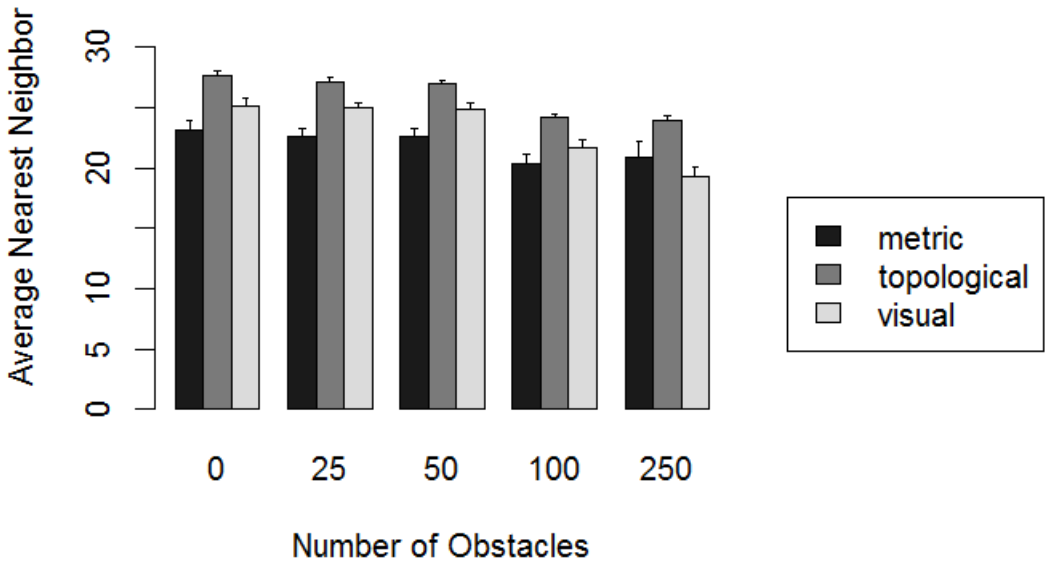

Figure IV.47: The distributions for each model in the Disperse task by number of obstacles.

cant affect of the model type on the nearest neighbor distance for each of the subgroups, with significance as detailed in Table IV.61. The Wilcoxon Rank-Sum test for the radius of repulsion equal to 5 found that there was a highly significant difference between the metric and topological models ($p < 0.001$, $z = 121{,}093$), the metric and visual models ($p < 0.001$, $z = 192{,}103$), and the topological and visual models ($p < 0.001$, $z = 1{,}629{,}281$). The Wilcoxon Rank-Sum test for the radius of repulsion equal to 25 found that there was a highly significant difference between the metric and topological models ($p < 0.001$, $z = 13{,}856$), the metric and visual models ($p < 0.001$, $z = 157{,}747$), and the topological and visual models ($p < 0.001$, $z = 856{,}532$). These results indicate that when the radius of repulsion was 5 or 25 the topological model had a significantly larger nearest neighbor distance and better performance than the visual and metric models, and the metric model had a significantly larger nearest neighbor distance and better performance than the visual model. The

Wilcoxon Rank-Sum test for the radius of repulsion equal to 50 found that there was a highly significant difference between the metric and visual models ($p < 0.001$, z = 53,527) and between the topological and visual models ($p < 0.001$, z = 224,041). The Wilcoxon Rank-Sum test for the radius of repulsion equal to 100 found that there was a highly significant difference between the metric and visual models ($p < 0.001$, z = 3,673) and between the topological and visual models ($p < 0.001$, z = 16,637). That is, when the radius of repulsion was equal to 50 or 100, the visual model had a significantly larger nearest neighbor distance, and better performance than the topological and visual models.

Radius of Repulsion	**Metric Mean (Std. Dev.)**	**Topological Mean (Std. Dev.)**	**Visual Mean (Std. Dev.)**
5	13.53 (9.42)	19.12 (6.14)	12.06 (3.90)
25	24.56 (2.26)	31.08 (4.35)	22.36 (5.32)
50	30.01 (9.24)	31.24 (11.25)	32.85 (9.90)
100	31.71 (9.39)	32.04 (9.88)	50.67 (7.10)

Table IV.60: The means and standard deviations of the Disperse task by radius of repulsion.

Radius of Repulsion	**Significance**	$\chi^2(2)$
5	$p < 0.001$	1,123.00
25	$p < 0.001$	1,088.28
50	$p < 0.001$	28.22
100	$p < 0.001$	536.17

Table IV.61: The significance results from the Kruskal-Wallis Test for the Disperse task by radius of repulsion.

The means and standard deviations for the results grouped by radius of orientation are provided in Table IV.62. The descriptive statistics are visualized in Figure IV.49. The Kruskal-Wallis test found a significant affect of the model type on the nearest neighbor distance for each of the subgroups, with significance as detailed in Table IV.63. The Wilcoxon Rank-Sum test found a significant difference for radius of orientation equal to 20 between the metric and topological models ($p < 0.001$, z = 14,095), the metric and visual models (p = 0.0218, z = 16,699), and the visual and topological models ($p < 0.001$, z = 154,467). That is, when the radius of orientation equaled 20, the metric model had a significantly larger nearest neighbor distance and better performance than the visual and topological models, and the topological model had a significantly larger nearest neighbor distance and better performance than the visual model. The Wilcoxon Rank-Sum test found a significant difference for radius of orientation equal to 40 between the metric and topological models ($p < 0.001$, z = 30,142) and the visual and topological models ($p < 0.001$, z = 211,920). The Wilcoxon Rank-Sum test found a significant difference for radius of orientation equal to 75 between the metric and topological models ($p < 0.001$, z = 70,453) and the visual and topological models ($p < 0.001$, z = 424,186). These results mean that when the radius of orientation equaled 40 or 75, the topological model had a significantly larger nearest neighbor distance and better performance than the visual and metric models. The Wilcoxon

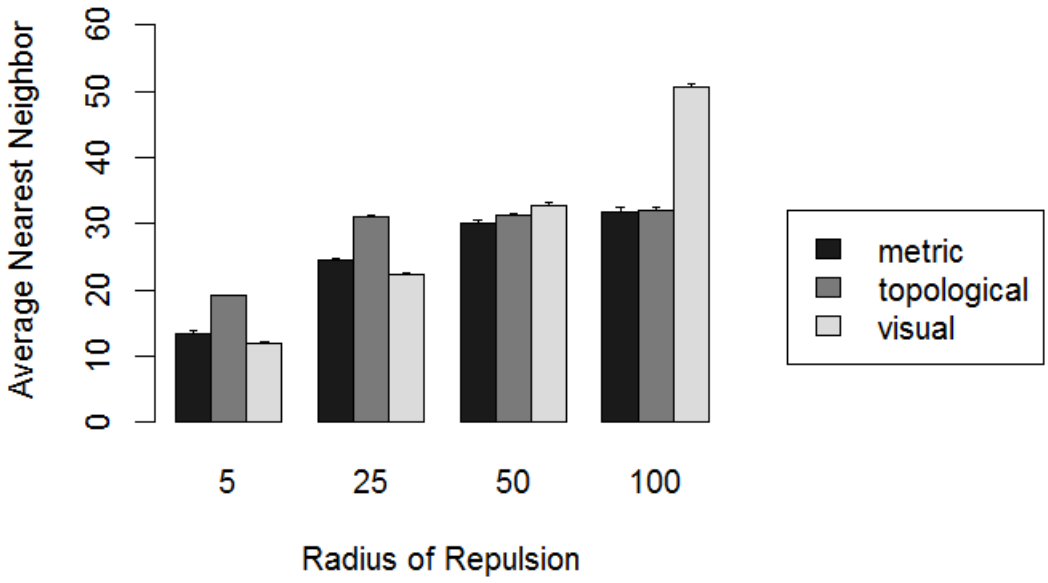

Figure IV.48: The distributions for each model in the Disperse task by radius of repulsion.

Rank-Sum test found a significant difference for radius of orientation equal to 150 between the metric and topological models ($p < 0.001$, z = 67,547), the metric and visual models ($p < 0.01$, z = 67,144), and the visual and topological models ($p < 0.001$, z = 355,908). The Wilcoxon Rank-Sum test found a significant difference for radius of orientation equal to 200 between the metric and topological models ($p < 0.001$, z = 27,659), the metric and visual models ($p < 0.01$, z = 29,296), and the visual and topological models ($p < 0.001$, z =158,457). These results mean that when the radius of orientation equaled 150 or 200, the topological model had a significantly larger nearest neighbor distance and better performance than the visual and metric models, and the metric model had a significantly smaller nearest neighbor distance and worse performance than the visual model. The Wilcoxon Rank-Sum test found a significant difference for radius of orientation equal to 300 between the metric and topological models ($p < 0.001$, z = 29,365), the metric and visual models ($p < 0.01$, z = 29,073), and the visual and topological models ($p < 0.01$, z = 151,989). That is, when the radius of orientation equaled 300, the topological model had a significantly larger nearest neighbor distance and better performance than the visual and metric models, and the visual model had a significantly smaller nearest neighbor distance and worse performance than the metric model.

The means and standard deviations for the results grouped by radius of attraction are presented in Table IV.64. The descriptive statistics are visualized in Figure IV.50. The Kruskal-Wallis test found a significant

Radius of Orientation	Metric Mean (Std. Dev.)	Topological Mean (Std. Dev.)	Visual Mean (Std. Dev.)
20	14.16 (11.32)	11.29 (0.78)	9.28 (0.37)
40	19.11 (11.28)	22.57 (5.81)	15.69 (7.11)
75	22.13 (10.27)	27.10 (6.91)	21.98 (10.96)
150	24.63 (10.62)	30.18 (8.34)	29.78 (15.16)
200	24.59 (9.74)	30.90 (8.78)	30.60 (14.84)
300	26.12 (8.74)	31.60 (9.57)	32.20 (13.73)

Table IV.62: The means and standard deviations of the Disperse task by radius of orientation.

Radius of Orientation	Significance	$\chi^2(2)$
20	$p < 0.001$	503.06
40	$p < 0.001$	216.55
75	$p < 0.001$	168.31
150	$p < 0.001$	66.67
200	$p < 0.001$	53.87
300	$p < 0.001$	40.08

Table IV.63: The significance results from the Kruskal-Wallis Test for the Disperse task by radius of orientation.

affect of the model type on the nearest neighbor distance for each of the subgroups, with significance as detailed in Table IV.65. The Wilcoxon Rank-Sum test found a significant difference with a radius of attraction equal to 25 between the metric and topological models ($p < 0.001$, z = 28) and the visual and topological models ($p < 0.001$, z = 4,165). That is, when the radius of attraction was 25, the topological model had a significantly larger nearest neighbor distance and better performance than the metric and visual models. The Wilcoxon Rank-Sum test found a significant difference when radius of attraction was equal to 35 between the metric and topological models ($p < 0.001$, z = 0), the metric and visual models ($p < 0.001$, z = 97), and the visual and topological models ($p < 0.001$, z = 4,331). This result implies that when the radius of attraction was 35, the topological model had a significantly larger nearest neighbor distance and better performance than the metric and visual models, and the visual model had a significantly larger nearest neighbor distance and better performance than the metric model. The Wilcoxon Rank-Sum test found a significant difference when the radius of attraction was equal to 80 between the metric and visual models (p = 0.02612, z = 22,205) and the visual and topological models ($p < 0.001$, z = 107,902). That is, when the radius of attraction was 80, the visual model had a significantly smaller nearest neighbor distance and worse performance than the metric and topological model. The Wilcoxon Rank-Sum test found a significant difference in trials with radius of attraction equal to 200 between the metric and topological models ($p < 0.001$, z = 58,057) and the visual and topological models ($p < 0.001$, z = 280,716). The Wilcoxon Rank-Sum test found a significant difference for a radius of attraction equal to 400 between the metric and topological models ($p < 0.001$, z = 153,159) and the visual and topological models ($p < 0.001$, z = 844,937). These results imply that when the

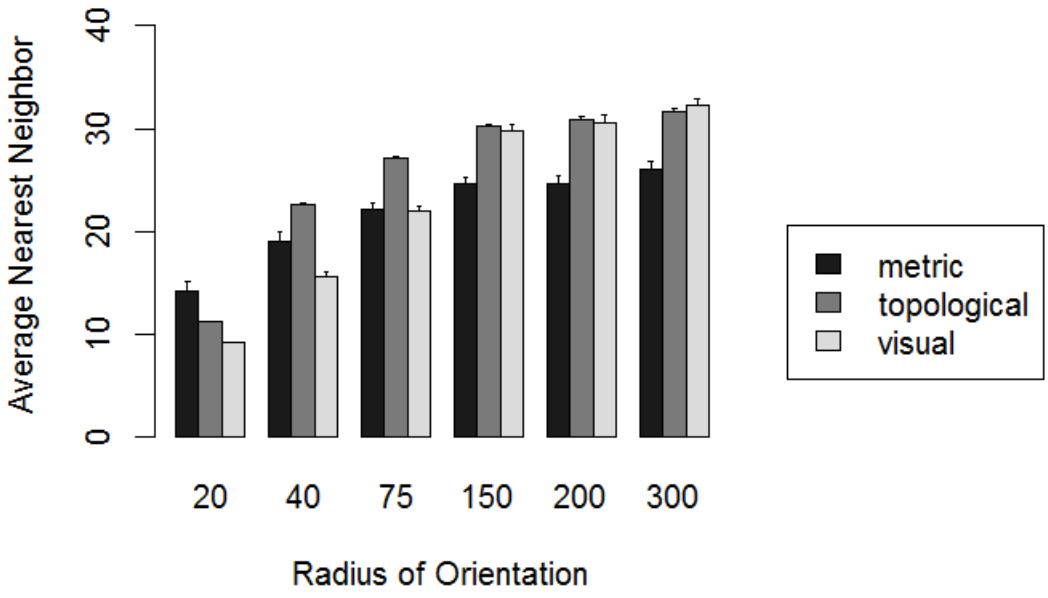

Figure IV.49: The distributions for each model in the Disperse task by radius of orientation.

radius of attraction was 200 or 400, the topological model had a significantly larger nearest neighbor distance and better performance than the metric and visual models. The Wilcoxon Rank-Sum test found a significant difference with a radius of attraction equal to 600 between the metric and topological models ($p < 0.001$, z = 148,174), the metric and visual models ($p < 0.01$, z = 156,863), and the visual and topological models ($p < 0.001$, z = 833,547.5). That is, when the radius of attraction was 600, the metric model had a signficantly smaller nearest neighbor distance and worse performance than the visual and topological models, and the topological model had a significantly larger nearest neighbor distance and better performance than the visual model.

Radius of Attraction	**Metric Mean (Std. Dev.)**	**Topological Mean (Std. Dev.)**	**Visual Mean (Std. Dev.)**
25	9.44 (0.46)	11.28 (0.74)	9.54 (0.57)
35	8.50 (0.26)	11.26 (0.76)	9.11 (0.36)
80	21.96 (10.57)	23.04 (8.13)	18.30 (10.15)
200	23.71 (13.28)	25.85 (8.97)	22.36 (13.47)
400	22.91 (9.94)	28.25 (9.47)	26.27 (14.45)
600	22.52 (10.21)	28.21 (9.45)	26.65 (14.90)

Table IV.64: The means and standard deviations of the Disperse task by radius of attraction.

The Rally task also ran 8,208 trials, with the same distribution across models as the Disperse task. The

Radius of Attraction	Significance	$\chi^2(2)$
25	$p < 0.001$	98.56
35	$p < 0.001$	120.34
80	$p < 0.001$	76.90
200	$p < 0.001$	85.64
400	$p < 0.001$	125.54
600	$p < 0.001$	126.44

Table IV.65: The significance results from the Kruskal-Wallis Test for the Disperse task by radius of attraction.

metric for the Rally task was also the nearest neighbor distance, *NearestNeighbor*. However, the Rally task requires a lower nearest neighbor distance for better performance, as opposed to the Disperse task which requires a higher nearest neighbor distance for better performance. The mean nearest neighbor distance for the metric model was 59.22 units (std. dev. = 31.37 units). The topological model had a mean nearest neighbor distance of 65.44 units (std. dev. = 31.68 units), while the visual models had a mean nearest neighbor distance of 67.20 units (std. dev. = 31.55 units). Each model's distribution can be seen in Figure IV.51.

The Kruskal-Wallis test found a significant affect of the model type on nearest neighbor distance ($p < 0.001$, $\chi^2(2) = 62.00$). The Wilcoxon Rank-Sum test found significant differences between all three pairings, as presented in Table IV.66. This analysis indicates that the metric trials had a significantly smaller nearest neighbor distance than the topological and visual models. The topological model had a significantly smaller nearest neighbor distance than the visual model.

Pairing	Significance	z-Value
Metric-Visual	$p < 0.001$	1,317,854
Metric-Topological	$p < 0.001$	1,838,365
Topological-Visual	$p < 0.05$	6,094,318

Table IV.66: The significance results from the Wilcoxon Rank-Sum Test for the Rally task.

The means and standard deviations by number of agents are presented in Table IV.67. The descriptive statistics are visualized in Figure IV.52. The Kruskal-Wallis test found a significant affect of the model type on the nearest neighbor distance by number of agents; the results are provided in Table IV.68. The Wilcoxon Rank-Sum test for 50 agents found that there was a significant difference between the metric and topological models ($p < 0.01$, z = 45,356) and the metric and visual models ($p < 0.001$, z = 31,850). The Wilcoxon Rank-Sum test for 100 agents found that there was a significant difference between the metric and topological models ($p < 0.001$, z = 37,002) and the metric and visual models ($p < 0.001$, z = 29,451). The Wilcoxon Rank-Sum test for 500 agents found that there was a highly significant difference between the metric and topological models ($p < 0.001$, z = 73,383) and the metric and visual models ($p < 0.001$, z = 51,889). These

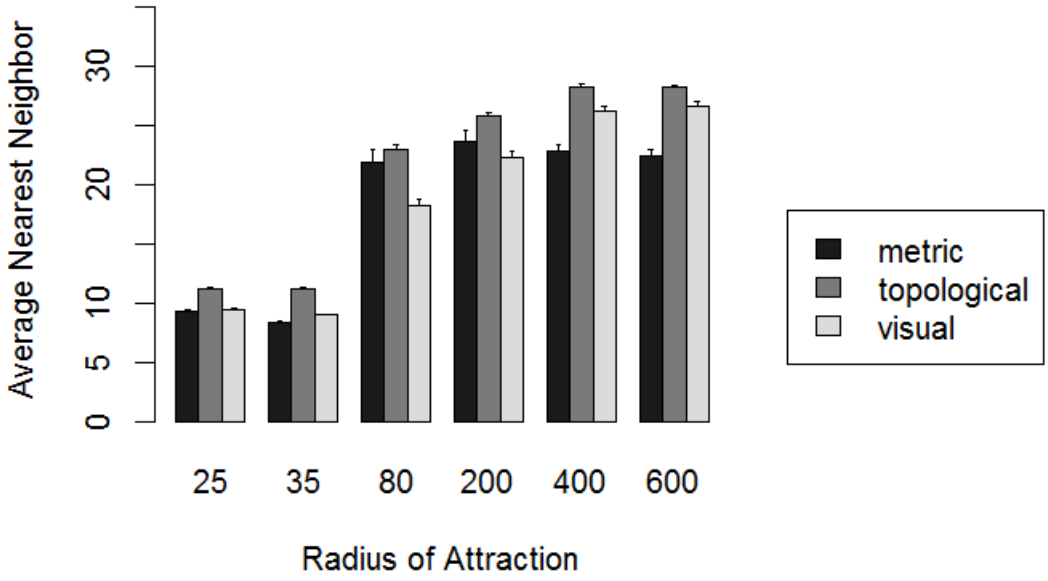

Figure IV.50: The distributions for each model in the Disperse task by radius of attraction.

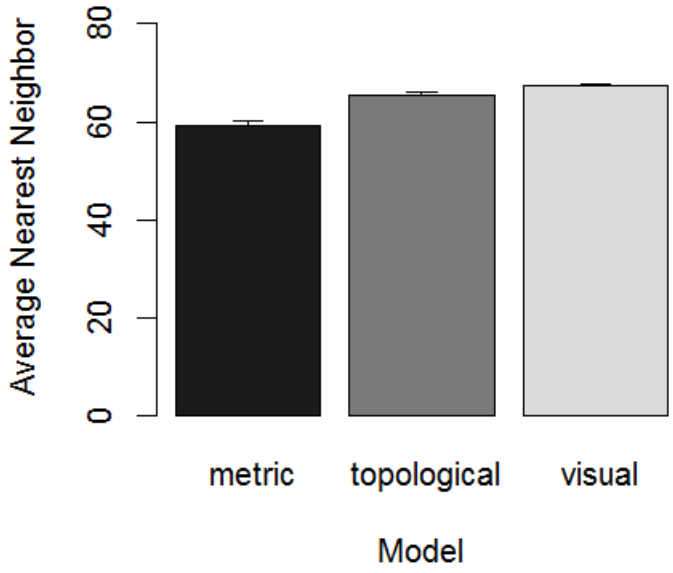

Figure IV.51: The distributions for each model in the Rally task.

results imply that when there were 50, 100, or 500 agents, the metric model had a significantly smaller nearest neighbor distance and better performance than the topological and visual models. The Wilcoxon Rank-Sum test for 250 agents found that there was a highly significant difference between the metric and topological models (p = 0.0387, z = 84,834), the metric and visual models ($p < 0.001$, z =56,928), and the topological and visual models (p = 0.0228, z = 260,800). The Wilcoxon Rank-Sum test for 1000 agents found that there was a highly significant difference between the metric and topological models (p = 0.0251, z = 132,964), the metric and visual models ($p < 0.001$, z = 88,681), and the topological and visual models ($p < 0.01$, z = 405,575). That is, when there were 250 or 100 agents, the metric model had a significantly smaller nearest neighbor distance and better performance than the topological and visual models and the visual model had a significantly larger nearest neighbor distance and worse performance than the topological model.

Number of Agents	**Metric Mean (Std. Dev.)**	**Topological Mean (Std. Dev.)**	**Visual Mean (Std. Dev.)**
50	71.61 (32.61)	77.64 (34.65)	79.30 (35.59)
100	49.57 (29.26)	61.07 (27.27)	59.18 (27.45)
250	65.53 (30.38)	69.24 (32.46)	72.69 (31.75)
500	47.43 (27.59)	55.33 (26.69)	56.40 (25.63)
1000	61.94 (30.92)	65.77 (32.31)	69.01 (31.55)

Table IV.67: The means and standard deviations of the Rally task by number of agents.

Number of Agents	**Significance**	$\chi^2(2)$
50	$p < 0.01$	13.17
100	$p < 0.001$	35.22
250	$p < 0.001$	15.57
500	$p < 0.001$	31.37
1000	$p < 0.001$	20.29

Table IV.68: The significance results from the Kruskal-Wallis Test for the Rally task by number of agents.

The means and standard deviations by number of obstacles are presented in Table IV.69. The descriptive statistics are visualized in Figure IV.53. The Kruskal-Wallis test found a significant affect of the model type on the nearest neighbor distance when the number of obstacles was less than 250; the results are provided in Table IV.70. The Wilcoxon Rank-Sum test for zero obstacles found that there was a significant difference between the metric and topological models (p = 0.0361, z = 133,790), the metric and visual models ($p <$ 0.001, z = 91,349) and the topological and visual models ($p < 0.01$, z = 401,600). These results imply that when there were zero obstacles, the metric model had a smaller nearest neighbor distance and better performance than the topological and visual models, and the visual model had a larger nearest neighbor distance and worse performance than the topological model. The Wilcoxon Rank-Sum results for 25 obstacles found that there was a highly significant difference between the metric and topological models ($p < 0.001$, z

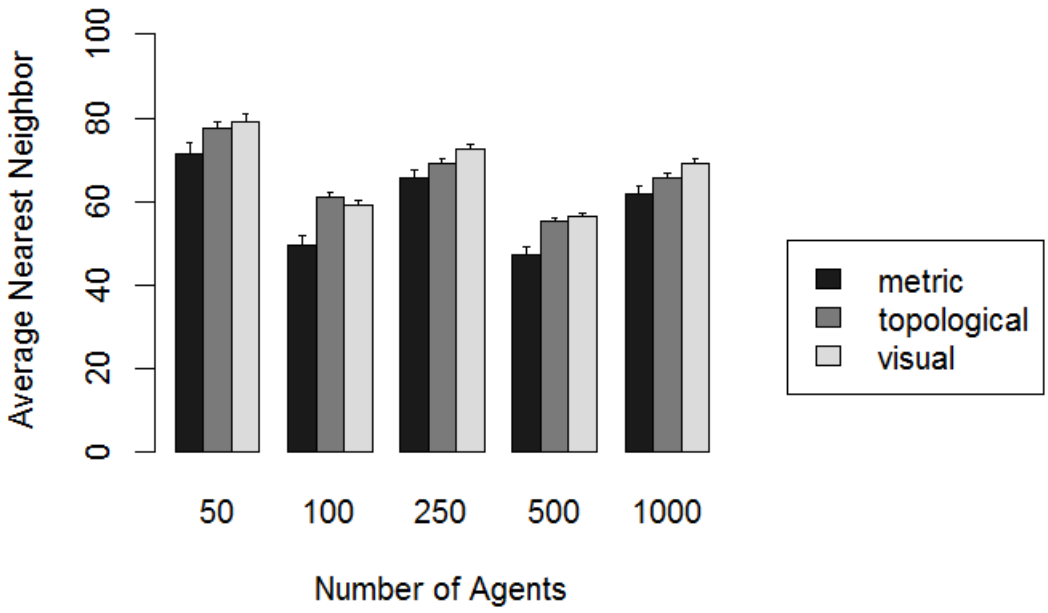

Figure IV.52: The distributions for each model in the Rally task by number of agents.

= 123,652) and the metric and visual models ($p < 0.001$, z = 91,400). The Wilcoxon Rank-Sum test for 50 obstacles found that there was a highly significant difference between the metric and topological models ($p < 0.001$, z = 122,524) and the metric and visual models ($p < 0.001$, z = 90,683). The Wilcoxon Rank-Sum analysis for 100 obstacles found that there was a significant difference between the metric and topological models (p = 0.0189, z = 46,232) and the topological and visual models ($p < 0.01$, z = 32,743). These results imply that when there were 25, 50, or 100 obstacles, the metric model had a smaller nearest neighbor distance and better performance than the topological and visual models.

Number of Obstacles	**Metric Mean (Std. Dev.)**	**Topological Mean (Std. Dev.)**	**Visual Mean (Std. Dev.)**
0	57.67 (31.90)	61.43 (31.73)	65.72 (32.02)
25	59.17 (31.49)	66.67 (31.45)	67.33 (31.82)
50	59.77 (31.38)	67.81 (31.58)	68.22 (31.46)
100	59.46 (30.59)	65.23 (31.27)	66.89 (30.44)
250	63.63 (31.04)	68.09 (32.67)	69.82 (31.56)

Table IV.69: The means and standard deviations of the Rally task by number of obstacles.

A similar analysis was conducted for the results grouped by the radii of attraction, orientation, and repulsion. The means and standard deviations for the results grouped by radius of repulsion are reported in Table

Number of Obstacles	Significance	$\chi^2(2)$
0	$p < 0.001$	19.11
25	$p < 0.001$	17.69
50	$p < 0.001$	19.26
100	$p < 0.01$	9.56
250	Not Significant	N/A

Table IV.70: The significance results from the Kruskal-Wallis Test for the Rally task by number of obstacles.

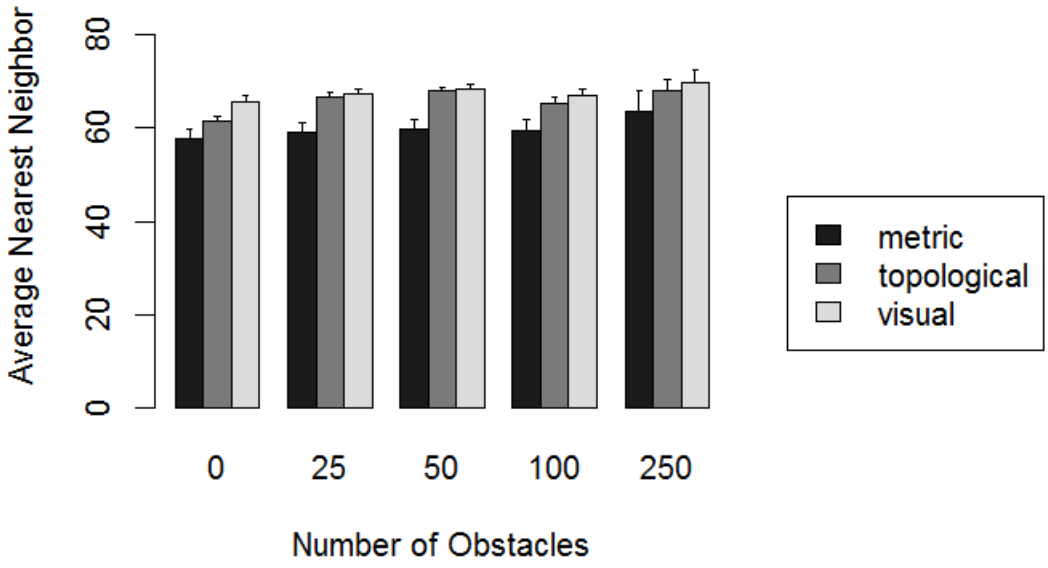

Figure IV.53: The distributions for each model in the Rally task by number of obstacles.

IV.71, and the descriptive statistics are visualized in Figure IV.54. The Kruskal-Wallis test found a significant affect of the model type on the nearest neighbor distance when the radius of repulsion was less than 100, with significance as detailed in Table IV.72. The Wilcoxon Rank-Sum test for the radius of repulsion equal to 5 found that there was a highly significant difference between the metric and topological models ($p < 0.001$, z = 260,150) and the metric and visual models ($p < 0.001$, z = 187,222). That is, when the radius of repulsion was 5, the metric model had a smaller nearest neighbor distance and better performance than the visual and topological models. The Wilcoxon Rank-Sum test for the radius of repulsion equal to 25 found that there was a highly significant difference between the metric and topological models ($p < 0.001$, z = 130,945), the metric and visual models ($p < 0.001$, z = 87,099), and the topological and visual models ($p < 0.01$, z = 449,102). The Wilcoxon Rank-Sum test for the radius of repulsion equal to 50 found that there was a highly significant

difference between the metric and topological models ($p < 0.001$, z = 74,481), the metric and visual models ($p < 0.001$, z = 49,187), and the topological and visual models (p = 0.0113, z = 241,834). These results imply that when the radius of repulsion was 25 or 50, the metric model had a smaller nearest neighbor distance and better performance than the visual and topological models, and the visual model had a significantly larger nearest neighbor distance and worse performance than the topological model.

Radius of Repulsion	**Metric Mean (Std. Dev.)**	**Topological Mean (Std. Dev.)**	**Visual Mean (Std. Dev.)**
5	37.42 (21.66)	45.89 (26.28)	47.40 (26.63)
25	51.62 (14.89)	58.80 (19.94)	61.42 (19.95)
50	73.41 (12.08)	77.66 (15.20)	79.65 (14.94)
100	118.57 (9.56)	119.08 (10.24)	119.45 (11.28)

Table IV.71: The means and standard deviations of the Rally task by radius of repulsion.

Radius of Repulsion	**Significance**	$\chi^2(2)$
5	$p < 0.001$	42.08
25	$p < 0.001$	45.00
50	$p < 0.001$	26.96
100	Not Significant	N/A

Table IV.72: The significance results from the Kruskal-Wallis Test for the Rally task by radius of repulsion.

The means and standard deviations for the results grouped by radius of orientation are provided in Table IV.73. The descriptive statistics are visualized in Figure IV.55. The Kruskal-Wallis test found a significant affect of the model type on the nearest neighbor distance for each of the subgroups, with significance as detailed in Table IV.74. The Wilcoxon Rank-Sum test found a highly significant difference for radius of orientation equal to 20 between the metric and topological models ($p < 0.01$, z = 21,681) and the metric and visual models ($p < 0.01$, z = 15,676). The Wilcoxon Rank-Sum test found a significant difference for radius of orientation equal to 150 between the metric and topological models ($p < 0.001$, z =85,690) and the metric and visual models ($p < 0.001$, z = 64,365). The Wilcoxon Rank-Sum test found a significant difference for radius of orientation equal to 200 between the metric and topological models ($p < 0.001$, z = 31,893) and the metric and visual models ($p < 0.001$, z = 24,849). This result implies that when the radius of orientation was 20, 150, or 200, the metric model had a significantly smaller nearest neighbor distance and better performance than the topological and visual models. The Wilcoxon Rank-Sum test found a significant difference for radius of orientation equal to 40 between the metric and visual models ($p < 0.001$, z = 26,167) and the visual and topological models ($p < 0.001$, z =113,291). The Wilcoxon Rank-Sum test found a significant difference for radius of orientation equal to 75 between the metric and visual models ($p < 0.001$, z = 256,970) and the visual and topological models ($p < 0.001$, z = 61,674). That is, when the radius of orientation was 40 or 75, the visual model had a significantly larger nearest neighbor distance and worse performance than the metric

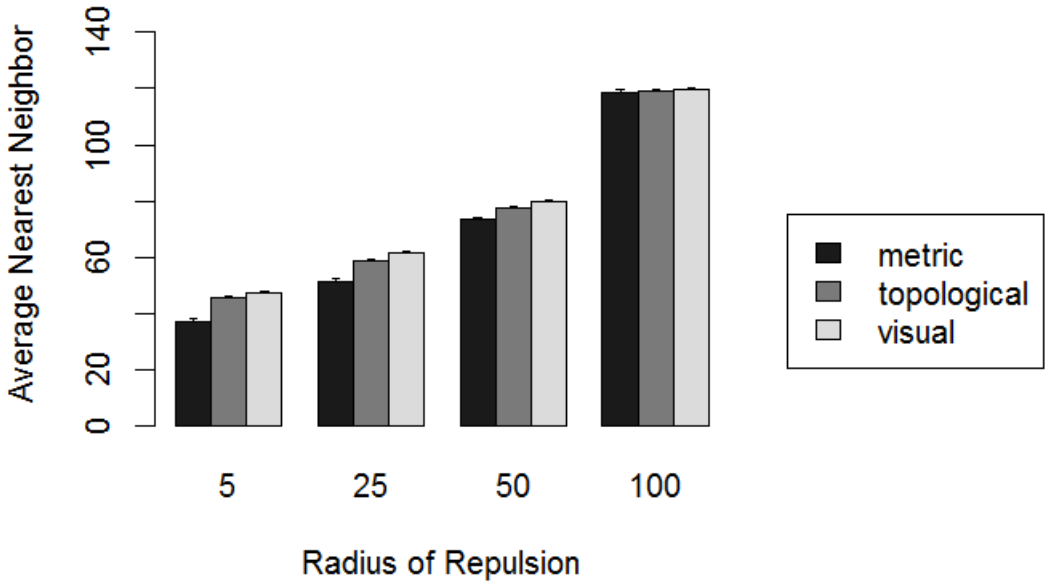

Figure IV.54: The distributions for each model in the Rally task by radius of repulsion.

and topological models. The Wilcoxon Rank-Sum test found a significant difference for radius of orientation equal to 300 between the metric and topological models ($p < 0.001$, $z = 32{,}626$), the metric and visual models ($p < 0.001$, $z = 27{,}930$), and the visual and topological models ($p < 0.01$, $z = 152{,}282$). This result implies that when the radius of orientation was 300, the metric model had a significantly smaller nearest neighbor distance and better performance than the topological and visual models, and the visual model had a smaller nearest neighbor difference and better performance than the topological model.

Radius of Orientation	**Metric Mean (Std. Dev.)**	**Topological Mean (Std. Dev.)**	**Visual Mean (Std. Dev.)**
20	23.13 (18.14)	25.00 (19.36)	28.33 (20.88)
40	38.02 (17.86)	40.12 (17.38)	45.80 (18.73)
75	50.75 (19.05)	52.79 (18.47)	58.13 (21.03)
150	74.16 (30.42)	81.41 (25.94)	82.15 (28.51)
200	77.72 (29.30)	90.61 (22.03)	89.74 (24.60)
300	79.25 (26.30)	90.92 (20.39)	86.41 (25.12)

Table IV.73: The means and standard deviations of the Rally task by radius of orientation.

The means and standard deviations for the results grouped by radius of attraction are presented in Table IV.75. The descriptive statistics are visualized in Figure IV.56. The Kruskal-Wallis test found a significant affect of the model type on the nearest neighbor distance when the radius of attraction was 25, 35, 400, or

Radius of Orientation	Significance	$\chi^2(2)$
20	$p < 0.01$	10.59
40	$p < 0.001$	33.95
75	$p < 0.001$	43.57
150	$p < 0.001$	19.23
200	$p < 0.001$	35.48
300	$p < 0.001$	32.75

Table IV.74: The significance results from the Kruskal-Wallis Test for the Rally task by radius of orientation.

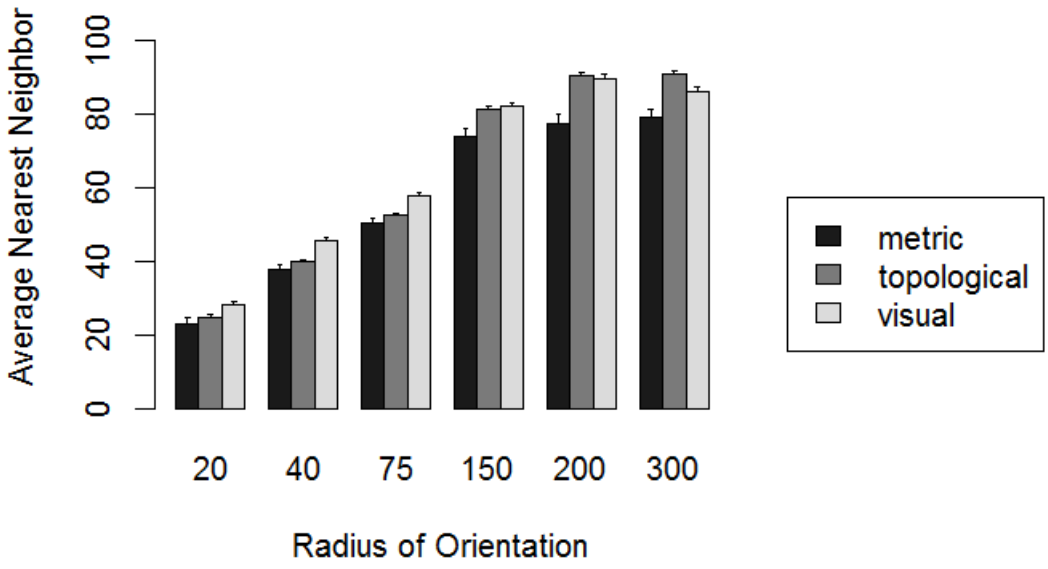

Figure IV.55: The distributions for each model in the Rally task by radius of orientation.

600, with significance as detailed in Table IV.76. The Wilcoxon Rank-Sum test found a significant difference when the radius of attraction was equal to 25 between the metric and topological models ($p < 0.001$, z = 105) and the visual and topological models ($p < 0.001$, z = 3,682). The Wilcoxon Rank-Sum test found a significant difference in trials with radius of attraction equal to 35 between the metric and topological models ($p < 0.001$, z = 33), the metric and visual models ($p < 0.001$, z = 116), and the visual and topological models ($p < 0.001$, z = 3,440). These results imply that when the radius of attraction was 25 or 35, the topological model had a significantly larger nearest neighbor distance and performed worse than the metric and visual models. Additionally, when the radius of attraction was 35, the visual model had a significantly larger nearest neighbor distance and performed worse than the metric model. The Wilcoxon Rank-Sum test found a significant difference when the radius of attraction was equal to 300 between the metric and

topological models ($p < 0.001$, z = 201,624), the metric and visual models ($p < 0.001$, z = 139,689), and the visual and topological models (p = 0.0103, z = 658,845). The Wilcoxon Rank-Sum test found a significant difference in trials with radius of attraction equal to 600 between the metric and topological models ($p <$ 0.001, z = 166,717), the metric and visual models ($p < 0.001$, z = 114,643), and the visual and topological models ($p < 0.01$, z = 657,839). These results imply that when the radius of attraction was 400 or 600, the metric model had a significantly smaller nearest neighbor distance and performed better than the topological and visual models, and the visual model had a significantly larger nearest neighbor distance and performed worse than the topological model.

Radius of Attraction	**Metric Mean (Std. Dev.)**	**Topological Mean (Std. Dev.)**	**Visual Mean (Std. Dev.)**
25	9.64 (0.14)	10.91 (0.77)	9.62 (0.83)
35	9.13 (0.29)	10.87 (0.73)	10.07 (0.67)
80	28.31 (16.66)	26.73 (14.66)	27.53 (15.40)
200	48.58 (27.22)	50.78 (25.78)	51.45 (24.15)
400	72.10 (27.47)	77.62 (25.88)	80.09 (24.11)
600	68.08 (28.23)	80.36 (24.11)	82.67 (23.87)

Table IV.75: The means and standard deviations of the Rally task by radius of attraction.

Radius of Attraction	**Significance**	$\chi^2(2)$
25	$p < 0.001$	61.86
35	$p < 0.001$	66.41
80	Not Significant	N/A
200	Not Significant	N/A
400	$p < 0.001$	31.51
600	$p < 0.001$	94.56

Table IV.76: The significance results from the Kruskal-Wallis Test for the Rally task by radius of attraction.

IV.2.6 Maintain Group / Flocking

The Flocking task ran a total of 8,208 trials, decomposed by model: metric = 1,026 trials, topological = 4,104 trials, and visual = 3,078 trials. The first metric for this task was the *change in dispersion*, $\Delta Dispersion$. The mean change in the dispersion for the metric model was 357,635,626,632 (std. dev. = 4,286,798,000,000). The topological model had a mean change in dispersion of 59,883,809 (std. dev. = 239,713,646), and the visual model had a mean change in dispersion of 239,292,507,151 (std. dev. = 3,520,467,000,000). The Kruskal-Wallis test indicated that there was a highly significant affect of the model type on the change in dispersion ($p < 0.001$, $\chi^2(2)$ = 16.39). The Wilcoxon Rank-Sum test found highly significant differences between all three pairings, as presented in Table IV.77. These results imply that the metric model had a significantly higher change in dispersion and worse performance than the topological and visual models, and the topological model had a lower change in dispersion and better performance than the visual model.

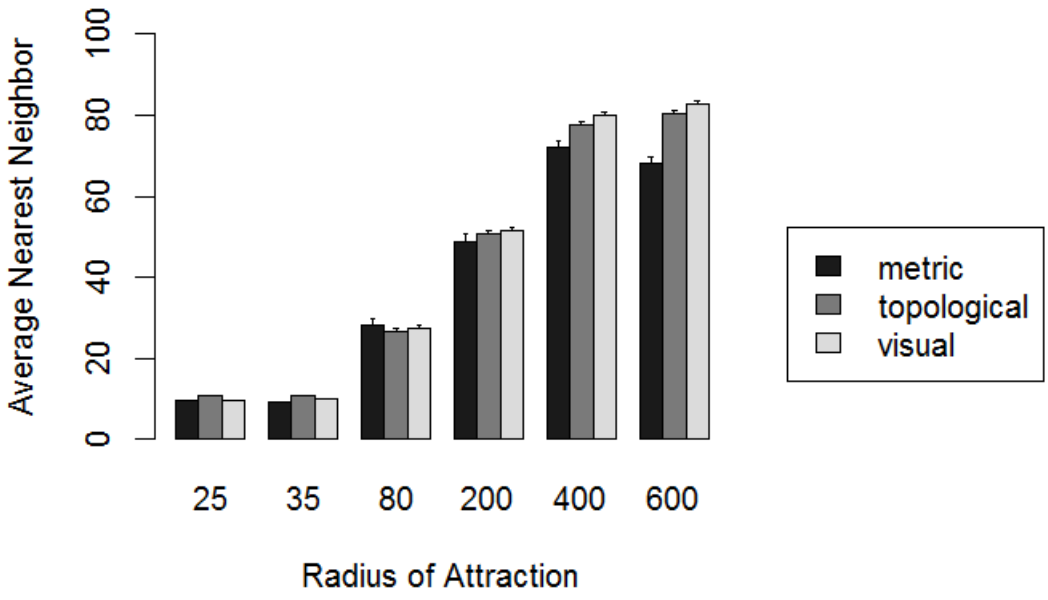

Figure IV.56: The distributions for each model in the Rally task by radius of attraction.

Pairing	**Significance**	***z*-Value**
Metric-Visual	$p < 0.001$	1,659,308
Metric-Topological	$p < 0.001$	2,272,305
Topological-Visual	$p < 0.001$	6,136,590

Table IV.77: The significance results from the Wilcoxon Rank-Sum Test for the Flocking task using the change in dispersion metric.

The means and standard deviations by number of agents are presented in Table IV.78. The Kruskal-Wallis test found a significant affect of model type on the change in dispersion for each subgroup, with significance as detailed in Table IV.79. The Wilcoxon Rank-Sum test for 50 agents found that there was a significant difference between the metric and visual models (p = 0.0192, z = 44,195) and the topological and metric models ($p < 0.01$, z =59,743). That is, when there were 50 agents the metric model had a significantly higher change in dispersion and worse performance than the topological and visual models. The Wilcoxon Rank-Sum test for the trials with 100 agents found that there was a highly significant difference between the metric and topological models ($p < 0.001$, z = 64,836), the metric and visual models ($p < 0.001$, z = 46,640), and the topological and visual models ($p < 0.001$, z = 139,039). This result implies that when there were 100 agents, the topological model had a significantly higher change in dispersion and worse performance than the metric and visual models, and the visual model had a singificantly lower change in dispersion and better

performance than the metric model. The Wilcoxon Rank-Sum test for the trials with 250 agents found that there was a highly significant difference between the topological and visual models ($p < 0.01$, z = 256,652). That is, when there were 250 agents, the topological model had a significantly lower change in dispersion and better performance than the visual model. The Wilcoxon Rank-Sum test for the trials with 500 agents found that there was a significant difference between the metric and topological models ($p < 0.001$, z = 106,913), the metric and visual models (p = 0.0318, z = 76,803), and the topological and visual models ($p < 0.001$, z = 251,461). This result implies that when there were 500 agents, the topological model had a significantly lower change in dispersion and better performance than the visual and metric models, and the visual model had a higher change in dispersion and worse performance than the metric model. The Wilcoxon Rank-Sum test for the trials with 1000 agents found that there was a highly significant difference between the metric and topological models ($p < 0.001$, z = 178,295), the metric and visual models ($p < 0.01$, z = 123,634), and the topological and visual models ($p < 0.001$, z = 375,341). This result implies that when there were 1000 agents, the topological model had a significantly lower change in dispersion and better performance than the visual and metric models, and the visual model had a lower change in dispersion and better performance than the metric model.

Number of Agents	**Metric Mean (Std. Dev.)**	**Topological Mean (Std. Dev.)**	**Visual Mean (Std. Dev.)**
50	3,736,087	2,636,684	2,824,896
	(2,952,971)	(1,783,581)	(1,905,783)
100	10,563,342	26,548,123	6,842,840
	(8,978,625)	(530,708,659)	(5,208,805)
250	38,201,943	28,010,942	28,672,674
	(38,881,264)	(30,777,258)	(24,079,711)
500	83,433,086	50,746,755	2,389,278,216
	(87,564,534)	(51,794,132)	(59,253,167,464)
1000	1,358,909,000,000	147,041,434	907,371,365,819
	(8,285,942,000,000)	(188,669,151)	(6,821,263,000,000)

Table IV.78: The means and standard deviations of the Flocking task by number of agents for change in dispersion.

Number of Agents	**Significance**	$\chi^2(2)$
50	$p = 0.0101$	9.19
100	$p < 0.001$	29.23
250	$p = 0.0158$	8.30
500	$p < 0.001$	18.89
1000	$p < 0.001$	49.36

Table IV.79: The significance results from the Kruskal-Wallis Test for the Flocking task by number of agents for change in dispersion.

The means and standard deviations by number of obstacles are provided in Table IV.80. The Kruskal-

Wallis test no found significant affect of the model type on change in dispersion when the number of obstacles was 0 or 25. The Kruskal-Wallis test found a significant affect of the model type on change in dispersion when the number of obstacles was 50, 100, or 250, with significance as detailed in Table IV.81. The Wilcoxon Rank-Sum test for the trials with 50 obstacles found that there was a highly significant difference between the metric and topological models ($p < 0.01$, z = 16,1457). That is, when there were 50 obstacles, the metric model had a significantly higher change in dispersion and worse performance than the topological model. The Wilcoxon Rank-Sum test for the trials with 100 obstacles found that there was a significant difference between the metric and topological models ($p < 0.01$, z = 60,441) and the topological and visual models (p = 0.0136, z = 143,988). The Wilcoxon Rank-Sum test for the trials with 250 obstacles found that there was a significant difference between the metric and topological models ($p < 0.001$, z = 7,650), the metric and visual models (p = 0.0288, z = 5,244), and the topological and visual models ($p < 0.01$, z = 14,523). These results imply that when there were 100 or 250 obstacles, the topological model had a significantly smaller change in dispersion and better performance than the metric and visual models. In addition, when there were 250 obstacles, the metric model had a significantly higher change in dispersion and worse performance than the visual model.

Number of Obstacles	**Metric Mean (Std. Dev.)**	**Topological Mean (Std. Dev.)**	**Visual Mean (Std. Dev.)**
0	1,248,949,582 (9,681,733,534)	54,943,073 (117,239,588)	64,909,213,598 (1,828,971,000,000)
25	194,930,435,979 (3,167,776,000,000)	47,831,707 (107,392,062)	193,631,948,060 (3,163,918,000,000)
50	580,218,854,250 (5,466,327,000,000)	61,469,067 (426,175,313)	195,293,000,000 (3,164,239,000,000)
100	3,558,359,049 (16,334,286,997)	69,649,397 (120,959,450)	433,297,000,000 (4,748,229,000,000)
250	2,902,411,000,000 (12,032,880,000,000)	107,624,952 (103,739,056)	977,495,680,891 (7,119,924,000,000)

Table IV.80: The means and standard deviations of the Flocking task by number of obstacles for change in dispersion.

Number of Obstacles	**Significance**	$\chi^2(2)$
0	Not Significant	N/A
25	Not Significant	N/A
50	$p = 0.0163$	8.23
100	$p < 0.01$	11.90
500	$p < 0.001$	17.15

Table IV.81: The significance results from the Kruskal-Wallis Test for the Flocking task by number of obstacles for change in dispersion.

The means and standard deviations for radius of repulsion are presented in Table IV.82. The Kruskal-

Wallis test found a significant affect of the model type on change in dispersion when the radius of repulsion was 5, 25, or 100. The Kruskal-Wallis test found a significant affect of the model type on change in dispersion when the radius of repulsion was 50 ($p < 0.001$, $\chi^2(2) = 17.29$). The Wilcoxon Rank-Sum test where the radius of repulsion was equal to 50 found that there was a highly significant difference between the metric and topological models ($p < 0.001$, $z = 100{,}944$) and the topological and visual models ($p < 0.01$, $z = 237{,}286$). That is, when the radius of repulsion was 50, the topological model had a significantly smaller change in dispersion and better performance than the metric and visual models.

Radius of Repulsion	**Metric Mean (Std. Dev.)**	**Topological Mean (Std. Dev.)**	**Visual Mean (Std. Dev.)**
5	89,510,643 (147,320,149)	65,802,919 (355,077,045)	1,324,076,091 (43,596,585,100)
25	86,108,623 (134,466,728)	65,892,832 (131,773,081)	65,223,687 (103,366,976)
50	11,935,905,044 (28,542,848,689)	60,494,991 (125,314,656)	4,144,922,683 (17,656,000,000)
100	2,739,694,000,000 (11,667,360,000,000)	28,289,574 (46,602,249)	1,835,345,000,000 (9,637,281,000,000)

Table IV.82: The means and standard deviations of the Flocking task by radius of repulsion for change in dispersion.

The means and standard deviations for the Flocking task results for change in dispersion grouped by radius of orientation are presented in Table IV.83. The Kruskal-Wallis test found no impact of the model type on change in dispersion when the radius of orientation was 40 or 75. The Kruskal-Wallis test found a significant impact of the model type on change in dispersion when the radius of orientation was 20, 150, 200, or 300, as detailed in Table IV.84. The Wilcoxon Rank-Sum test found that when the radius of orientation was equal to 20, there was a significant difference between the metric and topological models ($p = 0.0268$, $z = 22{,}508$) and the topological and visual models ($p = 0.0380$, $z = 84{,}661$). The Wilcoxon Rank-Sum test found that when the radius of orientation was equal to 300, there was a significant difference between the metric and topological models ($p < 0.01$, $z = 53{,}024$) and the topological and visual models ($p = 0.0448$, $z = 128{,}672$). That is, when the radius of orientation was 20 or 300, the topological model had a significantly lower change in dispersion and better performance than the metric and visual models. The Wilcoxon Rank-Sum test found that when the radius of orientation was equal to 150, there was a highly significant difference between the metric and topological models ($p < 0.01$, $z = 116{,}453$). This result implies that when the radius of orientation was 150, the topological model had a significantly lower change in dispersion and better performance than the metric model. The Wilcoxon Rank-Sum test found that when the radius of orientation was equal to 200, there was a significant difference between the metric and topological models ($p < 0.01$, $z = 52{,}566$) and the metric and visual models ($p = 0.0276$, $z = 38{,}788$). That is, when the radius of orientation was 20 or 300, the

metric model had a significantly larger change in dispersion and worse performance than the topological and visual models.

Radius of Orientation	Metric Mean (Std. Dev.)	Topological Mean (Std. Dev.)	Visual Mean (Std. Dev.)
20	33,325,247	23,627,768	29,496,714
	(64,237,966)	(22,762,142)	(43,931,615)
40	45,852,464	25,826,092	33,047,757
	(74,388,988)	(25,156,560)	(43,237,600)
75	3,915,940,705	30,192,818	1,443,171,908
	(17,221,026,157)	(30,154,833)	(10,540,507,613)
150	917,155,920,415	43,106,243	688,726,588,358
	(6,848,465,000,000)	(45,829,475)	(5,958,537,000,000)
200	687,654,758,099	90,872,275	343,404,000,000
	(5,950,859,000,000)	(550,739,666)	(4,212,733,000,000)
300	344,707,083,586	159,847,927	236,510,618,858
	(4,221,932,000,000)	(254,355,664)	(3,503,072,000,000)

Table IV.83: The means and standard deviations of the Flocking task by radius of orientation for change in dispersion.

Radius of Orientation	Significance	$\chi^2(2)$
20	$p = 0.0265$	7.26
40	Not Significant	N/A
75	Not Significant	N/A
150	$p = 0.0102$	9.18
200	$p = 0.0307$	6.97
300	$p < 0.01$	9.76

Table IV.84: The significance results from the Kruskal-Wallis Test for the Flocking Task task by radius of orientation for change in dispersion.

The means and standard deviations for the Flocking task results for change in dispersion grouped by radius of attraction are presented in Table IV.85. The Kruskal-Wallis test found a highly significant impact of the model type on change in dispersion for each subgroup by radius of attraction, as detailed in Table IV.86. The Wilcoxon Rank-Sum test found that when the radius of attraction was equal to 25, there was a highly significant difference between the metric and topological models ($p < 0.01$, $z = 352$) and the topological and visual models ($p < 0.01$, $z = 2{,}793$). That is, when the radius of attraction was 25, the metric model had a significantly smaller change in dispersion and better performance than the topological model and the topological model had a significantly smaller change in dispersion and worse performance than the visual model. The Wilcoxon Rank-Sum test found that when the radius of attraction was equal to 35, there was a significant difference between the metric and topological models ($p < 0.001$, $z = 274$), the metric and visual models ($p = 0.0318$, $z = 362$), and the topological and visual models ($p = 0.0210$, $z = 2{,}674$). These results imply that when the radius of attraction was 35, the metric model had a significantly smaller change

in dispersion and better performance than the topological and visual models and the topological model had a significantly smaller change in dispersion and worse performance than the visual model. The Wilcoxon Rank-Sum test found that when the radius of attraction was equal to 200, there was a highly significant difference between the metric and topological models ($p < 0.001$, z = 60,241) and the metric and visual models ($p < 0.01$, z = 45,954). That is, when the radius of attraction was 200, the metric model had a significantly larger change in dispersion and worse performance than the visual and topological models. The Wilcoxon Rank-Sum test found that when the radius of attraction was equal to 80, there was a highly significant difference between the metric and visual models ($p < 0.001$, z = 14,849), the topological and visual models ($p < 0.001$, z = 15,367), and the topological and visual models ($p < 0.001$, z = 93,435). The Wilcoxon Rank-Sum test found that when the radius of attraction was equal to 400, there was a significant difference between the metric and topological models ($p < 0.001$, z = 268,574), the metric and visual models ($p = 0.0257$, z = 189,563), and the topological and visual models ($p < 0.01$, z = 655,801). The Wilcoxon Rank-Sum test found that when the radius of attraction was equal to 600, there was a highly significant difference between the metric and topological models ($p < 0.001$, z = 312,540), the metric and visual models ($p < 0.001$, z = 220,918), and the topological and visual models ($p < 0.001$, z = 640,140). These results imply that when the radius of attraction was 80, 400, or 600, the topological model had a significantly lower change in dispersion and better performance than the metric and visual models and the metric model had a significantly larger change in dispersion and worse performance than the visual model.

Radius of Attraction	**Metric Mean (Std. Dev.)**	**Topological Mean (Std. Dev.)**	**Visual Mean (Std. Dev.)**
25	7,622,904	23,768,669	23,970,857
	(9,621,117)	(22,957,970)	(45,057,354)
35	4,449,229	23,779,814	24,602,065
	(3,891,698)	(22,983,799)	(43,472,650)
80	2,120,786,680	27,606,965	495,317,943
	(12,906,487,474)	(27,419,984)	(6,129,122,680)
200	551,331,524,968	33,794,284	461,024,224,923
	(5,326,128,000,000)	(36,739,567)	(4,891,529,000,000)
400	459,487,728,276	79,200,098	205,490,371,331
	(4,860,706,000,000)	(388,710,149)	(3,245,615,000,000)
600	306,416,260,402	69,832,824	256,094,776,244
	(3,974,658,000,000)	(137,751,279)	(3,651,661,000,000)

Table IV.85: The means and standard deviations of the Flocking task by radius of attraction for change in dispersion.

The second metric for the flocking task was the *change in center of gravity*. The mean change in center of gravity for the metric model was 78.39 units (std. dev. = 596.06 units). The topological model had a mean change in center of gravity of 32.48 (std. dev. = 59.57 units). The visual model mean change in center of

Radius of Attraction	Significance	$\chi^2(2)$
25	$p < 0.001$	15.38
35	$p < 0.001$	17.88
80	$p < 0.001$	57.25
200	$p < 0.01$	12.69
400	$p < 0.001$	20.34
600	$p < 0.001$	95.60

Table IV.86: The significance results from the Kruskal-Wallis Test for the Flocking Task task by radius of orientation for the change in dispersion.

gravity was 45.32 units (std. dev. = 489.56 units). These descriptive statistics are illustrated in Figure IV.57. The Kruskal-Wallis test found a significant affect of the model type on change in center of gravity ($p < 0.001$, $\chi^2(2) = 283.56$). The Wilcoxon Rank-Sum test indicated that there was a significant difference between the topological and visual models ($p < 0.001$, z = 7,604,785) and the visual and metric models ($p < 0.001$, z = 1,872,424). The test did not find a significant difference between the metric and topological models. These results show that the topological model had a significantly lower change in the center of gravity, than both the visual and topological models.

The means and standard deviations by number of agents are presented in Table IV.87. The descriptive statistics are displayed in Figure IV.58. The Kruskal-Wallis test found a significant affect of the model type on the change in center of gravity for each of the subgroups, with significance as detailed in Table IV.88. The Wilcoxon Rank-Sum test for the trials with 50 agents found that there was a highly significant difference between the topological and visual models ($p < 0.001$, z = 181,714). That is, when there were 50 agents, the visual model had a significantly lower change in center of gravity and better performance than the topological model. The Wilcoxon Rank-Sum test for the trials with 100 agents found that there was a highly significant difference between the metric and visual models ($p < 0.001$, z = 50,111) and the topological and visual models ($p < 0.001$, z = 193,245). The Wilcoxon Rank-Sum test for the trials with 250 agents found that there was a highly significant difference between the metric and visual models ($p < 0.001$, z = 84,940) and the topological and visual models ($p < 0.001$, z = 340,645.5). The Wilcoxon Rank-Sum test for the trials with 500 agents found that there was a highly significant difference between the metric and visual models ($p < 0.001$, z = 86,530) and the topological and visual models ($p < 0.001$, z = 329,871). These results imply that when there were 100, 250, or 500 agents, the visual model had a significantly lower change in center of gravity and better performance than the metric and topological models. The Wilcoxon Rank-Sum test for 1000 agents found that there was a highly significant difference between the metric and visual models (p = 0.0471, z = 134,426), and the topological and visual models ($p < 0.001$, z = 530,051). That is, when there were 1000 agents, the topological model had a significantly lower change in center of gravity and better

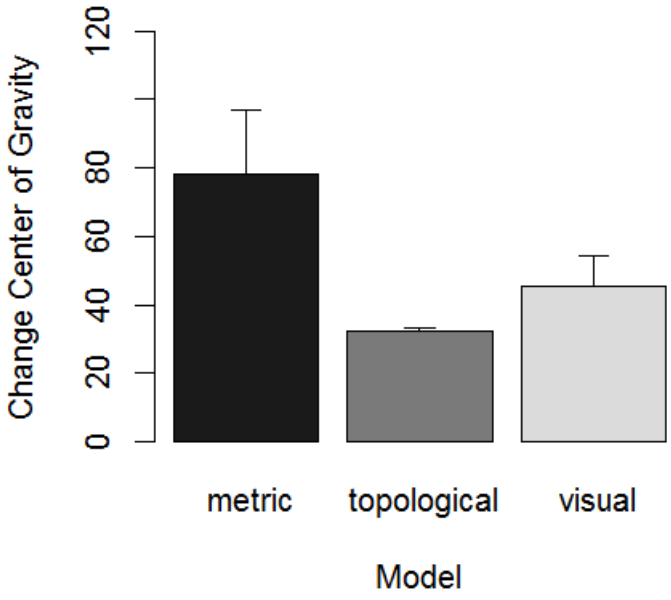

Figure IV.57: The distributions of change in center of gravity for each model in the Flocking task.

performance than the metric and visual models.

Number of Agents	**Metric Mean (Std. Dev.)**	**Topological Mean (Std. Dev.)**	**Visual Mean (Std. Dev.)**
50	15.42 (19.58)	22.84 (34.03)	11.16 (9.52)
100	25.16 (44.24)	39.15 (78.90)	11.53 (17.58)
250	20.28 (35.60)	27.26 (44.72)	7.13 (9.37)
500	29.23 (66.84)	48.25 (82.21)	13.56 (98.24)
1000	233.91 (1,146.63)	25.82 (41.42)	142.06 (943.82)

Table IV.87: The means and standard deviations of the Flocking task by number of agents for the change in center of gravity.

The means and standard deviations by number of obstacles are provided in Table IV.89. The descriptive statistics separated by number of obstacles are displayed in Figure IV.59. The Kruskal-Wallis test found a significant affect of model type on the change in center of gravity when the number of obstacles was less than 250, with significance as detailed in Table IV.90. The Wilcoxon Rank-Sum test when there were zero obstacles found that there was a significant difference between the metric and topological models ($p < 0.001$, z = 129,144), the metric and visual models ($p < 0.001$, z = 124,594), and the topological and visual models ($p < 0.001$, z = 544,510). That is, when there were zero obstacles, the topological model had a significantly higher change in the center of gravity and worse performance than the metric and visual models, and the

Number of Agents	Significance	$\chi^2(2)$
50	$p < 0.001$	20.08
100	$p < 0.001$	51.02
250	$p < 0.001$	56.91
500	$p < 0.001$	43.99
1000	$p < 0.001$	58.34

Table IV.88: The significance results from the Kruskal-Wallis Test for the Flocking task by number of agents for the change in center of gravity.

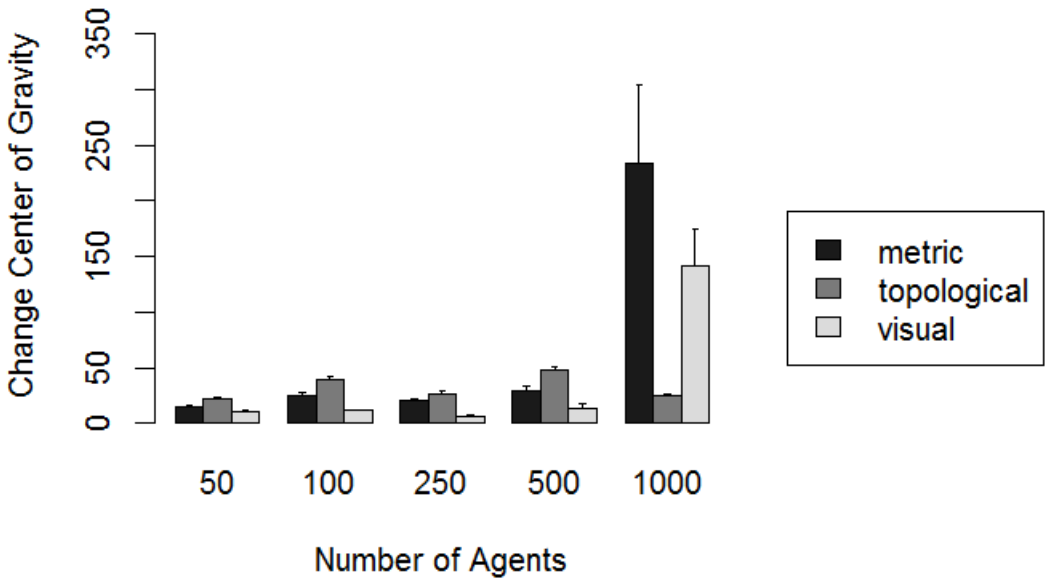

Figure IV.58: The distributions of the change in center of gravity by number of agents and model.

metric model had a higher change in the center of gravity and worse performance than the visual model. The Wilcoxon Rank-Sum test when there were 25 obstacles found that there was a highly significant difference between the metric and visual models ($p < 0.001$, z = 132,333) and the topological and visual models ($p < 0.001$, z = 520,516). The Wilcoxon Rank-Sum test when there were 50 obstacles found that there was a highly significant difference between the metric and visual models ($p < 0.001$, z = 130,361), and the topological and visual models ($p < 0.001$, z = 527,488). These results imply that when there were 25 or 50 obstacles, the topological model had a significantly lower change in center of gravity and better performance than the visual model, and the metric model had a higher change in center of gravity and worse performance than the visual model. The Wilcoxon Rank-Sum test when there were 100 obstacles found that there was a highly significant difference between the metric and visual models ($p < 0.001$, z = 47,175), and the topological and

visual models ($p < 0.001$, z = 185,418). That is, when there were 100 obstacles, the topological model had a significantly lower change in the center of gravity and better performance than the visual model, and the visual model had a higher change in the center of gravity and worse performance than the metric model.

Number of Obstacles	**Metric Mean (Std. Dev.)**	**Topological Mean (Std. Dev.)**	**Visual Mean (Std. Dev.)**
0	24.81 (55.38)	36.73 (64.66)	20.90 (254.89)
25	54.30 (441.79)	33.99 (58.65)	38.54 (439.25)
50	107.95 (757.99)	30.53 (62.27)	40.16 (447.56)
100	33.93 (71.78)	29.37 (52.85)	71.38 (655.97)
250	452.28 (1,662.10)	22.79 (37.14)	148.98 (982.59)

Table IV.89: The means and standard deviations of the Flocking task by number of obstacles for change in center of gravity.

Number of Obstacles	**Significance**	$\chi^2(2)$
0	$p < 0.001$	84.00
25	$p < 0.001$	57.17
50	$p < 0.001$	62.93
100	$p < 0.001$	30.10
250	Not Significant	N/A

Table IV.90: The significance results from the Kruskal-Wallis Test for the Flocking task by number of obstacles for change in center of gravity.

Similar evidence was discovered when the data was analyzed by the radii of repulsion, orientation, and attraction. The means and standard deviations for radius of repulsion are presented in Table IV.91. The descriptive statistics separated by radius of repulsion are displayed in Figure IV.60. The Kruskal-Wallis test found a significant affect of the model type on change in center of gravity for each of the subgroups, with significance as detailed in Table IV.92. The Wilcoxon Rank-Sum test when the radius of repulsion was equal to 5 found that there was a highly significant difference between the metric and visual models ($p < 0.001$, z = 281,828) and the topological and visual models ($p < 0.001$, z = 1,088,319). That is, when the radius of repulsion was 5, the visual model had a significantly lower change in center of gravity and better performance than the metric and topological models. The Wilcoxon Rank-Sum test for a radius of repulsion equal to 25 found that there was a highly significant difference between the metric and topological models ($p < 0.001$, z = 139,202), the metric and visual models ($p < 0.01$, z = 136,311), and the topological and visual models ($p <$ 0.001, z = 603,013). This result implies that when the radius of repulsion was 25, the topological model had a significantly higher change in center of gravity and worse performance than the metric and visual models, and the visual model had a significantly lower change in center of gravity and better performance than the metric model. The Wilcoxon Rank-Sum test where the radius of repulsion was equal to 50 found that there was a highly significant difference between the metric and visual models ($p < 0.001$, z = 82,040) and the topological

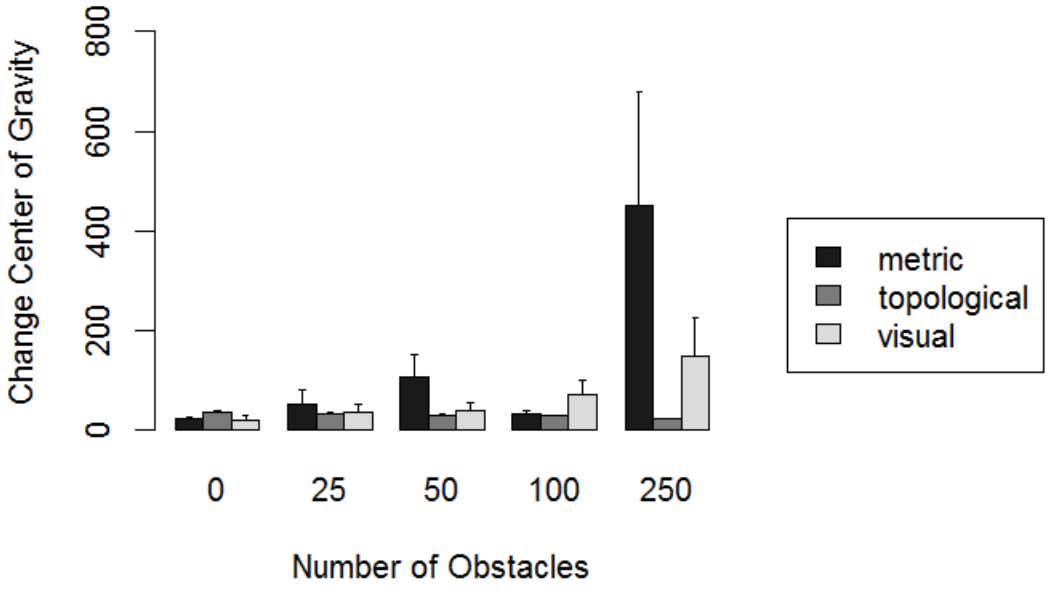

Figure IV.59: The distributions of change in center of gravity by number of obstacles and model.

and visual models ($p < 0.001$, z = 335,255). That is, when the radius of repulsion was 50, the visual model had a significantly lower change in center of gravity and better performance than the topological and metric models. The Wilcoxon Rank-Sum test for a radius of repulsion equal to 100 found that there was a highly significant difference between the metric and visual models ($p < 0.001$, z = 34,552) and the topological and visual models ($p < 0.001$, z = 137,012). This result implies that when the radius of repulsion was 100, the topological model had a significantly lower change in center of gravity and better performance than the visual model, and the visual model had a significantly higher change in center of gravity and worse performance than the metric model.

Radius of Repulsion	**Metric Mean (Std. Dev.)**	**Topological Mean (Std. Dev.)**	**Visual Mean (Std. Dev.)**
5	32.30 (62.11)	39.64 (75.63)	12.27 (72.98)
25	17.71 (32.13)	37.92 (59.00)	9.35 (13.06)
50	53.07 (99.51)	25.91 (34.34)	21.78 (62.73)
100	386.43 (1,618.14)	9.66 (10.61)	258.56 (1,333.35)

Table IV.91: The means and standard deviations of the Flocking task by radius of repulsion for the change in center of gravity.

The means and standard deviations for the Flocking task results for the change in center of gravity grouped

Radius of Repulsion	Significance	$\chi^2(2)$
5	$p < 0.001$	49.12
25	$p < 0.001$	85.38
50	$p < 0.001$	88.28
100	$p < 0.001$	64.27

Table IV.92: The significance results from the Kruskal-Wallis Test for the Flocking task by radius of repulsion for the change in center of gravity.

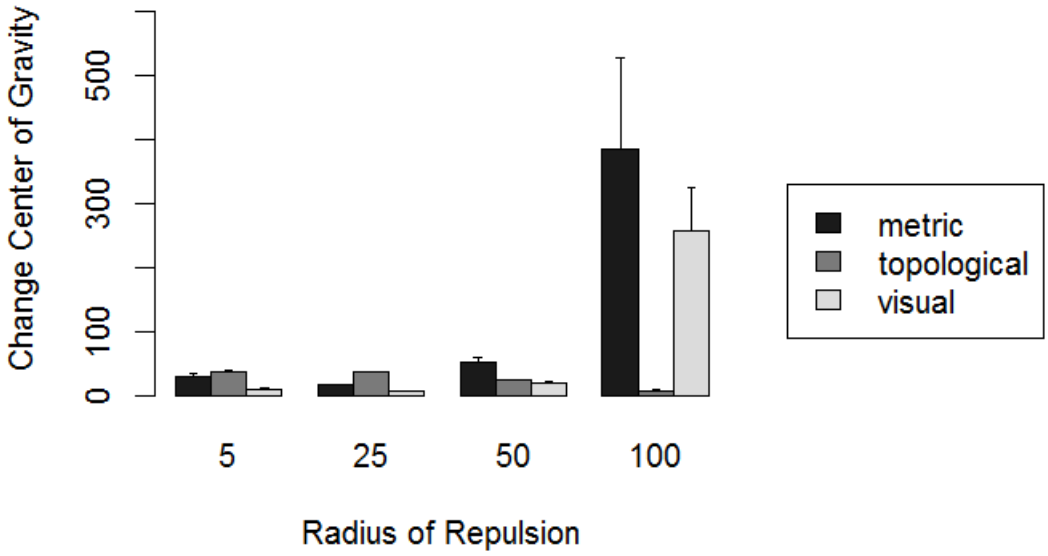

Figure IV.60: The distributions of the change in center of gravity by radius of repulsion and model.

by radius of orientation are presented in Table IV.93. The descriptive statistics are visualized in Figure IV.61. The Kruskal-Wallis test found a highly significant impact of the model type on change in center of gravity for each subgroup by radius of orientation, as detailed in Table IV.94. The Wilcoxon Rank-Sum test found that when the radius of orientation was equal to 20, there was a highly significant difference between the topological and visual models ($p < 0.001$, z = 65,382). The Wilcoxon Rank-Sum test found that when the radius of orientation was equal to 40, there was a highly significant difference between the topological and visual models ($p < 0.01$, z = 124,102). These results imply that when the radius of orientation was 20 or 40, the topological model had a lower change in center of gravity and better performance than the metric model. The Wilcoxon Rank-Sum test found that when the radius of orientation was equal to 75, there was a highly significant difference between the metric and topological models ($p < 0.001$, z = 119,980) and the

metric and visual models ($p < 0.001$, z = 91,487). That is, when the radius of orientation was 75, the metric model had a significantly higher change in center of gravity and worse performance than the topological and visual models. The Wilcoxon Rank-Sum test found that when the radius of orientation was equal to 150, there was a highly significant difference between the metric and topological models ($p < 0.01$, z = 92,019), the metric and visual models ($p < 0.001$, z = 105,967), and the topological and visual models ($p < 0.001$, z = 460,964). The Wilcoxon Rank-Sum test found that when the radius of orientation was equal to 200, there was a highly significant difference between the metric and topological models ($p < 0.001$, z =28,510), the metric and visual models ($p < 0.001$, z = 45,645), and the topological and visual models ($p < 0.001$, z = 226,490). These results imply that when the radius of orientation was 150 or 200, the topological model had a significantly lower change in the center of gravity and better performance than the visual and metric models, and the metric model had a significantly higher change in the center of gravity and worse performance than the visual model. The Wilcoxon Rank-Sum test found that when the radius of orientation was equal to 300, there was a highly significant difference between the metric and topological models ($p < 0.001$, z = 36,011), the metric and visual models ($p < 0.001$, z = 48,392), and the topological and visual models ($p < 0.001$, z = 227,230). That is, when the radius of orientation was 300, the visual model had a significantly lower change in the center of gravity and better performance than the topological and metric models, and the metric model had a significantly higher change in the center of gravity and worse performance than the topological model.

Radius of Orientation	**Metric Mean (Std. Dev.)**	**Topological Mean (Std. Dev.)**	**Visual Mean (Std. Dev.)**
20	4.56 (4.00)	3.59 (2.15)	4.29 (2.86)
40	4.71 (3.90)	3.94 (2.52)	4.21 (2.35)
75	20.28 (60.80)	5.21 (3.96)	9.70 (37.50)
150	156.95 (948.52)	25.24 (26.40)	106.19 (824.82)
200	125.95 (824.16)	59.40 (68.51)	61.28 (584.44)
300	129.18 (587.77)	107.53 (95.97)	63.40 (494.79)

Table IV.93: The means and standard deviations of the Flocking task by radius of orientation for the change in center of gravity.

Radius of Orientation	**Significance**	$\chi^2(2)$
20	$p < 0.001$	14.59
40	$p = 0.0183$	8.00
75	$p < 0.001$	16.36
150	$p < 0.001$	271.75
200	$p < 0.001$	324.80
300	$p < 0.001$	317.11

Table IV.94: The significance results from the Kruskal-Wallis Test for the Flocking Task task by radius of orientation for the change in center of gravity.

The means and standard deviations for the Flocking task results for change in center of gravity grouped

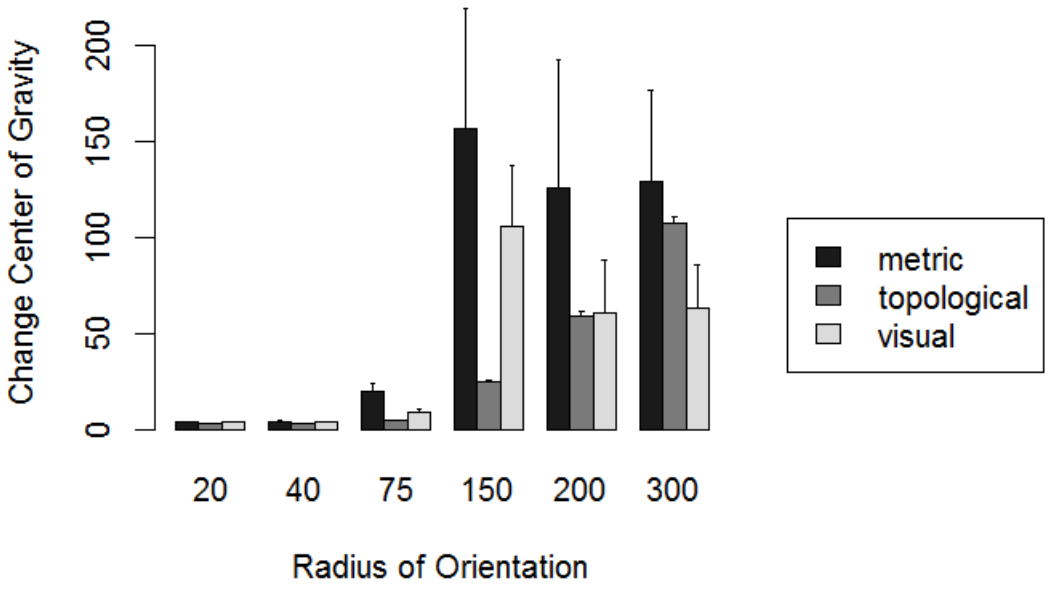

Figure IV.61: The distributions of the change in center of gravity by radius of orientation and model.

by radius of attraction are presented in Table IV.95. The descriptive statistics are visualized in Figure IV.62. The Kruskal-Wallis test found a highly significant impact of the model type on change in center of gravity when the radius of attraction was not equal to 35, as detailed in Table IV.96. The Wilcoxon Rank-Sum test found that when the radius of attraction was equal to 25, there was a significant difference between the topological and visual models (p = 0.0215, z = 1,660). The Wilcoxon Rank-Sum test found that when the radius of attraction was equal to 200, there was a highly significant difference between the topological and visual models ($p < 0.001$, z = 247,598). These results imply that when the radius of attraction was 25 or 200, the visual model had a significantly higher change in center of gravity and worse performance than the topological model. The Wilcoxon Rank-Sum test found that when the radius of attraction was equal to 80, there was a significant difference between the metric and visual models (p = 0.0249, z = 22,228) and the topological and metric models ($p < 0.001$, z = 31,540). That is, when the radius of attraction was 80, the metric model had a significantly higher change in the center of gravity and worse performance than the topological and visual models. The Wilcoxon Rank-Sum test found that when the radius of attraction was equal to 400, there was a highly significant difference between the metric and topological models ($p < 0.001$, z = 203,110), the metric and visual models ($p < 0.001$, z = 199,660), and the topological and visual models ($p < 0.001$, z = 910,044). This result implies that when the radius of attraction was 400, the topological model

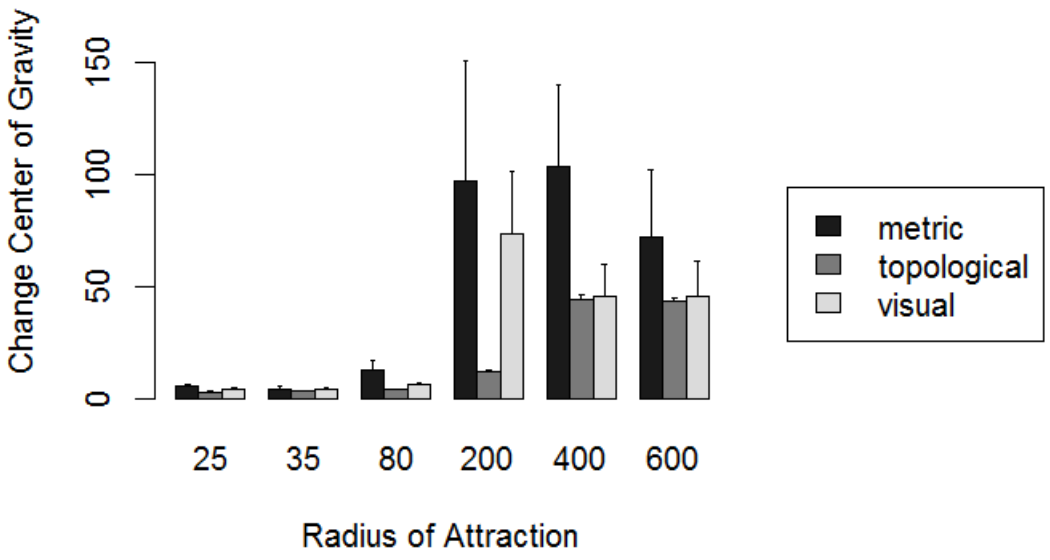

Figure IV.62: The distributions of the change in center of gravity by radius of attraction and model.

had a significantly lower change in the center of gravity and better performance than the metric and visual models, and the metric model had a significantly higher change in center of gravity and worse performance than the visual model. The Wilcoxon Rank-Sum test found that when the radius of attraction was equal to 600, there was a highly significant difference between the metric and visual models ($p < 0.001$, $z = 241{,}045$) and the topological and visual models ($p < 0.001$, $z = 929{,}481$). That is, when the radius of attraction was 600, the topological model had a significantly lower change in the center of gravity and better performance than the visual model, and the metric model had a significantly higher change in the center of gravity and worse performance than the visual model.

Radius of Attraction	**Metric Mean (Std. Dev.)**	**Topological Mean (Std. Dev.)**	**Visual Mean (Std. Dev.)**
25	5.79 (5.76)	3.51 (2.14)	4.87 (4.11)
35	4.62 (4.98)	3.65 (2.22)	4.74 (3.44)
80	13.29 (45.71)	4.57 (3.56)	6.61 (21.93)
200	97.23 (739.13)	12.61 (19.23)	73.64 (676.51)
400	103.60 (675.39)	44.68 (72.34)	46.04 (457.35)
600	72.53 (552.63)	43.84 (66.03)	46.28 (504.91)

Table IV.95: The means and standard deviations of the Flocking task by radius of attraction for the change in center of gravity.

Radius of Attraction	Significance	$\chi^2(2)$
25	$p = 0.03609$	6.64
35	Not Significant	N/A
80	$p < 0.01$	151.57
200	$p < 0.001$	19.46
400	$p < 0.001$	224.29
600	$p < 0.001$	214.98

Table IV.96: The significance results from the Kruskal-Wallis Test for the Flocking Task task by radius of orientation for the change in center of gravity.

Task	Hypothesis	Description	Result
Go To Location	H_{GTL}	$PercentReached_{Visual} > PercentReached_{Topo} > PercentReached_{Metric}$	Partially Supported
Search	H_{S1}	$PercentFound_{Visual} > PercentFound_{Topo}$	Not Supported
	H_{S2}	$PercentFound_{Visual} > PercentFound_{Metric}$	Partially Supported
Monitor	H_M	$TotalCoverage_{Visual} > TotalCoverage_{Metric} > TotalCoverage_{Topo}$	Partially Supported
Avoid Object	H_{A1}	$Expanse_{Visual} < Expanse_{Metric}$	Partially Supported
	H_{A2}	$Expanse_{Topo} < Expanse_{Metric}$	Not Supported
Follow Object	H_{F1}	$Efficiency_{Visual} > Efficiency_{Topo} > Efficiency_{Metric}$	Partially Supported
	H_{F2}	$Error_{Visual} < Error_{Topo} < Error_{Metric}$	Fully Supported
Disperse	H_{D1}	$NearestNeighbor_{Metric} > NearestNeighbor_{Visual}$	Partially Supported
	H_{D2}	$NearestNeighbor_{Metric} > NearestNeighbor_{Topo}$	Not Supported
Rally	H_{R1}	$NearestNeighbor_{Visual} < NearestNeighbor_{Metric}$	Not Supported
	H_{R2}	$NearestNeighbor_{Topo} < NearestNeighbor_{Metric}$	Not Supported
Maintain Group	H_{MG1}	$\Delta Dispersion_{Visual} > \Delta Dispersion_{Topo}$	Fully Supported
	H_{MG2}	$\Delta Dispersion_{Metric} > \Delta Dispersion_{Topo}$	Fully Supported
	H_{MG3}	$\Delta COG_{Visual} > \Delta COG_{Topo}$	Fully Supported
	H_{MG4}	$\Delta COG_{Metric} > \Delta COG_{Topo}$	Fully Supported

Table IV.97: A summary of the hypotheses and if they were supported, either fully, partially, or not at all.

IV.3 Discussion

Each of the eight tasks presented a different result as to which of the swarm communication models was best suited to accomplishing the task. The topological model had a better performance in the Go To Location, Search, Monitor, Disperse, and Flocking tasks. The metric model performed better in the Rally task, while the visual model performed better in the Follow task. The visual and metric models both outperformed the topological model in the Avoid task. The difference in optimal communication models implies that the overall research hypothesis, that each task requires a different model for optimal performance, was supported.

H_{GTL}, the hypothesis that the visual model will have a higher percent of agents reach the goal than the topological and metric models, while the topological model will have a higher percentage of agents reach the goal than the metric model, was partially correct in that the topological model had a higher percentage of agents reach the goal than the metric model. However, the topological model performed better than the

visual model for this task. This result occurs because the topological model communicates with a limited number of agents, as compared to the metric and visual models (Strandburg-Peshkin et al., 2013), which allows for a greater cohesiveness among the agents in the topological model swarm. The visual and metric models have a greater sensing range and; thus, were more likely to become obstructed by the presence of an obstacle in the environment, while the topological agents were limited to the closest agents within the swarm and ignored the obstacles. As a result, a greater percentage of the topological model swarms was able to reach the goal area. The data was consistent across the number of agents and number of obstacles, but there were large differences across the radii of attraction, repulsion, and orientation. The larger values for these radii demonstrated a significantly better ability for the agents to reach the goal area, which implies that the increased sensing range was necessary for reaching the goal area. Future experiments may consider providing the agents with prior knowledge regarding the goal location, perhaps by directing them towards the correct area at the start of the trial.

The hypothesis for the Search task, H_{S1}, that the visual model will find more goals than the topological model, was not supported. The results demonstrated the opposite outcome, that the visual model found fewer goals, on average than the topological model. The significantly larger percentage of goals found by the topological model agents, as compared to the visual model can be explained by the constrained number of objects to which the topological model agents react, as compared to the visual model agents. The agents were required to come within a certain radius of a goal in order to successfully find a goal. Thus, if a small number of topological agents sense the goal, they will all be attracted to the goal object, and end up within the required radius. The visual model agents, while more likely to be able to sense the goal, may be misdirected by an obstacle or attracted by two goals simultaneously because they can sense more objects. Hypothesis H_{S2}, that the visual model will find more goals than the metric model was partially supported. The visual model's greater sensing range was better able to detect the goals than the metric model, which led to a higher percentage of goals being found by swarms using the visual model. However, on the whole, this difference was not significant.

The hypothesis, H_M for the Monitor task that the visual model will have better coverage than the metric and topological models, while the topological model will have better coverage, was also partially verified. The topological model provided the best coverage of all the models. The hypothesis was supported by the fact that the metric model had a significantly lower percentage of coverage than the visual model. This result can be explained by the potential sensing range of the agents for each communication model. The visual model's sensing range is anywhere within the field of view, which can be anywhere from the size of the radius of attraction to the size of the environment, while the metric model is limited to the radius of attraction. The topological model agent's sensing range is limited by the distance of the nearest neighbor that is farthest away

from the agent. Any object closer to the agent than the farthest neighbor can be sensed by the agent. An agent in the corner of the map can only sense objects, within at most a specific radius under the metric or visual models, where the metric agent's sensing range is the radius of attraction and the visual model's sensing range is at most the visual range, if no occlusion occurs. However, if the nearest neighbors of the agent are spread across the map, under the topological model, the agent is able to see much farther than under the metric or visual models. The trends in the data considered by radius of repulsion, orientation, and attraction all support this conclusion. The lower values for radius of attraction, where the metric and visual models have a constrained sensing range, show that the topological model has a significantly higher percent coverage. The higher values for radius of attraction show that when the visual and metric models have enhanced sensing range, they achieve a higher coverage percentage than the topological model. Across all of the parameters, the metric model is less able to sense the environment than the visual model. The lower sensing range of the metric model is illustrated in the lower values for radius of attraction, as the metric model has a significantly lower coverage percentage. The visual model agents are able to sense more of the environment than the metric model agents, as predicted by the hypothesis. The radii of orientation and repulsion followed a similar pattern, because the radius of attraction is constrained by those two values. The trends in the data by number of agents and number of obstacles were consistent across all values, providing no further support.

Neither of the Avoid task hypotheses were fully supported. H_{A1} stated that the metric model will have higher expanse than the visual model, and received partial support, while H_{A2} hypothesized that that the topological model will have lower expanse than the metric model and received no support. The topological model had a greater expanse than the metric model in many instances when the data was considered by individual parameters, and the topological model was almost always significantly better than the metric model. However, H_{A1} received support in several of the parameter specific analyses, as the metric model had a higher mean expanse than the visual model, occasionally with a significant difference. The trends when the data was considered by the different patterns were consistent. There was an increase in expanse along with the increasing number of agents, which is a result of the increasingly large areas within which the agents can operate as the number of agents increases. The metric model had a higher expanse than the visual model when the sensing range of the agent was low; that is, when the radii of repulsion, orientation, and attraction were low. As the radii decreased, the metric agent's ability to sense and stay close to its neighbors decreased. The reason the hypothesis is not fully supported is due to the interaction between the agents and the adversary. The topological model agents only interact with a set number of closest agents, which means that the repulsive reaction to the adversary has a greater relative impact on the topological agent. The metric and visual model agents sense a much wider array of objects, which allows the attractive force towards other agents to counteract the adversary's repulsive effect. The additional attractive force prevents the metric and visual

swarms from spreading out and having a higher expanse. As the radius of attraction, and thus the maximum sensing range of the metric model is limited, the performance of the metric model suffers, leading to higher and higher mean expanse values as the radius of attraction decreases. The metric model generally has a larger expanse than the visual model, due to the metric model's limited sensing range. The visual model senses objects outside of the radius of attraction when the field of view is greater than the radius, whereas the metric model is always limited to the radius of attraction as its maximum.

The results demonstrated a result that was counter to the Follow task hypothesis, H_{F1}, which stated that the visual model will have a higher efficiency than the topological and metric models, while the metric model will have lower efficiency than the topological model. This result can be explained by the communication models' interaction patterns; the agents were generated in one corner of the map, and thus, the original interactions were likely based more on repulsion because all of the agents are within a small distance of each other. The metric model agents, which can sense all objects within the radii, were able to interact with more agents in the confined space and become informed faster. The topological model agents were limited to the nearest objects, and the visual model agents were limited to the visible agents. The visual model has the lowest latency, because the near agents were occluded when all of the agents are concentrated in the corner of the environment at the trial start. The trends for network efficiency, when considered by the different radii showed that there was a markedly higher time for information propagation in the metric model, than the topological model when the sensing range of the agent was small. That is, when the radius of attraction is constrained to 25 or 35, with the radius of orientation at 20 and the radius of repulsion at 5, the metric model was unable to sense as many agents as the topological model and unable to propagate information as effectively as the topological model. Thus, the metric model's superior ability to react to agents within the radius of repulsion positively influenced its network efficiency. A future experiment can better measure network efficiency by increasing the area in which the original agents are generated, in order to allow for non-repulsive actions to have an effect on the swarm's network efficiency. The second Follow task hypothesis, H_{F2}, in which the metric model has higher error than the topological and visual models, and that the visual model has lower error than the topological model, was supported by the results. The lowest error and highest percentage of agents following the target occurred with the visual model, followed by the topological model, with the metric model having the lowest percentage of agents following the target and the highest error. The results were consistent when considered by number of agents and obstacles, as well as by the radii of repulsion, orientation, and attraction. More visual agents, after expanding from the corner in which they were generated, are able to sense the target, than the metric or topological model agents, and are better able to remain aligned with the target.

The Disperse task's first hypothesis, H_{D1}, states that the metric model will have a higher nearest neighbor

distance and perform better than the visual model. H_{D2} hypothesizes that the metric model can have a higher nearest neighbor distance and perform better than the topological model. H_{D1} was partially supported, while H_{D2} was not supported. The topological model had a significantly higher nearest neighbor distance than the visual and metric models, which was mostly consistent when considered by the different parameters. This result can be explained by the topological model only focusing on a constrained number of nearest agents, compared to the visual and topological models. The hypothesis determined that the greater number of agents that the visual and metric models can respond to and repulse from is an advantage. However, the data implies that the larger number of agents that the visual and metric models respond to prevents the desired repulsion, as they will attempt to move away from objects in multiple directions and not make any significant movements. The topological model's nearest neighbor distance remained more constant than the metric and visual models even when varying the number of agents or obstacles. The metric and visual models were dependent on the changes in number of objects. Partial support for H_{D1} occurs in small radii and crowded environments (i.e., those with large numbers of agents and obstacles). The trend of higher distances for the metric model at low values for radius of repulsion and orientation indicate that as the sensing range of the metric model decreases, the metric model focuses better on closer objects and repels away from other objects. The smaller sensing range allows the metric model to sense fewer objects and behave more like the topological model.

The hypotheses for the Rally task, H_{R1}, hypothesized that the metric model will have a higher nearest neighbor distance and perform worse than the visual model. H_{R2} stated that the metric model will have a higher nearest neighbor distance and perform worse than the visual model. Neither hypothesis was supported. The metric model had the lowest nearest neighbor distance, significantly lower than the topological and visual models. The hypotheses for this task were predicated on the idea that the topological and visual models' greater sensing range will allow more attraction than the metric model. However, the results suggest that the ability to communicate with more objects misdirected the visual and topological models. The topological and visual models' greater sensing range meant that they were more likely to be attracted to agents in opposite directions or to be repulsed by an obstacle. The metric agents only responded to those agents within the radius of attraction and actually moved closer together. The topological model sensed fewer objects at a distance, due to the limited topological number. As such, the topological model agents came together more effectively than the visual model agents. The hypotheses' logic was correct in identifying the sensing range as a key performance determinant, but did not fully consider the effect that the sensing range had on the each model's performance. The nearest neighbor distances were consistent across the various parameters.

The Flocking task hypothesis, H_{MG1}, stated that the visual model will have a higher change in dispersion than the topological model, while H_{MG2} hypothesized that the metric model will have a higher change in dispersion than the topological model. H_{MG3} stated that the visual model will have a higher change in center

Task	Recommended Model(s)
Go To Location	Topological
Search	Topological
Monitor	Topological
Avoid Object	Metric, Visual
Follow Object	Visual
Disperse	Topological
Rally	Metric
Maintain Group / Flocking	Topological

Table IV.98: Summary of recommended models for tasks.

of gravity than the topological model, and H_{MG4} conjectured that the metric model will have a higher change in center of gravity than the topological model. All four hypotheses were supported by the results. The topological model's lower level of interaction proved to be the key in maintaining a relatively stable center of gravity and dispersion, as proposed in the hypotheses. The results' trends indicated that as there were more objects within the environment, the topological model's limited interaction allowed the swarm's change in dispersion and center of gravity to remain low. The larger sensing range of the metric and visual model caused the changes in dispersion and center of gravity to skyrocket. A similar pattern was observed as the agents' radii of repulsion, orientation, and attraction increased; the topological model would have a consistent performance, while the metric and visual models would have exponentially larger changes in swarm position and density. The topological model swarms, in which agents were less likely to sense an obstacle, maintained a low change in center of gravity and dispersion across different parameters.

Across all of the tasks, there was a clear difference between the topological model and the visual or metric models. This difference is particularly evident for the Disperse, Go To Location, Avoid, and Flocking tasks, and partially true for the Search task. Each task appears to have a clearly identified model that is the best alternative for the most successful task completion. The recommended models for each task are presented in Figure IV.98. The recommendations in which there was a clear model choice, as in the Go To Location, Monitor, Avoid, Disperse, Flocking, and Rally tasks were straightforward. One or two models in each of these tasks perform significantly better than the other model or models. The Search task contained only partial indication of which model was best, but the topological model was better than the metric model, even if no significant difference was found. The Follow Object task had conflicting results. The error metric was deemed to be more immediately relevant to the task, and thus the visual model was selected.

The three biologically inspired communication models were able to perform most of the tasks, although not always in the manner expected. The models performed as predicted in some cases, but more frequently the result was different from what was predicted, but reasonable in hindsight.

CHAPTER V

Contributions, Conclusions, and Future Work

V.1 Conclusions

This Thesis analyzed the applicability of biologically inspired swarm communication models to typical swarm robotics tasks. Progress has been made in determining which communication models are applicable to a given task, by simulating potential tasks and analyzing the results using swarm specific metrics. Some specific tasks seem to favor the usage of a given model, like the topological model for the Disperse task or the Flocking task. Others have a less clear difference between the models, favoring a pair of models over the third. An example is how the visual and the metric models are preferred over the topological model in the Go To Location task.

Biological swarms have been shown to have the ability to complete swarm robotics tasks. The abilities of different swarm communications models have been contrasted, illustrating the strengths and weaknesses of each model. This Thesis uses these differences to provide evidence for where one model is preferable to another of the models.

V.2 Contributions

There are two primary contributions of this Thesis. The first component is the creation of algorithms representing the biological swarm communication models that can be applied for use in swarm robotics. A novel application of the biological communication models as viable algorithms for completing swarm robotics tasks was introduced. The models analyzed in this thesis had been used primarily to describe biological swarms. The models were used to either describe a property of the biological swarms (Couzin et al., 2002; Ballerini et al., 2008), or to emulate a facet of swarm behavior (Abaid and Porfiri, 2010). This was the first application of these models to a variety of tasks useful for swarm robotics.

The second primary contribution is the analysis of the performance of these models in the context of swarm robotics task. A wide range of exemplar robotics tasks were used for this Thesis, laying the groundwork for the application of these models to actual robots. The biological models were shown to be capable of completing the tasks, and performing in a swarm robotics environment. This capability means that further research can be conducted on the capabilities of biological swarm models in robotics scenarios.

V.3 Future Work

This work only begins to explore the potential of these biologically inspired swarm models. Further applications fall into one of two groups; the application based group or the theory based group. Future work from the applications perspective involves implementing these models in physical swarms of robots and assessing the performance of the models in real world scenarios. The models can be implemented for a variety of robots; unmanned aerial vehicles, small insectlike robots, or even submersibles. Determining which models work in certain environments will be a viable research topic. The visual model, for example, may not work as efficiently in situations where the field of view is heavily occluded by dust or obstacles. The implementation for use in the real world will not pose any great challenge using the algorithms described in Chapter III and an appropriate abstraction layer (Brutschy et al., 2015).

The other perspective to consider is more theoretical, studying the more abstract capabilities and properties of biologically inspired swarms. While the analyzed swarms are homogenous swarms, further research can prove that a mixture of different models of interaction will perform more effectively in the tasks. If each robot is required to hold a single model, mixing the algorithms through the swarm may provide a way for the properties of individual models to complement each other. A mixture of topological and visual model agents, for example, can allow swarm to have the cohesiveness presented by the topological model and the sensing capabilities of the visual model. Alternatively, the research can focus on adapting and optimizing a specific model to perform in a more broad environment. The analysis environments were chosen to distinguish the differences of the models for each task, and were held constant for a given swarm size; variations in the environment's shape or properties can provide interesting differences for research. Larger obstructions in the environment may mean that the advantages of the visual model, for example, can be negated due to a reduction in the number of visible objects.

An alternative approach to the research perspective involves the completion of more complex tasks. Swarms can be required to navigate first through an environment full of obstacles, and then search for goals once they have reached a given location. The chaining of the primitive tasks more closely resembles potential applications in the real world. Transitions from one model of interaction to another will provide an interesting avenue for research, as after one task is complete, the swarm might need to transition to a model more suitable for the follow-up task. Endless possibilities stem from these simple biologically inspired models.

BIBLIOGRAPHY

Abaid, N. and Porfiri, M. (2010). Fish in a ring: Spatio-temporal pattern formation in one-dimensional animal groups. *Journal of The Royal Society Interface*, page rsif20100175.

Aoki, I. (1982). A simulation study on the schooling mechanism in fish. *Nippon Suisan Gakkaiski*, 48(8):1081–1088.

Attanasi, A., Cavagna, A., Del Castello, L., Giardina, I., Grigera, T. S., Jelić, A., Melillo, S., Parisi, L., Pohl, O., Shen, E., et al. (2013). Superfluid transport of information in turning flocks of starlings. *arXiv preprint arXiv:1303.7097*.

Ballerini, M., Cabibbo, N., Candelier, R., Cavagna, A., Cisbani, E., Giardina, I., Lecomte, V., Orlandi, A., Parisi, G., Procaccini, A., Viale, M., and Zdravkovic, V. (2008). Interaction ruling animal collective behavior depends on topological rather than metric distance: Evidence from a field study. *Proceedings of the National Academy of Sciences*, 105(4):1232–1237.

Beni, G. (2005). From swarm intelligence to swarm robotics. In Sahin, E. and Spears, W., editors, *Swarm Robotics*, volume 3342 of *Lecture Notes in Computer Science*, pages 1–9. Springer Berlin Heidelberg.

Bialek, W., Cavagna, A., Giardina, I., Mora, T., Silvestri, E., Viale, M., and Walczak, A. M. (2012). Statistical mechanics for natural flocks of birds. *Proceedings of the National Academy of Sciences*, 109(13):4786–4791.

Bode, N. W., Franks, D. W., and Wood, A. J. (2011). Limited interactions in flocks: relating model simulations to empirical data. *Journal of The Royal Society Interface*, 8(55):301–304.

Brito, R., Schaerf, T., Myerscough, M., Heard, T., and Oldroyd, B. (2012). Brood comb construction by the stingless bees tetragonula hockingsi and tetragonula carbonaria. *Swarm Intelligence*, 6(2):151–176.

Brutschy, A., Garattoni, L., Brambilla, M., Francesca, G., Pini, G., Dorigo, M., and Birattari, M. (2015). The tam: abstracting complex tasks in swarm robotics research. *Swarm Intelligence*, 9(1):1–22.

Cavagna, A., Cimarelli, A., Giardina, I., Parisi, G., Santagati, R., Stefanini, F., and Viale, M. (2010). Scale-free correlations in starling flocks. *Proceedings of the National Academy of Sciences*, 107(26):11865–11870.

Cavagna, A., Queirós, S. D., Giardina, I., Stefanini, F., and Viale, M. (2013). Diffusion of individual birds in starling flocks. *Proceedings of the Royal Society B: Biological Sciences*, 280(1756):20122484.

Cianci, C. M., Raemy, X., Pugh, J., and Martinoli, A. (2007). Communication in a swarm of miniature robots: The e-puck as an educational tool for swarm robotics. In Sahin, E., Spears, W. M., and Winfield, A. F., editors, *Swarm Robotics*, volume 4433 of *Lecture Notes in Computer Science*, pages 103–115. Springer Berlin Heidelberg.

Couzin, I. D. (2009). Collective cognition in animal groups. *Trends in Cognitive Sciences*, 13(1):36 – 43.

Couzin, I. D., Krause, J., Franks, N. R., and Levin, S. A. (2005). Effective leadership and decision-making in animal groups on the move. *Nature*, 433(7025):513–516.

Couzin, I. D., Krause, J., James, R., Ruxton, G. D., and Franks, N. R. (2002). Collective memory and spatial sorting in animal groups. *Journal of Theoretical Biology*, 218(1):1 – 11.

Dorigo, M., Roosevelt, A. F. D., and Dorigo, M. (2004). Swarm robotics. *Special Issue, Autonomous Robots*, pages 111–113.

Dornhaus, A. and Chittka, L. (1999). Insect behaviour: Evolutionary origins of bee dances. *Nature*, 401(6748):38–38.

Du, Q., Faber, V., and Gunzburger, M. (1999). Centroidal voronoi tessellations: Applications and algorithms. *SIAM review*, 41(4):637–676.

Fujisawa, R., Dobata, S., Sugawara, K., and Matsuno, F. (2014). Designing pheromone communication in swarm robotics: Group foraging behavior mediated by chemical substance. *Swarm Intelligence*, 8(3):227–246.

Handegard, N. O., Boswell, K. M., Ioannou, C. C., Leblanc, S. P., Tjøstheim, D. B., and Couzin, I. D. (2012). The dynamics of coordinated group hunting and collective information transfer among schooling prey. *Current Biology*, 22(13):1213–1217.

Handl, J. and Meyer, B. (2007). Ant-based and swarm-based clustering. *Swarm Intelligence*, 1(2):95–113.

Hayes, S. T. (2014). Swarm tasks. personal communication.

Hecker, J. and Moses, M. (2015). Beyond pheromones: evolving error-tolerant, flexible, and scalable ant-inspired robot swarms. *Swarm Intelligence*, 9(1):43–70.

Huth, A. and Wissel, C. (1992). The simulation of the movement of fish schools. *Journal of Theoretical Biology*, 156(3):365 – 385.

Karaboga, D. and Akay, B. (2009). A survey: Algorithms simulating bee swarm intelligence. *Artif. Intell. Rev.*, 31(1-4):61–85.

Kolpas, A., Busch, M., Li, H., Couzin, I. D., Petzold, L., and Moehlis, J. (2013). How the spatial position of individuals affects their influence on swarms: A numerical comparison of two popular swarm dynamics models. *PloS one*, 8(3):e58525.

Krause, J., Hoare, D., Krause, S., Hemelrijk, C., and Rubenstein, D. (2000). Leadership in fish shoals. *Fish and Fisheries*, 1(1):82–89.

Krause, J. and Ruxton, G. D. (2002). *Living in groups*. OUP Oxford.

Leca, J.-B., Gunst, N., Thierry, B., and Petit, O. (2003). Distributed leadership in semifree-ranging white-faced capuchin monkeys. *Animal Behaviour*, 66(6):1045–1052.

Makris, N. C., Ratilal, P., Jagannathan, S., Gong, Z., Andrews, M., Bertsatos, I., God, O. R., Nero, R. W., and Jech, J. M. (2009). Critical population density triggers rapid formation of vast oceanic fish shoals. *Science*, 323(5922):1734–1737.

Manning, M. D., Harriott, C. E., Hayes, S. T., Seiffert, A. E., and Adams, J. A. (2015). Heuristic evaluation of swarm metrics effectiveness. In *Proceedings of the 10th ACM/IEEE International Conference on Human-Robot Interaction*, Portland, OR.

Mersch, D. P., Crespi, A., and Keller, L. (2013). Tracking individuals shows spatial fidelity is a key regulator of ant social organization. *Science*, 340(6136):1090–1093.

Murray, L., Timmis, J., and Tyrrell, A. (2013). Modular self-assembling and self-reconfiguring e-pucks. *Swarm Intelligence*, 7(2-3):83–113.

Nunnally, S., Walker, P., Kolling, A., Chakraborty, N., Lewis, M., Sycara, K., and Goodrich, M. (2012). Human influence of robotic swarms with bandwidth and localization issues. In *Proceedings of the 2012 IEEE International Conference on Systems, Man, and Cybernetics*, pages 333–338.

Olson, R. S., Hintze, A., Dyer, F. C., Knoester, D. B., and Adami, C. (2013). Predator confusion is sufficient to evolve swarming behaviour. *Journal of The Royal Society Interface*, 10(85).

Parrish, J. K., Viscido, S. V., and Grünbaum, D. (2002). Self-organized fish schools: an examination of emergent properties. *The biological bulletin*, 202(3):296–305.

Reynolds, C. W. (1987). Flocks, herds and schools: A distributed behavioral model. *ACM Siggraph Computer Graphics*, 21(4):25–34.

Saska, M., Vakula, J., and Preucil, L. (2014). Swarms of micro aerial vehicles stabilized under a visual relative localization. In *Robotics and Automation (ICRA), 2014 IEEE International Conference on*, pages 3570–3575.

Seyfried, J., Szymanski, M., Bender, N., Estana, R., Thiel, M., and Worn, H. (2005). The i - swarm project: Intelligent small world autonomous robots for micro-manipulation. In Sahin, E. and Spears, W. M., editors, *Swarm Robotics*, volume 3342 of *Lecture Notes in Computer Science*, pages 70–83. Springer Berlin Heidelberg.

Shen, C.-C. and Jaikaeo, C. (2005). Ad hoc multicast routing algorithm with swarm intelligence. *Mobile Networks and Applications*, 10(1-2):47–59.

Spears, W. M., Spears, D. F., Hamann, J. C., and Heil, R. (2004). Distributed, physics-based control of swarms of vehicles. *Autonomous Robots*, 17(2-3):137–162.

Strandburg-Peshkin, A., Twomey, C. R., Bode, N. W., Kao, A. B., Katz, Y., Ioannou, C. C., Rosenthal, S. B., Torney, C. J., Wu, H. S., Levin, S. A., and Couzin, I. D. (2013). Visual sensory networks and effective information transfer in animal groups. *Current Biology*, 23(17):R709 – R711.

Walker, P., Nunnally, S., Lewis, M., Kolling, A., Chakraborty, N., and Sycara, K. (2012). Neglect benevolence in human control of swarms in the presence of latency. In *2012 IEEE International Conference on Systems, Man, and Cybernetics*, pages 3009–3014.

Wilson, E. O. (1962). Chemical communication among workers of the fire ant solenopsis saevissima (fr. smith) 1. the organization of mass-foraging. *Animal behaviour*, 10(1):134–147.

Young, G. F., Scardovi, L., Cavagna, A., Giardina, I., and Leonard, N. E. (2013). Starling flock networks manage uncertainty in consensus at low cost. *PLoS computational biology*, 9(1):e1002894.